TECHNICAL REPORT
NATICK/TR-06/023

AD_____

THE REDUCTION OF SOLID WASTE ASSOCIATED WITH MILITARY RATION PACKAGING

by
Jo Ann Ratto
Jeanne Lucciarini
Christopher Thellen
Danielle Froio
and
Nandika Anne D'Souza*

***University of North Texas**
Denton, Texas 76203

September 2006

Final Report
January 2003 – December 2005

U.S. Army Research, Development and Engineering Command
Natick Soldier Center
Natick, Massachusetts 01760-5020

DISCLAIMERS

The findings contained in this report are not to be construed as an official Department of the Army position unless so designated by other authorized documents.

Citation of trade names in this report does not constitute an official endorsement or approval of the use of such items.

DESTRUCTION NOTICE

For Classified Documents:

Follow the procedures in DoD 5200.22-M, Industrial Security Manual, Section II-19 or DoD 5200.1-R, Information Security Program Regulation, Chapter IX.

For Unclassified/Limited Distribution Documents:

Destroy by any method that prevents disclosure of contents or reconstruction of the document.

REPORT DOCUMENTATION PAGE

Form Approved
OMB No. 0704-0188

1. REPORT DATE *(DD-MM-YYYY)*	2. REPORT TYPE	3. DATES COVERED *(From - To)*
19-09-2006	FINAL	January 2003 - December 2005

4. TITLE AND SUBTITLE

THE REDUCTION OF SOLID WASTE ASSOCIATED WITH MILITARY RATION PACKAGING

5a. CONTRACT NUMBER

5b. GRANT NUMBER

SERDP 1270

5c. PROGRAM ELEMENT NUMBER

622786

6. AUTHOR(S)

Jo Ann Ratto, Jeanne Lucciarini, Christopher Thellen, Danielle Froio and Nandika Anne D'Souza*

5d. PROJECT NUMBER

AH-99 (SERDP - 1270)

5e. TASK NUMBER

5f. WORK UNIT NUMBER

7. PERFORMING ORGANIZATION NAME(S) AND ADDRESS(ES)

U.S. Army Research, Development and Engineering Command
Natick Soldier Center
Nanomaterials Science Team
ATTN: AMSRD-NSC-SS-NS
Natick, MA 01760-5020

8. PERFORMING ORGANIZATION REPORT NUMBER

NATICK/TR-06/023

9. SPONSORING/MONITORING AGENCY NAME(S) AND ADDRESS(ES)

Strategic Environmental Research and Development Program (SERDP)
901 N. Stuart St. Suite 303
Arlington VA 22203-1821

10. SPONSOR/MONITOR'S ACRONYM(S)

SERDP

11. SPONSOR/MONITOR'S REPORT NUMBER(S)

SERDP 1270

12. DISTRIBUTION/AVAILABILITY STATEMENT

Approved for public release; distribution is unlimited.

13. SUPPLEMENTARY NOTES

*University of North Texas, Department of Materials Science and Engineering, Denton, Texas

14. ABSTRACT

Nanocomposites were researched as a potential technology to produce environmentally friendly food packaging for military rations that not only meet the military performance requirements but also decrease the amount of solid waste generated by the military. These nanocomposites formulations were melt processed into films and characterized for barrier, mechanical, thermal and biodegradation properties. The polymers investigated were: poly (ethylene co-vinyl alcohol) (EVOH), low-density polyethylene (LDPE), polyamides (nylon), polylactic acid (PLA), and polyethylene terephthalate (PET). The nanoparticles used for all the formulations were from the family of montmorillonite-layered silicates (MLS) that are organically modified to be compatible with the polymer. Formulations varied on the amount of MLS and in some cases compatibilizers were also incorporated to enhance polymer/MLS interactions. In all cases, the nanocomposites had improved barrier and mechanical properties from the homopolymer. The outcome of the research showed that LDPE nanocomposites are the most promising for the Meal, Ready-to-Eat Meal Bag while the EVOH nanocomposites sandwiched within a polyolefin is a potential candidate for the non-retortable and retortable food pouches.

15. SUBJECT TERMS

BARRIER	POLYAMIDE	POLYETHYLENE	WASTE DISPOSAL	MILITARY RATIONS
DISPOSAL	CAST FILMS	SOLID WASTES	BIODEGRADATION	MONTMORILLONITE
POLYMERS	BLOWN FILMS	NANOPARTICLES	NANOCOMPOSITES	LAYERED SILICATES
PACKAGING	WATER VAPOR	POLYLACTIC ACID	WASTE RECYCLING	MRE(MEAL READY TO EAT)

16. SECURITY CLASSIFICATION OF:			17. LIMITATION OF ABSTRACT	18. NUMBER OF PAGES	19a. NAME OF RESPONSIBLE PERSON
a. REPORT	b. ABSTRACT	c. THIS PAGE			Jo Ann Ratto
U	U	U	UU	85	19b. TELEPHONE NUMBER *(Include area code)* 508-233-5315

Table of Contents

List of Figures

Page

List of Tables

Page

Preface

This report documents research on the processing and characterization of nanocomposites for military rations performed by the Natick Soldier Center (NSC), U.S. Army Research, Development and Engineering Command, under project number AH-99, funded by the Department of Defense Strategic Environmental Research and Development Program (SERDP) during the period January 2003 to December 2005.

Acknowledgements

The principal investigator greatly appreciates the team at Natick Soldier Center who worked on this project and generated this report with her. The team members include: Jeanne Lucciarini (co-principal investigator), Danielle Froio (materials engineer) and Christopher Thellen (materials engineer).

The authors are most grateful to the Strategic Environmental Research and Development Program (SERDP) for the continuous technical and financial support during the three years of this project. The authors especially would like to thank the following people at SERDP: Bradley Smith, Jeffrey Marqusee, Charles Pellerin, Jason Campiti, Christopher Swallow, Jeff Houff, Robert Holst, the Science and Advisory Board and all the reviewers for the In-progress Reviews.

The authors also would like to acknowledge Bert Powell of Texas State University and Randy Chapman of Southern Clay Products, Gonzales, Texas for supplying various grades of montmorillonite-layered silicates as well as providing x-ray diffraction patterns for many of the nanocomposites. The authors are grateful for the collaboration with Nandika D'Souza. and Ajit Ranade at the University of North Texas. The authors also thank John Facinelli of Honeywell, Morristown, NJ and Tie Lan of Nanocor, Arlington Heights, IL for their technical support of the nylon nanocomposite work. The authors thank Richard Farrell for the biodegradation studies of PLA nanocomposites, Michael Mullern for the insect resistance testing, Triton Corporation, Chelmsford, MA, Foster Corporation, Dayville, CT and Alcan Corporation, Neenah, WI for the LDPE compounding and scale-up processing. The authors acknowledge Brian Koene, formerly of Triton Corporation, for his technical discussions on nanocomposites. Also, thank you to Andrew Myers of TDA Research, Boulder, Colorado for the PET barrier data. The authors give thanks to Megan Coyne, Elizabeth Culhane, Caitlin Orroth and Sarah Schirmer for their assistance at NSC on a variety of processing and testing of the polymers and nanocomposites. The authors also thank Mona Bray, Environmental Program Manager, from NSC, for her constant support. The authors are extremely grateful to Jean Herbert, Nanomaterials Science Team Leader, for her technical support and guidance.

THE REDUCTION OF SOLID WASTE ASSOCIATED WITH MILITARY RATION PACKAGING

1. Executive Summary

The Meal, Ready-to-Eat (MRE) is key field survival food for the military. Each soldier in combat potentially eats several MRE rations per day. The US Army, US Marine Corps, and the US Air Force consume approximately 46.6 million meals in the field in an average year, generating approximately 14,117 tons of waste per year (0.66 lb of packaging waste per warrior per meal). Currently, the MRE packaging contains foil-laminated films that provide the required three-year shelf life. The existing military specification for barrier properties for the retortable pouch is: oxygen transmission rate: 0.06 cc/m²/day and water vapor transmission rate of 0.01 g/m²/day with a shelf life of 3 years at 27°C (80°F) or 6 months at 38°C (100°F). Inherent problems such as flex cracking and pinholes exist with the use of these films, especially when exposed to freezing temperatures and airdrop scenarios. In addition, the use of foil-based structures limits the potential for recycling as well as the development of packaging systems for novel food processes currently being investigated, such as microwave and radio frequency sterilization. There is a need to develop recyclable and/or biodegradable MRE packaging, which offers high performance and sufficient barrier properties for the required shelf life. Nanotechnology is being explored in this project to improve the physical, thermal and barrier properties of MRE packaging. The main objective of this study was to evaluate and characterize the behavior and properties of blown and cast nanocomposite films consisting of a variety of recyclable and biodegradable polymers and montmorillonite layered silicates (MLS) nanoparticles. These nanocomposites were compared to neat polymer films and the exisiting MRE materials with respects to barrier properties, mechanical performance, and thermal stability as well as soil biodegradation properties. The program deliverables were the following: a nanocomposite meal bag, a non-retortable and a retortable food pouch.

The research explored a variety of polymers and organically modified nanoparticles to enhance the compatibility and interaction between the polymer and nanoparticle. The polymers investigated were: low-density polyethylene (LDPE), poly (ethylene co-vinyl alcohol) (EVOH), polyamides (nylon), polylactic acid (PLA) and polyethylene terephthalate (PET). The polymers were selected based on some of the following properties and criteria: barrier to oxygen and water vapor, mechanical properties, ease of melt processing, price, food and drug administration approval, recyclability and biodegradability.

The nanoparticles used for all the formulations were from the family of MLS that are organically modified to be compatible with the polymer. These MLS platelets, if correctly dispersed and exfoliated in the polymer matrix, can significantly lengthen the path that oxygen and water molecules travel through the nanocomposite film. This should significantly improve barrier properties, but would the improvement be enough to replace the aluminum foil barrier currently used in the MRE packaging? The research focused on varying the MLS content and in some cases, compatibilizers to enhance polymer/MLS interactions. The recyclability of the

The degree of MLS interaction affects mechanical and barrier properties, so these interactions were analyzed with respect to processing methods and parameters. To achieve good interaction between MLS and polymer, the chemistry of the polymer and nanoparticle needs to be compatible. However, processing parameters are also key in achieving maximum interaction, and therefore different shear profiles were investigated to see the influence on these interactions. For all of the polymer/MLS systems, exfoliation was the goal to achieve for morphology, since reported exfoliated systems have obtained the most improvement in performance properties.

Complete exfoliation is a challenge. Previous studies reveal that only nylon nanocomposites have achieved complete exfoliation. The concentration of nanoparticles along with changes in extruder screw speed, residence time, temperature, and screw configuration during melt processing were optimized for each formulation. Formulations of compounded pellets and films were prepared at the laboratory scale and characterized for morphological, mechanical, barrier, thermal, and biodegradable properties. Blown film and cast films were produced to see which processing method produced the best quality films in terms of barrier performance. Since there is bi-axial orientation in the blown film process, studies focused on this method speculating that the orientation of the platelets would also enhance the barrier performance. Optimal nanocomposite formulations were determined from the laboratory scale studies to target the Meal Bag and Food Pouches. Scale-up of these formulations (5 lbs to 25 lbs to 300 lbs) was performed to see if the same polymer/MLS interaction, as well as performance properties, could be achieved at larger scale operations. For the one biodegradable polymer used in this study, PLA, biodegradation studies were performed in soil to see if, in this system, the nanoparticles enhanced biodegradation.

A nanocomposite meal bag was targeted with low density polyethylene and MLS. The current Meal Bag is made from a low density polyethylene but is 11 mil in thickness so tha the bag has resistance to insects. LDPE/7.5% MLS nanocomposite films were melt processed at the laboratory and pilot scale level. The LDPE/MLS formulation contained a compatiblizer and showed significant improvements in mechanical, thermal and barrier performance properties over neat films. This was first demonstrated using laboratory scale equipment for 5-pound processing trials and the MLS concentration varied from 1-7.5%. Subsequently, these trials obtained the optimal formulation (7.5% MLS) and were successfully scaled-up to 300-pound pilot plant trials. Through optimization of the film formulation and processing techniques, a 6-mil LDPE/7.5% MLS nanocomposite Meal Bag prototype was generated that has superior performance to the existing MRE meal bag structure. At both the laboratory and pilot scale level, intercalated nanocomposites were achieved with some degree of exfoliation. Also, Young's modulus of the film was improved by 100%, which is a significant accomplishment given that MRE's can be subjected to extreme rough handling, including free fall and parachute airdrop. The oxygen barrier was also improved with the 7.5% nanocomposite, having nearly twice the barrier properties of the pure LDPE film. Oxygen barrier improvements of this magnitude would make the meal bag a dual-use item, and could be influential in further material reduction. Thermal stability improved by over 80°C for the nanocomposite, as compared to the pure LDPE. The onset of degradation of the nanocomposite film occurred at 450°C vs. 370°C for pure LDPE film. Meal bags fabricated from these films have undergone and passed insect resistance and rough handling testing, which is a major requirement for military food packaging applications.

The Meal Bag would not only contain the MRE components and protect from insect infestation, but would also have built-in barrier, which could potentially lead to down gauging of materials for inner components.

Another candidate for the Meal Bag was PLA/MLS nanocomposites. PLA/MLS nanocomposites were the only biodegradable nanocomposite system studied. This was based on the availability, properties and price of the polymer. Improvement in mechanical, barrier and thermal properties of the nanocomposites was significant in comparison to the neat PLA; however, the properties were not acceptable for MRE packaging. The biodegradation rates in soil were too slow also for the military to consider PLA/MLS nanocomposites. The addition of MLS did not really affect the rate of biodegradation significantly.

EVOH nanocomposites were targeted for the non-retortable and retortable food pouch. Studies were done varying the organically modified MLS as well as the MLS concentration from 1-6% by weight. Blown and cast films were produced and the films were characterized at varying relative humidity (RH), since EVOH is a hydrophilic polymer and its moisture content influences properties. All of the EVOH/MLS nanocomposites had a dispersed /intercalated morphology with perhaps some small degree of exfoliation that was confirmed by X-ray diffraction and transmission electron microscopy (TEM). The cast film nanocomposites had 23% improvement of Young's modulus at 0% RH in comparison to the neat film. The blown film nanocomposites did not show improvement at 0%RH, but did show a 58% improvement in comparison to the neat EVOH at high humidity (93% RH). The oxygen barrier was the best for the cast film nanocomposite, with a 57% improvement from the neat EVOH (0.5 cc-mil/m^2-day for the nanocomposite, 1.4 cc-mil/m^2-day for the neat EVOH). The thermal properties, onset of thermal degradation, melt temperature and enthalpy did not change significantly for the nanocomposites in relation to the neat EVOH films. Since EVOH is extremely sensitive to moisture, multilayer films (5 layers) were produced using LDPE as the outer layer to protect the EVOH from atmospheric moisture along with a tie layer that helps adhere the EVOH to the LDPE. Studies were performed to vary the EVOH thickness in order to optimize the barrier properties. Barrier properties were again studied at 0 and 93% RH and the films had twice the oxygen barrier at 93% RH. Selected formulations were reprocessed and even scaled up from 5 lbs to 25 lbs to obtain additional nanocomposites of EVOH/MLS to make multilayer films. The scale up had some dispersion and processing problems with the MLS, and these processing runs are being repeated. EVOH nanocomposites did demonstrate promising oxygen barrier data, but it would need to be in a multilayer system for use in MRE packaging.

EVOH films were made into pouches and underwent thermal processing in a retort, which subjects the packaging to extreme heat and pressure while submerged in water. The entrée food pouch in the MRE is retorted to achieve commercial sterility. These trials included multilayered film structures of LDPE and multilayer EVOH/MLS nanocomposite films processed at NSC. The following properties were tested before and after retorting to determine its affect on the package in terms of: seal strength, tensile properties and oxygen permeability. In addition, the pouches were subjected to a visual inspection to determine if any of the seals had ruptured after the retort trial was complete. In all samples, the seal strength and tensile properties were maintained, but the barrier properties after retorting could not be measured. The pouches did not retain their original size, shape or color. Studies are underway to reduce the

thickness of the EVOH layer and use a retortable-grade of polypropylene (PP) for the outer layer.

Several nylons were also targeted for the non-retortable and retortable food pouch. A variety of nylons was first processed into films and characterized for barrier and mechanical performance to see which nylon would be the best candidate for the nanocomposite study. Nylon/ MLS nanocomposite films were processed and characterized as monolayer and multilayer films. The nylon/MLS nanocomposites did display some exfoliation and intercalation. The mechanical properties all showed significant improvement from the neat nylon. The oxygen and water barrier properties of monolayer nylon 6 films were improved by 40% and 30% respectively through the addition of MLS. MLS additives did not significantly affect the glass transition temperature (Tg) and melting temperature (Tm) of the nylon 6. Thermal stability of the neat nylon film is roughly 4°C higher than that of the nanocomposite.

Multilayer nylon films formed through co-extrusion processing provided similar results and were examined for packaging applications. A multilayer structure that may contain nylon and EVOH is being considered. Multilayer films based on nanocomposite nylon MXD6 technology demonstrated the highest barrier against oxygen. Oxygen permeation through this 10-mil thick film at 0%RH was 0.49cc/m^2-day.

There was an interest to explore PET nanocomposites also for the non-retortable and retortable food pouch as PET is currently used as a recyclable packaging material with promising barrier properties. If a monolayer of PET nanocomposite could be produced with significantly improved barrier values, this would simplify the MRE packaging. Polyethylene terephthalate glycol (PETG) /MLS nanocomposites were prepared using maleic anhydride (MA) as the compatibilizer. The nanocomposites had some degree of intercalation and the morphology of the films with and without MA was not significantly different. Intercalated dispersion was observed in x-ray diffraction (XRD) and TEM confirmed the platelet spacing observed in XRD. Non-maleated nanocomposites showed 10% increase in ultimate tensile strength and 16% increase in Young's modulus. Barrier properties were difficult to measure for oxygen and water vapor because of the quality of the films. A different instrument using helium gas did show improvement with the nanocomposite compared to the PETG pure film. A slight decrease in degradation temperature of the nanocomposites was observed. Addition of MLS showed a decrease in Tg of the PETG. MA served as an effective compatibilizer but the un-reacted MA contributed to decreased thermal stability due to reactivity with the hydrogenated tallow of the MLS.

An intercalated PET/MLS film has been produced through film extrusion processing. XRD analysis and TEM microscopy has shown that the d-spacing of the MLS platelets has increased as a result of melt processing, but layered-structures are still present in the samples. The PET/MLS systems with and without the MA-coupling agent demonstrated an increased Young's modulus along with a substantial loss in film toughness and strain. Maleated PET/MLS systems do not show any improvement in mechanical properties over the non-maleated PET/MLS films. There were no significant improvements in oxygen and water vapor barrier data for the nanocomposite compared to the neat PET. Maleated and non-maleated PET/MLS films show an increased degree of crystallization and crystallization rate over the neat PET films. It is believed that both the MA and MLS act as nucleating agents for crystallization to occur

upon cooling of the nanocomposites from the melt state. No substantial differences were found between the maleated and non-maleated systems in relation to crystallization properties. The MLS also appears to plasticize the PET, as the Tg of the PET/MLS systems is lower than the neat PET film. This effect is not observed in the maleated PET sample; therefore this was concluded to be directly related to the MLS additive.

Overall in this SERDP study, the nanocomposite structures and formulations have been optimized. Films at the laboratory and pilot scale level have been produced and the properties are compared to the existing MRE components and military specifications. A LDPE nanocomposite and a multi-layered nylon/EVOH nanocomposite are targeted for the meal bag and food pouch respectively. This research is now being transitioned to a 6.3 Solid Waste Reduction Program, Nanocomposites for Optimized Packaging System (NANOPS) until FY10 where this remains focused on the improvement of military ration with dual use for the commercial sector.

2. Objective

The technical objective is to research and develop a cost effective, environmentally friendly technology that will reduce the amount of solid waste associated with current and future military rations and packaging. Nanocomposite packaging will be demonstrated to reduce DoD specific waste problems by the development of environmentally friendly packaging while meeting the combat ration operational requirements. This research involves processing and characterizing nanocomposite systems and determining the mechanical, thermal, barrier and biodegradation properties of these systems. The results will be compared to MRE specifications and the existing MRE packaging. The polymers used to prepare nanocomposites were: ethylene co-vinyl alcohol (EVOH), low-density polyethylene (LDPE), polyamides (nylons), polylactic acid (PLA), and polyethylene terephthalate (PET).

3. Background

The development of environmentally friendly food packaging is an interest for the military to significantly reduce the amount of solid waste. Nanotechnology is being applied to military food packaging research since it has shown large improvements in barrier properties (resistance to water vapor/oxygen transmission), as well as in physical properties such as tensile strength, Young's modulus, and heat distortion temperature.[1-3] Applied to food packaging materials, nanotechnology can be used to meet the shelf life and survivability required for existing combat ration packaging systems, thereby eliminating the necessity of the currently used aluminum foil laminates, while dramatically improving disposal and recycling.

The current outer Meal Bag that holds all the individual components is now made from a thermoplastic polyolefin, but is extremely thick to resist burrowing insects. Figure 1. depicts the MRE Meal Bag, the components, and plastic waste from the MRE.

a) b) c)

Figure 1. MRE Meal Bag and Components a.) sealed MRE b.) opened MRE and c) plastic waste of 1 MRE.

The current MRE packaging for the MRE entree consists of a retortable four-layer pouch using aluminum foil as the barrier along with polyethylene, nylon and polyester. Other food items, such as crackers, are packaged in three-layer foil pouches. Figure 2. illustrates the current MRE structures and materials. This system can only be land filled due to the aluminum foil. The goal of the research is to remove this aluminum foil barrier layer and replace the pouch with nanocomposite materials. Figure 3 shows the potential nanocomposite multilayered structure that may replace the current structure. Overall, the amount of trash generated from MREs will be reduced because the packaging will be thinner and lighter as well as being recyclable and/or biodegradable.

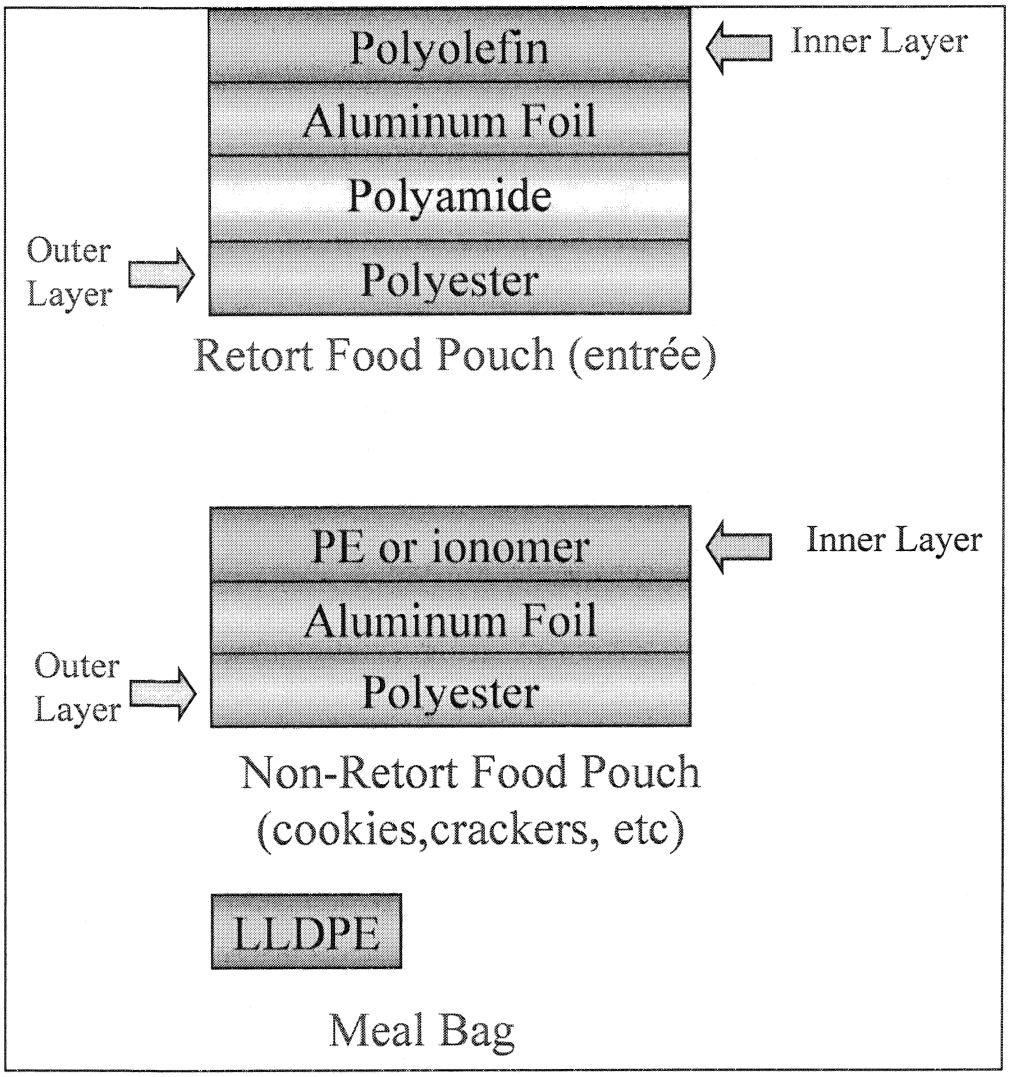

Figure 2. Current MRE structures and materials.

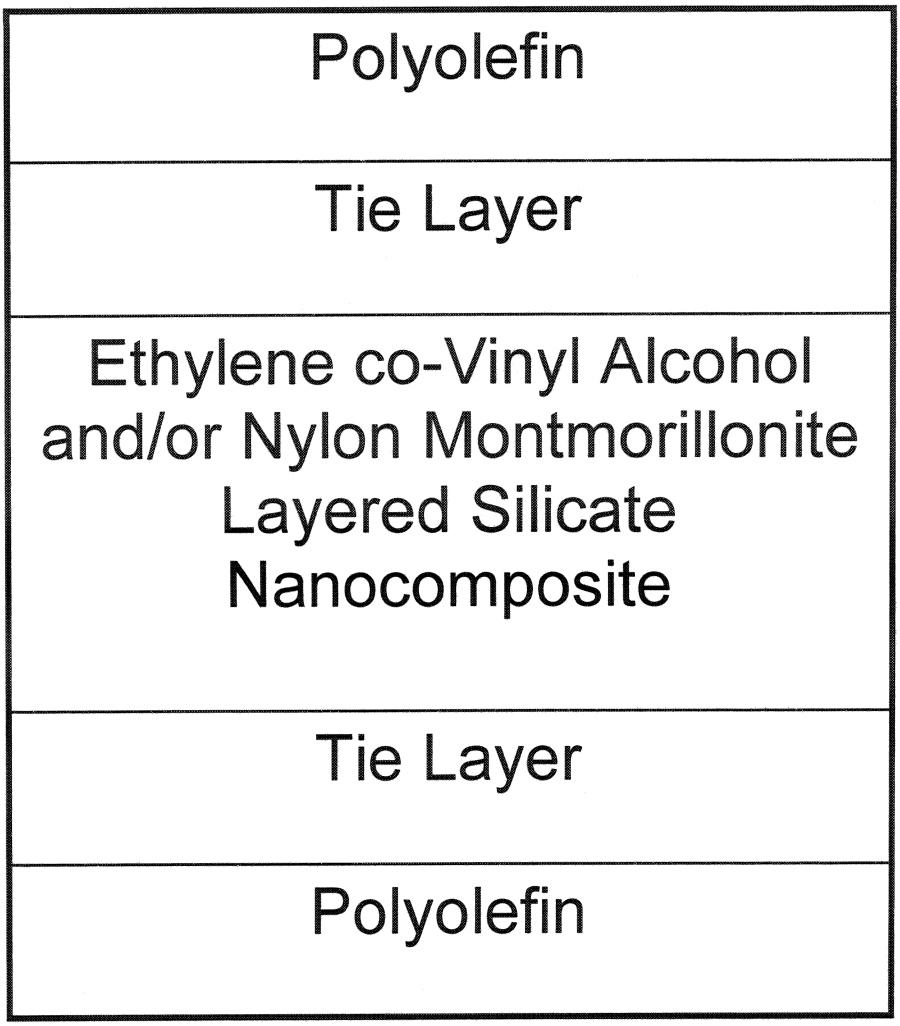

Figure 3. Potential nanocomposite structure for the MRE.

The existing military specification for barrier properties for the retortable pouch is: oxygen transmission rate: 0.06 cc/m²/day and water vapor transmission rate of 0.01 g/m²/day with a shelf life of 3 years at 27°C (80°F) or 6 months at 38°C (100°F). With such stringent shelf life requirements, an exceptional barrier material is necessary for this application. The packaging also needs to be robust enough to withstand airdrop and rough handling associated with the military logistics system. MREs also suffer from flex cracking or pinholing in the foil-based laminates especially when exposed to the cold weather. With nanocomposites, not only are the barrier properties improved, but the mechanical and thermal properties improve as well.

The use of polymers containing nanoclays, in particular MLS, is targeted to be a recyclable and/or biodegradable system to replace the current MRE packaging components that contain metallic foil and to down gauge components that use excessive material. Although foil-based laminated films are capable of providing the necessary barrier properties, they have inherent problems such as flex cracking and pinholing. These problems are exacerbated during in-plant handling, and when exposed to cold temperatures within the military logistics system. This cracking and pinholing can lead to vastly shortened shelf life for military rations and could result in considerable discards as well as increasing disposal costs for a mixed plastic/metal waste stream. A need exists for a polymer/nanoparticle system that can correct these deficiencies, while still meeting the operational requirement of 3 years at ambient temperatures.

For nanotechnolgy to be successful in improving properties there must be compatibility of the polymer/MLS as well as dispersion of the MLS within the polymer matrix. The MLS typically used in this study was organically modified montmorillonite, a mica-type silicate, which consists of sheets arranged in a layered structure. MLS is used due to its high cation exchange capacity and its high surface area, approximately 750 m^2/g and large aspect ratio (larger than 50) with a platelet thickness of 10Å (angstroms). [4]

The large aspect ratio of the silicate layers has several benefits for food packaging applications. The interface between the tremendous surface area of the MLS and the polymer matrix minimizes chain mobility, creating a reinforcement effect. In addition, this interface facilitates stress transfer to the reinforcement phase, thus improving physical properties such as tensile strength and tensile modulus. Because the MLS contain so many individual particles in a relatively small amount of material, it takes low levels of loading (1-5%) to obtain a high concentration of constrained areas within the polymer.

Melt processing has proven to be one of the more attractive and preferred methods in producing nanocomposites for commercial use. Significant interest is being paid to the development of proper processing techniques and process optimization for the extrusion of nanocomposite films. [5,6] Optimization of nanocomposite morphology relies heavily on polymer/nanoparticle chemistry, along with processing parameters, which has been shown to enhance these interactions.[3]

The emphasis of the project was to optimize the nanocomposite formulations with compatible polymers and nanoparticles. Nanocomposites and control films were produced via melt compounding and the blown film extrusion process. The films were characterized for polymer/nanoparticle interaction as well as mechanical, thermal, barrier and biodegradation properties. The processing parameters in the extrusion process were varied (temperature, residence time, screw speed and screw configuration) to see if this influenced the polymer/nanoparticle interactions.

Several polymers were chosen for this study due to their performance and properties as a homopolymer. (i.e. barrier properties to oxygen and moisture, mechanical properties, ease of melt processing, price, food and drug administration approval, recyclability and biodegradability)

Low- density polyethylene (LDPE), a polymer in the polyolefin family, was studied with MLS for the Meal Bag. Polyolefin nanocomposites with compatibilizers have been widely studied in the literature and prepared by a variety of preparation methods.[7-14] Achieving exfoliation and significantly improving the properties of a polyethylene with nanoparticles is a challenge because of the non-polarity of the structure. In this study, blown films of the nanocomposites are produced at the laboratory and pilot scale level to determine if the same properties could be achieved after scale up. Morphological, barrier, thermal and mechanical properties of the films are evaluated and compared for the different trials. These LDPE nanocomposites are targeted to make a thinner Meal Bag, which is currently made from polyethylene. Also, these nanocomposites can be used as an outer layer for the EVOH nanocomposite to protect it from moisture.

Polylactic acid (PLA) was another polymer investigated as a potential nanocomposite for a biodegradable Meal Bag. PLA has proven to be of interest over the recent years in both the scientific and industrial realms with its decrease in price and increased production.[15] It has demonstrated impressive physical properties, processability on common plastics processing equipment, and biodegradability in industrial and municipal compost. Most importantly, it is derived from plant starch in corn, which makes PLA a completely renewable resource. Within the last few years, Natureworks™ has become the only United States supplier of the material and has transformed it to the only commercially viable, natural-based polymer on the market. [16,17] Prior to the beginning of this research, there were no reported studies on PLA/ MLS nanocomposites in blown-film technology. Authors such as Pluta and Ray, report nanocomposite formation and characterization using compression molding and simple melt extrusion.[18,19] In these reports, intercalation of the nanocomposites was observed and remarkable property enhancements were indicated. Also, noted is the increase in the rate of PLA biodegradability when the modified montmorillonite MLS was added. [27,28] It is believed that the addition of the MLS platelets increases the surface area of the sample, thereby providing more area for the organisms that degrade the polymer to attack. Increasing the rate of biodegradability would be extremely important and useful. Biodegradation is dependent on crystallinity and surface area. Since the nanoparticles have such huge surface area, this is expected to help the biodegradation of the polymer. The microorganism can easily attack the polymer, especially in an exfoliated nanocomposite system. However, the nanoparticles can often enhance crystallinity in the polymer and this will hinder biodegradation

The polymer investigated for the food pouches was EVOH. It was chosen based on its excellent oxygen barrier properties, and can be targeted for a military retort or non-retort food pouch. Also, the work from an environmental Quality 6.1 Programs (FY01-FY03) showed a compatible EVOH /nanoparticle formulation that led to significantly improved oxygen barrier properties. Nanocomposites with these enhanced barrier properties would be ideal for high barrier packaging applications.

EVOH is a random copolymer of polyvinyl alcohol (PVOH) and polyethylene; therefore, it is less hydrophilic than PVOH. Its properties depend on the ethylene vinyl alcohol composition ratio. EVOH with an ethylene content of 44% exhibits good mechanical properties (Young's modulus = 2062 MPa; tensile strength = 58.87 MPa; elongation = 280%) and excellent oxygen barrier properties (oxygen transmission rate = 31.00 $cm^3 \cdot mil/(m^2 \cdot d)$). [20.21] This EVOH

was chosen for this study; however, all EVOH grades are sensitive to moisture which can render it unsuitable for certain applications. Consequently, nanocomposites of EVOH can be sandwiched between polyolefins to enhance barrier properties and extend shelf life.

Nanocomposites based on polyamide (nylon) materials were also investigated as a potential high barrier film for the MRE. The polyamide nanocomposites became popular when Toyota researchers began a detailed examination of polymer layered silicate mineral nanocomposites [22] Since then, there have been numerous studies focused on nylon-based nanocomposites and their formation. Fornes et al. [23] discusses how the temperatures associated with melt processing of nylon 6 nanocomposites as well as the chemical structure of the surfactant in the MLS affects the extent of polymer degradation during processing. Ranade et al. [24] discuss how the MLS particles took an active role in the nucleation of nylon 6 films processed through twin-screw extrusion. These nanocomposites exhibited an increase in modulus, ultimate tensile strength, and yield strength as the concentration of MLS increased.

Numerous papers have focused on nylon nanocomposite films with improved barrier properties to oxygen, water vapor, and other gases. [25-27] Due to the hydroscopic properties of nylon materials, nylons are typically coated or co-extruded along with other polymers in order to maintain barrier performance at various RH conditions. A patent written by Mueller et al.[28] describes such a structure in which nylon and nylon nanocomposite barrier layers are co-extruded along with ethylene vinyl acetate and MA grafted polyesters. The resultant film is a high-barrier thermoplastic material suitable for packaging meats and cheese, cereal, crackers, and over-the-counter drugs.

This polyamide work focused on the melt processing and resulting barrier properties of various types of monolayer nylon films. From these base materials and their oxygen barrier properties, one was selected for use in a nylon nanocomposite structure. The barrier and mechanical properties of these nanocomposites were closely examined in relation to the neat films. Finally, neat and nanocomposite materials were co-extruded along with polyethylene and tie layers in order to develop high-barrier multilayer structures for the MRE that perform in higher RH environments.

Another candidate for the MRE packaging is a PET/MLS nanocomposite. PET is a desirable polymer for packaging waste reduction since it is a recyclable polymer that is used extensively in packaging, in particular for the boil-in-bag, heat-and-serve, and beverage bottles. There have been several commercial attempts to incorporate PET nanocomposites into beverage bottles. [29] However, PET is not easily processed with crystallinity being a contributing factor; therefore, having a well-dispersed and exfoliated PET nanocomposite can be a challenge to obtain. PET does have attractive barrier properties and the idea was to obtain a PET nanocomposite monolayer that would meet the Army's requirements.

Films were produced via extrusion compounding and blown film and cast film processes. The films were characterized for polymer/nanoparticle interaction (x-ray and TEM) as well as mechanical, thermal, and barrier properties. The processing parameters in the extrusion process were varied (temperature, residence time, screw speed and screw configuration) to try to maximize the polymer/MLS interactions.

The approach here is to develop a high barrier system of PETG via the MLS based nanotechnology. Prior research has indicated the significant impact of the crystalline regions on the properties of the resultant nanocomposite.[29,30] The influence of increased matrix polarity on dispersion of the PETG by incorporating MA onto the PETG backbone was studied. The influence of the MLS concentration and maleation are separately investigated.

PETG, described generally as polyethylene 1,4 cyclohexylenedimethylene terephthalate, is an amorphous thermoplastic of the PET family. PETG has excellent clarity, good impact and tear strength at low temperatures, and excellent resistance to stress and bend whitening. PETG has excellent gas barrier properties, which makes it an outstanding choice for storing biologicals. [29,30]

A second system that has been examined is the semi-crystalline PET/MLS nanocomposite. Through compression molding methods, Ke et al.[31] prepared PET/MLS nanocomposites that exhibited a 40°C increase in heat deflection temperature (HDT) and a 250% enhancement of Young's modulus. The MLS played a strong nucleating-role in the polymer and had strong interactions with the PET polymer chains. Ou et al.[32] also observed similar results in PET/MLS nanocomposites prepared through solution mixing techniques. The PET exhibited heterogeneous nucleation and an increased crystallization rate in the presence of MLS. Sanchez-Solis et al.[33] made PET/MLS bottles through the injection-stretch blow-molding process. Thermal, mechanical, and rheological properties of PET were all affected by the addition of 2% MLS into the blow-molded bottles. A mixed intercalated/exfoliated structure was present in all blow-molded samples.

This study concentrated on the production of PET/MLS films, with and without MA coupling agent, through twin-screw extrusion. It is our hope that we will produce highly intercalated/exfoliated nanocomposite films that demonstrate improved physical, thermal, and barrier properties over the neat PET film.

4. Materials and Methods

4.1 Materials

4.1.1 LDPE Nanocomposite Study

Low Density Polyethylene 683 I was supplied by Dow Chemical Company. The MLS was supplied by Southern Clay Products, under the trademark Cloisite 20A. The compatibilizer was Polybond (PB) 3109 supplied by Crompton Chemical.

4.1.2 PLA Nanocomposite Study

Polylactic Acid (PLA) was supplied by NatureWorks, Minnetonka, MN. The grade was Natureworks 4041D with a molecular Weight (Mw): 180,000 g/mole. Plasticizer was supplied by Morflex, Inc. North Carolina and specifically acetyltriethyl citrate; Citroflex A-2 was used for this study with PLA. MLS supplied by Southern Clay Products, Gonzales, TX were used for the study. In particular, for the PLA study, alkyl quaternary ammonium montmorillonite, Cloisite® 25A, as well as alkyl quaternary Ammonium MLS Cloisite® 20A was used

4.1.3 EVOH Nanocomposite Study

Commercially available EVOH (EVAL® E-105) was used as the matrix polymer. E-105 has an ethylene copolymer ratio of 44 mol%. Southern Clay's organically modified MLS, Cloisite 25A, was compounded with EVOH. Cloisite 25A is modified with a quaternary ammonium salt.

4.1.4 Nylon Nanocomposite Study

The un-filled nylon materials used as controls for the nanocomposite films were Novamid 1020 (Nylon 6-Mitsubishi Plastics), Zytel 42A (Nylon 6,6-Dupont), and Capron (Nylon 6-Honeywell). Pre-compounded polyamide nanocomposite resins used to produce extruded films were Aegis NC73ZP Aegis NC73ZP is a commercially available, high-barrier nylon nanocomposite material based on Capron nylon 6) and Imperm 105 (Nanocomposite Nylon MXD6-Mitsubishi/Nanocor. Un-filled nylon MXD6, also provided by Nanocor, was used as a control for the MXD6 nanocomposite. For clarification purposes, listed in Table 1 are the nylon materials used along with the nanocomposites that are based on them. During multi-layer co-extrusion, ethylene bis-stearamide (EBS) was used at a concentration of 200 ppm as a slipping agent for the proper pellet feeding of the MXD6 resins into our extrusion system. LDPE (683I-Dow) was used as the outer layer in the multi-layer films to provide water vapor barrier, while Modic-AP (Maleic Anhydride Grafted Polyolefin-Mitsubishi Chemical Corp) was used as the tie layer ensure proper adhesion between the LDPE and polyamide layers.

Table 1. List of Materials for Nylon Nanocomposites

Base Nylon Material	Nanocomposite Using Base Nylon
Capron	Aegis NC73ZP
Novamid	N/A
Zytel 42A	N/A
Nylon MXD6	Imperm 105

4.1.5 PETG Nanocomposite Study

An extrusion grade of amorphous co-polyester resin (Eastar 6763) was supplied in pellet form by Eastman Chemical Company, Tennesee. Montmorillonite layered silicate (MLS Cloisite® 20A) was supplied by Southern Clay Products. A 99% pure grade of MA from Research Chemicals Ltd. was used as a compatibilizer for the polymer and MLS. Its purpose was to assist in developing a copolymer in which a more hydrophobic end (PETG) is tied to a more hydrophilic end (MA).

4.1.6 PET Nanocomposite Study

The polymer used in this study was a semi-crystalline, extrusion grade of PET (KOSA 1101) supplied by KOSA. Organically modified MLS (Cloisite® 30B) provided by Southern Clay Products was used to process a series of PET/MLS nanocomposites. MLS percentages in the nanocomposites varied from 2 to 5% by weight. One half percent by weight MA, supplied by Avocado Research Chemicals, was incorporated into the nanocomposites as a polymer-MLS coupling agent.

4.2 Processing

4.2.1 LDPE Nanocomposite Study

4.2.1.1 Laboratory Scale

Compounding

The MLS at 7.5% loading was compounded with LDPE using a Zenix ZPT-30 30 mm co-rotating twin-screw extruder using a standard mid shear configuration for additive blending. Temperature was varied across the nine zones from 165°C in the feed section to 215°C at the die. Extruded strands were pelletized for secondary processing.

Film Processing

Blown films were prepared with a Haake® Polylab twin-screw extruder, 24:1 L/D. The screws were conical, counter–rotating and intermeshing with a diameter of 31.8 mm and a length of 300 mm. The die has an interior diameter of 24 mm and outer diameter of 25 mm with an adjustable ring gap. Screw speeds ranged from 40-200 rpm and processing temperatures varied from 215 to 235°C.

4.2.1.2 Pilot Scale

Compounding

Foster Corporation processed 300 lbs of the same LDPE nanocomposite formulation that was used with the laboratory scale trial with a 30 mm twin-screw extruder at temperatures varying from 160 to 215C, and a screw speed of 300 rpm. Melt temperature was measured at 234°C.

Film Processing

Alcan Packaging conducted a trial production run of LDPE nanocomposite blown film. The LDPE nanocomposite pellets that were compounded at Foster were shipped to Alcan's Neenah Technical Center in Neenah, WI. Several hundred linear feet of pure LDPE film and LDPE nanocomposite film were successfully processed on a 5-layer blown film pilot plant co-extrusion line. Films were fabricated at 2 mil and 6 mil thicknesses.

4.2.2 PLA Nanocomposite Study

Compounding

Before blown-film processing could be accomplished, the PLA and MLS had to be compounded into pellets. Compounding was done on a Thermoprism Twin-Screw Extruder with the attached strand die, cooling bath, and pelletizer. The pure PLA pellets were initially dried for 4 hours @ 80°C and then cooled to room temperature for an additional hour. Once cooled, the dried PLA resin was compounded by a normal shear screw with MLS 25A by way of a

secondary volumetric feeder located downstream of the extruder. The nanocomposite strands were pulled through a water bath at 20°C and cut into pellets by the Thermoprism pelletizer. The pure PLA pellets were also pelletized in the same fashion so that the control would have the same number of thermal histories as the nanocomposite pellets. Processing took place at 200 to 225°C and 80 rpm.

Blown Film Processing

To prepare for blown film processing, the compounded PLA/MLS resin and the pelletized PLA resin were dried for 4 hours @ 80°C to remove moisture absorbed during the pelletizing process. Again, the resin was allowed to cool to room temperature for 1 hour. The dried resin was mechanically mixed for 20 minutes with 10% Morflex A-2 Plasticizer. The polymer and plasticizer mixture was allowed to sit at room temperature for 2 hours in an airtight bag to absorb any remaining plasticizer.

The polymer pellets with plasticizer were loaded into the extruder hopper and fed by way of the primary volumetric feeder. The average thickness of the blown film samples was 0.003 inches. Various sets of processing conditions were run to produce blown films of neat PLA and the nanocomposite respectively. Processing temperatures ranged from 150 to 165°C at 80, 110 and 130 rpm. Specifications for the processing equipment are as follows: Screw Diameter: 16mm, L/D Ratio: 24:1, Dies: Spiral Blown-Film, Single Strand, Diameter: 25.4mm, Forming Apparatus: Water Trough, Blown-Film Tower, Air Knife pelletizer

4.2.3 EVOH Nanocomposite Study

Compounding

Compounding was performed at Triton Systems, Inc. using a Zenix ZPT-30 30mm co-rotating twin-screw extruder with a standard mid-shear configuration. The temperature profile of the nine zones increased from 170°C at the feed zone to 205°C at the die. E-105 was compounded with 3% 25A, at a screw speed of 300 rpm. Extruded strands were pelletized for secondary processing. MLS concentrations varied from 3 to 6%.

Film Processing

Blown and cast film samples were melt processed on a ThermoPrism co-rotating; completely intermeshing, twin-screw extruder with a 16 mm bore size and a L/D ratio of 24:1. The temperature profile increased from 195°C at the feed section to 200°C at the die, at a screw speed of 50 and 90rpm.

Multi-layer films were processed using a Collin Teach Line multi-layer extrusion system. This system uses 3 different single-screw extruders to process multi-layer films by way of a feedblock. By controlling the speed of each extruder along with the speed of the forming rolls, the individual layer thicknesses can be altered to produce films with varying layer thickness.

4.2.4 Polyamide (Nylon) Nanocomposite Study

4.2.4.1 Monolayer Processing

Extrusion of the control nylon materials was performed on a ThermoPrism TSE-16 twin-screw extruder with 16 mm co-rotating, completely intermeshing screws. The screw configuration of the system was set to yield a low to medium shear environment during extrusion. The nylon resins were pre-dried in a Dri-Air X-10B dessicant dryer for 8 hours at 80°C. Films were formed through a 15 cm adjustable-thickness cast film die onto chill rolls set

at 20°C. The Aegis monolayer nanocomposite film was processed in this same way as a direct comparison to the neat control. Listed in Table 2 are the extrusion processing conditions for all of the monolayer film trials.

Table 2. Extrusion Processing Conditions for Nylon Nanocomposites

Nylon Barrier Layer Material	Extruder Temp. (°C) (Nylon Layer)	Die Temp. (°C)	Screw Speed (rpm)
Capron Nylon 6	280-295	275	65
Aegis Nano Nylon 6	280-295	275	65
MXD6 Nylon	270-275	275	60
Imperm MXD6 Nano Nylon	270-275	275	60

4.2.4.2 Multilayer Processing

Multilayer extrusion processing was performed on a Collin GmbH Teach Line multi-layer extrusion system. Three 20 mm single-screw extruders were used in the system along with a feed block and 10cm adjustable thickness film die. The extrusion screws had a L/D ratio of 25:1 and a compression ratio of 3:1. This configuration allows for the processing of 5-layer films consisting of 3 different polymers. Table 3 lists the multilayer extrusion processing conditions for the multilayer film trials. Figure 4 illustrates the structure of the multi-layer films processed using this method.

Table 3. Multilayer Extrusion Processing Conditions

Sample	Extruder Temp. (°C)	Screw Speed (rpm)	T_{Die} (°C)
Novamid 1020 Nylon 6	270-290	65	265
Zytel 42A Nylon 66	285-300	70	265
Capron Nylon 6	230-270	70	250
Aegis NC73ZP Nylon 6 Nanocomposite	230-255	65	240

LDPE
MODIC-AP
NYLON BARRIER LAYER
MODIC-AP
LDPE

Figure 4. Structure of the multilayer film

4.2.5 PETG Nanocomposite Study

Compounding

PETG pellets were dried overnight in a vacuum oven at 80°C to remove any moisture from the polymer. The MLS and polymer were compounded on a ThermoPrism twin-screw extruder (TSE-16) with co-rotating, completely intermeshing, 16mm screws at a L/D ratio of 24:1. Individual compositions of (1, 2, 3 and 5%) were prepared by mixing appropriate amount of master batch with neat PETG. PETG/MA master batch of pellets was prepared under the same processing conditions. Pure MA was mixed with PETG pellets in a twin-screw extruder. Individual MLS concentrated nanocomposites (1, 2, 3 and 5% by weight) were prepared from PETG-MA master batch.

Preparation of Nanocomposite Film

All PETG/MLS nanocomposite pellets were dried overnight in a vacuum oven at 80°C to remove moisture from the polymer. PETG nanocomposite films of 0.010 inches (10-mil) thickness were extruded into films on a ThermoHaake Polydrive Single Screw Extruder equipped with a slit die. Chilled rolls set at a temperature of 17.5°C were used to form the films.

4.2.6 PET Nanocomposite Study

Compounding

Once the proper PET/MLS system was determined, it was possible to compound the PET/MLS nanocomposites. KOSA PET was dried overnight at 65°C in a vacuum oven and fed into the feeding zone of a ThermoPrism TSE-16 co-rotating, twin-screw extruder (16mm-bore, 24:1 L/D) using a volumetric feeder. A PET/MLS nanocomposite master batch was pelletized at a concentration of 10% MLS by hand feeding the MLS into the second zone of the extruder. Nanocomposite pellets with MLS percentages of 2,3, and 5% 30B, by weight, were processed using the master batch and a measured amount of pure PET. 0.5% by weight MAwas added during this final extrusion to compatibilize the polymer and MLS. Control samples were also processed in this way without MA. Extruder temperatures ranged from 270°C in the feed zone, to 290°C in the die. The screw speed of the extruder was 65 rpm. The PET strand was pulled through a water bath and pelletized using a Thermoprism mechanical pelletizer.

Film Processing

The compounded PET/MLS pellets, with and without MA, were extruded into films by way of a ThermoHaake Polydrive Single Screw Extruder. A PET melt-temperature of 250°C

provided the proper melt viscosity for quality film extrusion. Chill rolls set at a temperature of 17.5°C were used to form the film. PET was processed with the following temperatures in zones 1-9 respectively, 200, 210, 220, 230, 230, 240, 240, 240, and 235°C with a screw speed of 225 rpm. The MLS 30B Cloisite varied in concentration from 1.5% to 4.5%.

4.3. Characterization

4.3.1 Transmission Electron Microscopy

The morphology of the nanocomposites was determined by TEM. Samples were prepared in a mixture of epoxy and hardener to enable slicing of the samples in the ultra-microtome, using a diamond knife. The microtomed samples were then observed in Philips EM400 Transmission Electron Microscope at 120kV at various magnifications. Also, for the PET study, TEM was conducted on a JEOL JEM-100CX II electron microscope.

4.3.2 X-ray Diffraction (XRD)

XRD experiments were carried out on a Siemens D500 x-ray diffractometer. The experiments were carried out at room temperature with a scanning speed of 1°/min and the step size of 0.02°. Experiments were carried out on a powdered sample of MLS nanocomposites. The basal spacing or the d spacing was calculated by using Bragg's equation.

4.3.3 Gel Permeation Chromatography (GPC)

GPC was used to analyze the molecular weight of the PLA after each processing step to determine the degree (if any) of degradation occurring during processing. To prepare samples for GPC analysis, 0.1% solutions were prepared by dissolving 4.0mg of each film sample in 4.0ml of tetrahydrofuran (THF) solvent. The pelletized PLA and PLA/MLS pellets were also included to observe the effect of pelletization on their molecular weight. After the samples were completely dissolved, the solutions were filtered through a Wattman 0.45 μm glass micro fiber filter. The injections of solution into the column were done at an injection volume of 10.0μL over a period of 40 minutes. Two injections were done for each sample, and the average values of Mn, Mw, and PDI were reported based on polystyrene standards.

4.3.4 Mechanical Properties

Tensile properties were evaluated with a 4200 series Instron® in accordance with ASTM D882. The load cell was 50 lb and cross head speed was 2.0 mm/min. Rectangular or dog bone shape samples, with a gauge length of 2 inches, were used. Each result was based on the average of 10 replicates. Measurements were made in both the machine and radial directions at room temperature and ambient conditions. Tensile Properties that were determined include tensile strength at yield, toughness, Young's modulus, and percent strain. An MTS 810 hydraulic system was used for tensile testing of PETG nanocomposite films. ASTM standard (D882-95a) was used to measure tensile properties of thin PETG films.

4.3.5 Barrier Properties

4.3.5.1 Water Vapor and Oxygen Barrier Testing

Water vapor barrier testing and oxygen barrier testing were carried out according to ASTM F1249 and D3985, respectively. Water vapor transmission rate (WVTR) was measured

on the MOCON Perma-Tran 3/33, while the oxygen transmission rate (OTR) was measured on the MOCON Ox-Tran 2/20. The test samples were measured and either cut into50 cm^2 pieces or masked down to 5 cm^2, for appropriate fit into the testing area. The thickness of each sample was measured and incorporated into the test to determine normalized values for the permeation constant. WVTR was tested at 37.8 °C and 90% RH, while OTR was tested at 23 °C and 0-90% RH.

4.3.5.2 Helium Permeability

Helium permeability experiments were performed on an instrument built at the University of North Texas. The principle of the instrument is based on measuring the rate of diffusion of a penetrant gas molecule in a closed high seal system. All the experiments were carried out on 10-mil thick PETG films. Helium was used as an experimental gas.

4.3.6 Thermogravimetric Analysis (TGA)

A TA Instruments TGA was used to analyze the decomposition temperature of films, compounded pellets, and plasticizer, as well as to determine the exact amount of MLS in the sample. The percent weight loss was recorded as a function of temperature at a heating rate of 20°C/min. Nitrogen was used as the testing environment to eliminate any weight fluctuations caused by oxidation of the samples in the testing furnace. Residue values (MLS remaining) were taken at 800°C to ensure that all moisture and organics had been eliminated from the sample pan.

4.3.7 Differential Scanning Calorimetry (DSC)

A DSC (either TA Instruments or Perkin Elmer) was used for the determination of both the Tg and the Tm of the polymers and nanocomposites. The Tg values of the films were taken as the half Cp extrapolation of the step-transition commonly associated with the glass transition temperature. Onset temperatures were also recorded for this transition. The Tm peak of each DSC curve was analyzed for the peak Tm and also for ΔH of the melt. It is the ΔH value that describes the amount of crystals in the polymer film as well as the amount of energy it takes to melt these crystals. A heating rate of 20°C/min was employed for all samples tested.

4.3.8 Biodegradation Testing Using a Soil Respirometry Test

The ultimate biodegradability (i.e. mineralization) of the PLA/MLS nanocomposites was assessed using standard laboratory scale reactors to simulate a bioactive soil burial site. All film samples were cryogenically milled into powder for the testing. Prior to testing, appropriate sub-samples of each material were dried to a constant weight in a convection oven (50°C for 12–18 h) and cooled to room temperature in a desiccator.

Polymer mineralization studies were conducted using a static soil biometer system incorporating elements of both the soil biometer system of Bartha & Pramer and ASTM standard D 5988. The soil used was a standard soil mix composed of a 1:1:0.1 (w:w:w) mix of potting soil, sand, and composted manure (water holding capacity = 46.4 g H_2O per 100 g soil; pH 7.0; C:N ratio = 17:1). Test samples yielding a substrate loading of 5.0 mg C g^{-1} soil were mixed with the soil; buried in test reactors (1-L mason jars fitted with Plexiglas compression lids and a Swagelok gas sampling port) containing 75 g of soil at a water content of 60% water-holding capacity (WHC); and incubated in a controlled environment chamber at 22 ± 1°C in the dark. Soil

water content was maintained at 55 ± 5% WHC by periodically watering the soils with either sterile tap water or dilute (½-strength) Hoagland's solution.

Samples of the headspace gas were withdrawn from the reactors at 12 to 120 hour intervals and analyzed for CO_2 content using a Varian Model CP2003 Micro-GC equipped with a Poraplot U column and a micro-TCD (thermal conductivity detector). Each time the headspace gas was sampled, the systems were aerated by allowing the atmosphere in the bioreactors to exchange and equilibrate with atmospheric air for 5 to 10 minutes; at the same time, the soils were hand-mixed to ensure that anaerobic microenvironments did not develop. Daily and cumulative CO_2 production (total and net) was then calculated relative to a control reactor (soil without added polymer). In addition, net mineralization of a positive control (i.e., microcrystalline cellulose; Sigma Chemical Corp., St. Louis, MO) was monitored to ensure that the soil supported an actively degrading microbial population throughout the test exposure. All analyses were run in triplicate.

Biodegradation data was plotted in the form of net CO_2 production *vs.* time curves and analyzed using a combination of linear (1st order polynomial) and non-linear (3-parameter, single exponential rise to a maximum) regression techniques.

4.3.9 Insect Resistance Testing

4.3.9.1 Study I

In addition to the current 11 mil MRE Meal Bag, four prototype Meal Bags were analyzed in the insect resistance test. They included the following: the current 11 mil MRE Meal Bag, 2 mil LDPE, 6 mil LDPE, 2 mil nanocomposites of LDPE/MLS and 6 mil nanocomposites of LDPE/MLS. The samples were exposed to the saw-toothed grain beetle, the warehouse beetle, the cigarette beetle, the red flour beetle and the Indian meal moth. Packages were placed into an environmentally controlled chamber and were held at 72 ± 4° F. Thirty samples of each package type (total of 150) were used in this study. Before being placed into the chambers each package was examined for signs of existing damage and those found to have bad seals or with holes were discarded. Approximately, 500 beetles were added to the chamber along with 200 adult Indian meal moths. After 4 weeks 10 packages of each type were removed and examined for insect damage. The packages were checked for insect penetration and penetration attempts. Packages with no obvious insect penetrations were submerged in water to detect unseen penetration or leaks in the seals. After the initial examination the packages were opened and the contents checked for insect activity. The results were recorded. The remaining packages were removed and examined at 8 and 12 weeks.

4.3.9.2 Study II

This study was carried out in two parts. The initial study was to determine if stored-product insect pests would penetrate nanocomposite packaging films in the presence or absence of food odors. The second part of the study was to determine if insects would penetrate accessory packets containing standard contents or with no contents.

4.3.9.2.1 Part 1

In this study 6 films (6 mil LDPE, 6 mil LDPE/MLS, Pure LDPE 6 mil, Pure LDPE 11 mil, multilayer LDPE/NANO LDPE /LDPE 6 mil, and multilayer pure LDPE/NANO LDPE /LDPE 11 mil) were cut into 7 cm disks. The disks were attached to 0.47 L glass jars and were

held in place with a threaded ring. Each jar contained 10 larvae of the warehouse beetle, Trogoderma variable. Warehouse beetle larvae were selected for this study because they are powerful penetrators and have the ability to survive for long periods without food. The jars were inverted so that the insect had contact with the test film. The jars with the film side down were then placed over a Petri dish containing dry dog food or dishes with no food. The smooth glass of the jars prevented the larvae from climbing and ensured that they would remain in contact with the film. Six replications each of food and no food were done for each film. Films were checked weekly for 4 weeks for evidence of penetration.

4.3.9.2.2 Part 2

In this study over wrapped accessory packets were tested to determine if they were susceptible to insect penetration. Empty packets made of the same materials were used as controls. The packets were separated into 3 groups each containing 6 of each of the 7 film types. The film types were the current MRE film, pure LDPE 6 mil, pure LDPE 11 mil, nano LDPE 6 mil, nano LDPE 11 mil, blown pure LDPE and blown 6-mil nano LDPE. The packets were placed into 3 separate chambers and the test insects were added. The insects used were the Indian meal moth, Plodia interpunctella, red flour beetle, Tribolium casteneum, saw-toothed grain beetle, Oryzaephilus surinamensis and warehouse beetle, Trogoderma variable. A small amount of dry dog food was added to each chamber to sustain the insects. At 4, 8 and 12 weeks the packets in one chamber were removed and examined for insect damage. The packets were visually inspected for damage and they were further pressure tested to find less obvious damage. Pressure tests were conducted by submerging the packet in water and looking for escaping air. Packets with air leaks were further examined to determine if the escaping air was from flaws in the seals or from insect damage. Packets with leaks were opened to determine if insects were present.

4.3.10 Vibration and Drop Test

The LDPE/MLS nanocomposite blown films of 6-mil thickness were made into Meal Bags. Twenty-four Meal Bags (1 case for each film) using the 2mil and 6 mil films were filled with the contents of MRE food and then heat-sealed. They were inspected and placed in the fiberboard MRE shipping container and sealed. Two cases of MREs were used as controls. ASTM D775, Standard Test Method for Drop Test for Loaded Boxes, was performed for each case of MRE. The purpose of the test is to provide an indication of the damage that can be caused by sudden shock induced by dropping a package. This test is important for the MRE and MRE shipping containers as they can experience significant rough handling throughout the military's logistic cycle.

5. Results and Accomplishments

5.1 Meal Bag - LDPE Nanocomposite Study

5.1.1 Morphology

The nanocomposite blown films were more translucent and yellow in color than the pure LDPE films. They do appear similar in ductility. TEM and X-ray diffraction was used to determine the morphology and interaction of the polymer and MLS. TEM data is shown below. Figure 5 is a representative TEM of the LDPE/MLS nanocomposite with 7.5% MLS for the laboratory and pilot scale films. The threadlike strands in the high magnification photograph in

Figure 5a represent the MLS stacked platelets. It is difficult to determine the spacing in between the platelets as it is clearly an intercalated morphology. Figure 5b is at a lower magnification that shows the aggregates of MLS in the polymer matrix. A series of photographs have been taken for both the trials to show the degree of dispersion at the lowest magnification and the degree of intercalation at the highest magnification. Both laboratory and pilot scale films show similar dispersion and intercalation from the TEM photographs.

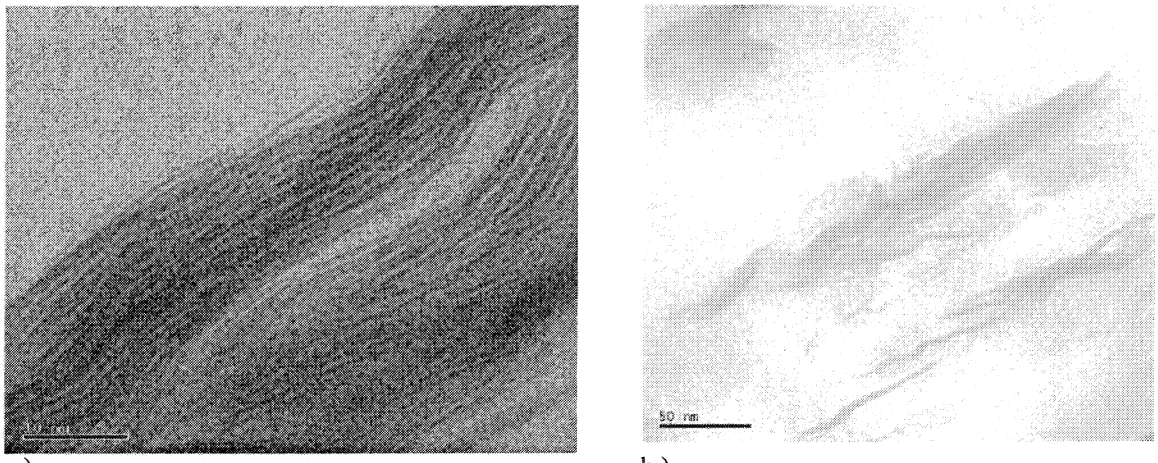

a.) b.)

Figure 5a and 5b. Typical TEM images for LDPE nanocomposite with 7.5% MLS

5.1.2 Mechanical Properties

The Young's modulus increased in the machine direction by approximately 80% for the 7.5% montmorillonite nanocomposite in both laboratory and pilot scale trials in comparison to the pure LDPE. For the laboratory scale trial the Young's modulus was plotted as a function of MLS concentration and the screw speed, as shown in Figure 6a and Figure 6b, respectively. The 7.5% MLS showed the greatest improvement in Young's modulus while the screw speed did vary significantly Young's modulus. Figure 7 showed even greater improvements in the transverse direction than seen in the machine direction of the films for the pilot scale trial. The results showed that the pure LDPE transverse direction films had about a 30% improvement in Young's modulus over the pure LDPE machine direction films. Mechanical properties such as modulus usually increase in the direction of orientation of polymer molecules. However, these films are blown films with biaxial orientation. The improvement in modulus can be seen in both machine and transverse directions for the nanocomposites, since there is orientation in both the parallel and perpendicular directions as well as random orientation of the MLS platelets throughout the matrix. For the laboratory scale trial, only machine direction samples could be analyzed due to the size of the films.

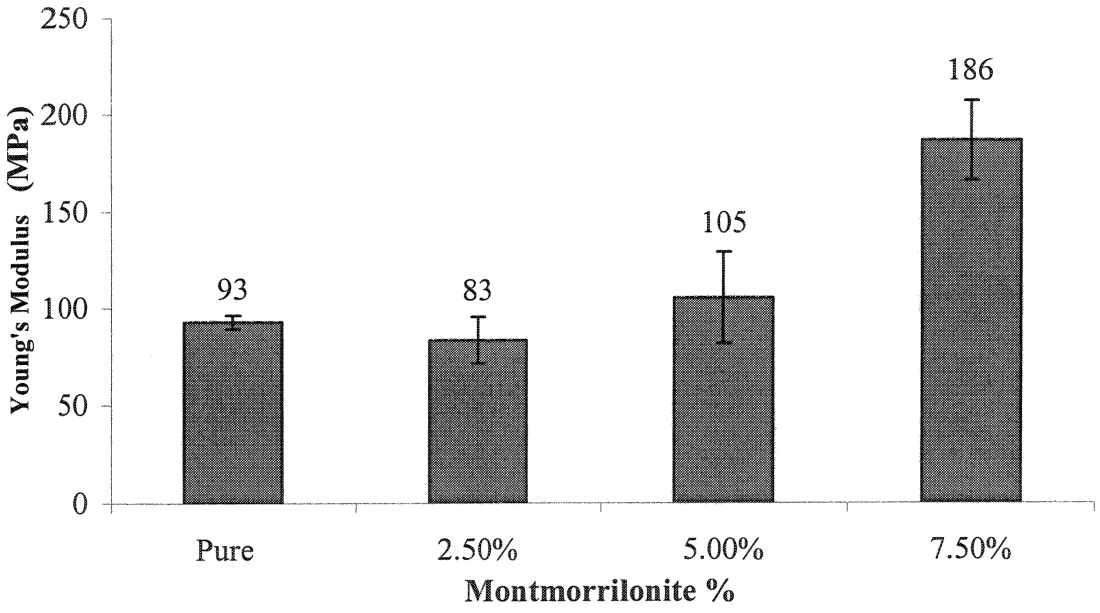

a.)

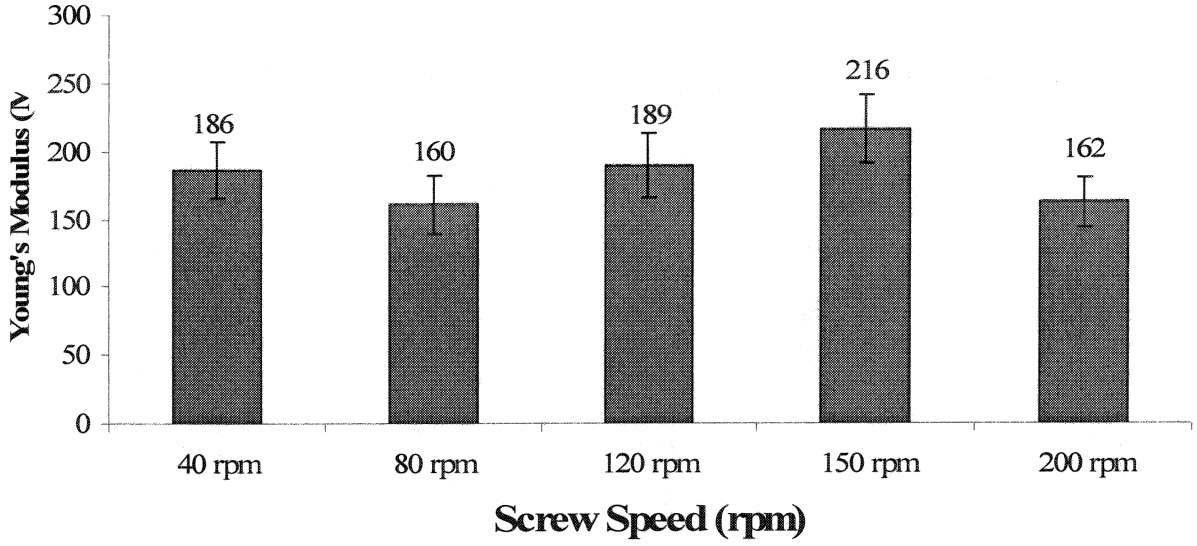

b.)

Figure 6. Young's modulus for laboratory scale trial as a function of a.) montmorillonite % and b.) screw speed

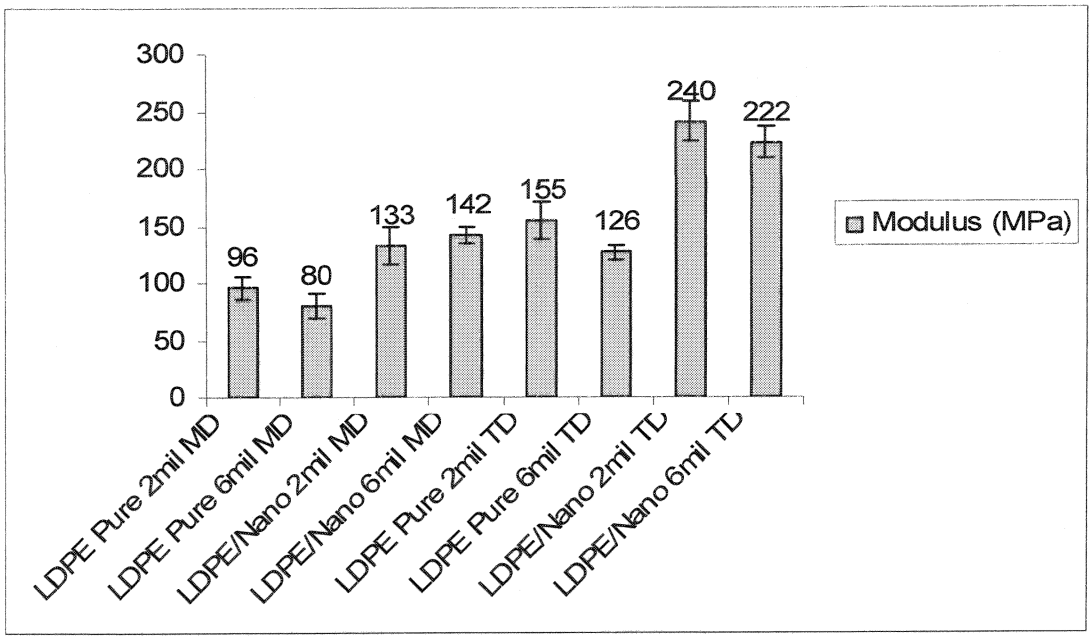

Figure 7. Young's modulus data for the pilot trial of LDPE and LDPE/MLS nanocomposite films

5.1.3 Barrier Properties

The oxygen barrier performance improved with the 7.5% nanocomposite films having almost twice the barrier of the pure LDPE films. These results are also attributed to the degree of intercalation in the LDPE nanocomposites. For both trials, water vapor barrier performance showed approximately 40% improvement for the LDPE nanocomposites films as compared to the pure LDPE films (Figure 8)

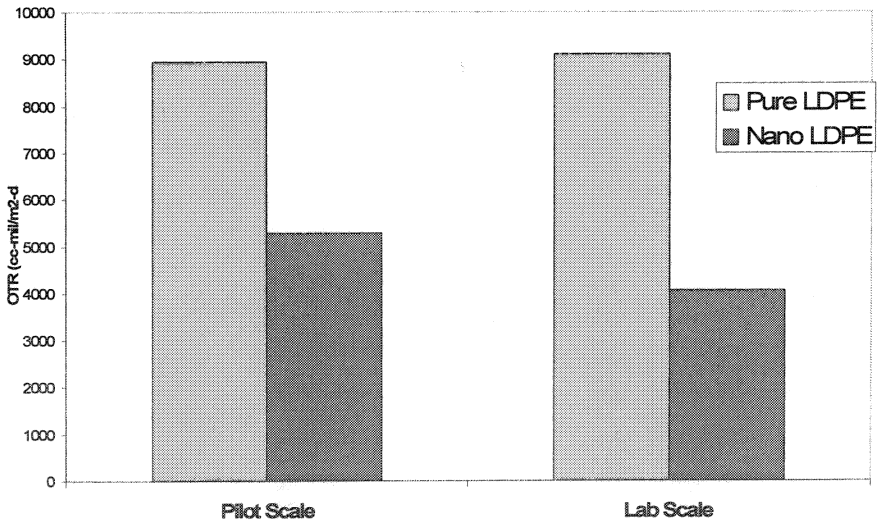

Figure 8. Oxygen Transmission Rates for LDPE Nanocomposites for pilot and laboratory scale trials

5.1.4 Thermal Properties

Thermogravimetric analysis (TGA) data of the laboratory and pilot scale trials were compared. The TGA data representing the laboratory scale samples showed an 80°C improvement in thermal stability while the pilot scale data showed a 50°C improvement. The calculated residue after heating the samples in the TGA does show that the pilot scale film samples have slightly less MLS than the laboratory scale samples, which may have influenced these results. Possible variations in the degree of dispersion and orientation of the platelets may have also influenced this difference in thermal stability. Figure 9 shows the onset of degradation temperature for the pure LDPE and LDPE nanocomposites for the pilot scale trial. Both the 2 and 6 mil thick samples have similar onset temperatures for the pure LDPE, but vary slightly for the LDPE/MLS nanocomposite.

The melting temperatures determined from DSC for the pure LDPE and the LDPE/MLS nanocomposite films were equivalent. These values remained constant from the laboratory to the pilot scale blown film trial.

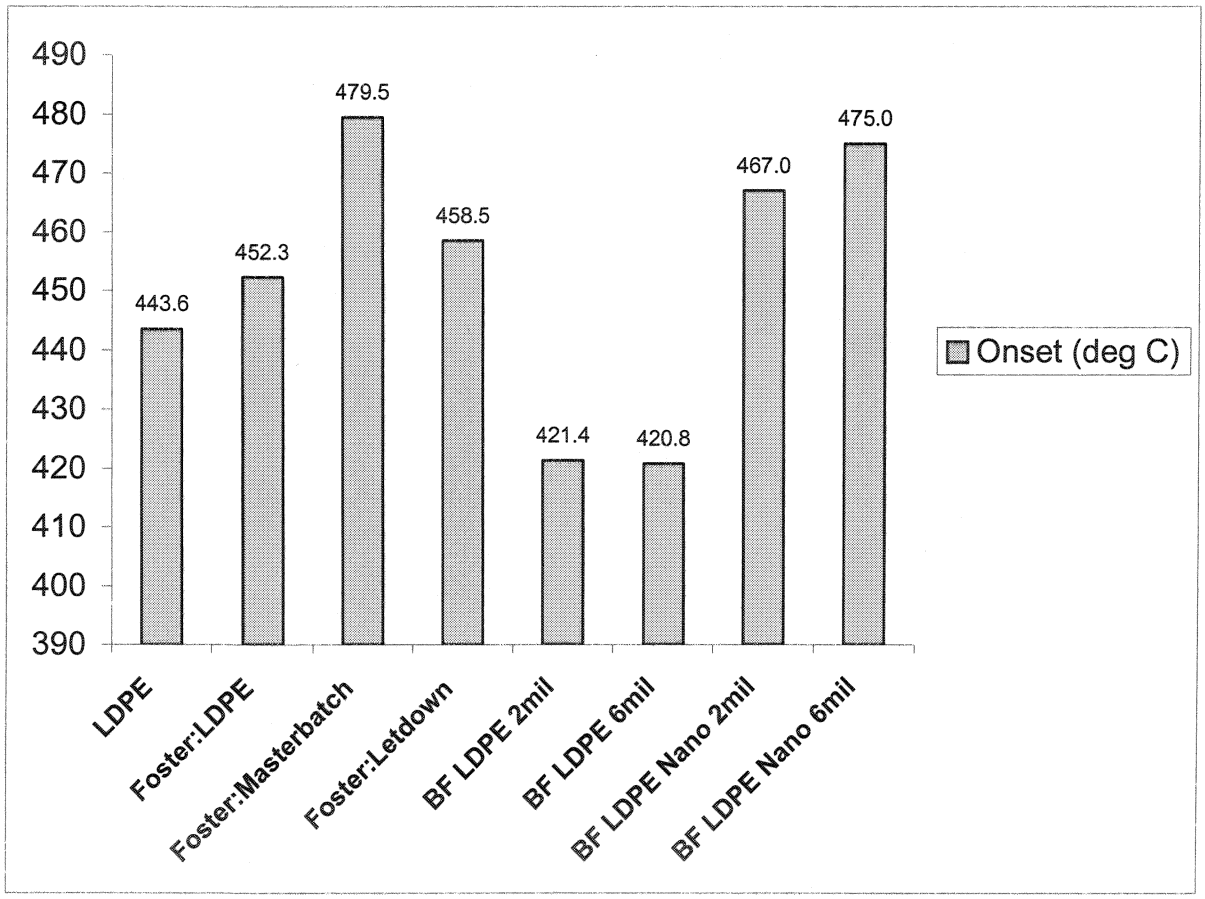

Figure 9. Onset degradation temperatures for the pilot trial of the various pure and LDPE/MLS nanocomposites

5.1.5 Insect Resistance Tests of LDPE Nanocomposites

5.1.5.1 Study 1.

These are results after 12 weeks of testing. The 11-mil LDPE had no penetration and only one package had any chew marks. The 2-mil pure LDPE had insect penetrations in all 10 packages with 5 of the packages having insects inside of the outer wrap (Meal Bag); however, the inner contents showed no signs of infestation. The 6-mil pure LDPE had one package with a suspected penetration and insects were found inside. Most of the 6-mil LDPE packages had moisture inside that may indicate that either some of the food was spoiling or that excessive moisture was inside the package when it was sealed. None of the contents of the packages appeared to be leaking. The 2-mil NANO/LDPE showed significant failure, with all 10 packages having insect penetrations numbering from 2 to over 80. Insects were found in all of the packages. In the case of the 2-mil NANO/LDPE insect penetrations were found in two inner components: one spoon package and one accessory package. However, none of the food contents were infested. Two of the 6-mil NANO/LDPE bags had insect penetrations and both had insects inside. One package had moisture inside and 2 had bad seals. No contents were infested.

During the 12th week breakdown little change was noted from the 8th week breakdown. The 11-mil LDPE remained free of insects with only one showing chew marks. The 2-mil LDPE bags all failed. The 6-mil LDPE had one suspicious hole and one saw-toothed grain beetle adult was found inside. As previously noted the hole was not made by the saw-toothed grain beetle, but may have been made by a warehouse beetle larvae. The concern was the presence of moisture inside most of the 6-mil LDPE packages. This moisture was present before the packages were immersed in water. The 2-mil NANO/LDPE also failed and all of the packages had large numbers of insects of various stages. One package had penetrations in the spoon package and another had warehouse beetle larvae in the accessory pack. The 6-mil NANO/LDPE packages failed in 2 of the 10, but two packages had a bad seal and insects were found inside one. Moisture was found in two of the packages. The food content of all of the MRE's appears to be adequately protected from insect invasion and no attempts to penetrate were found.

Based on the information derived from this study the 6 and 11 mil LDPE are the only packages recommended for insect resistance. The moisture in the 6-mil was somewhat bothersome. The 2 mil overwraps (Meal Bags) both failed early in the study. The 6-mil NANO/LDPE was good for the first 8 weeks and based on the conditions of the test may provide adequate protection.

5.1.5.2 Study 2

The LDPE nanocomposite blown film scale-up had comparable thermal, mechanical, and barrier properties to the small scale blown films processed at NSC. However, these films showed poor resistance to insect infestation. A re-examination of the scaled-up films was conducted, and it was determined that the rough, grainy surface of the film may have affected the results of the insect study. This type of surface may have attracted the insects or made it easier for them to chew through the film.

In response to this a small scale multilayer film with a pure LDPE skin and LDPE nanocomposite core was produced using NSC's Collin Teach Line Co-extrusion System. An SEM image of this structure is shown in Figure 10. . This film showed a significantly smoother surface than the monolayer LDPE nanocomposite. Two multilayer films were produced, with a

total film thickness of approximately 6mil and 11mil. Characterization of these films included layer thickness measurement, mechanical (ASTM D 638) and oxygen barrier testing (ASTM D 3985), as well as an insect infestation study. Exact layer thickness was calculated using the SEM images, and are presented in Table 4.

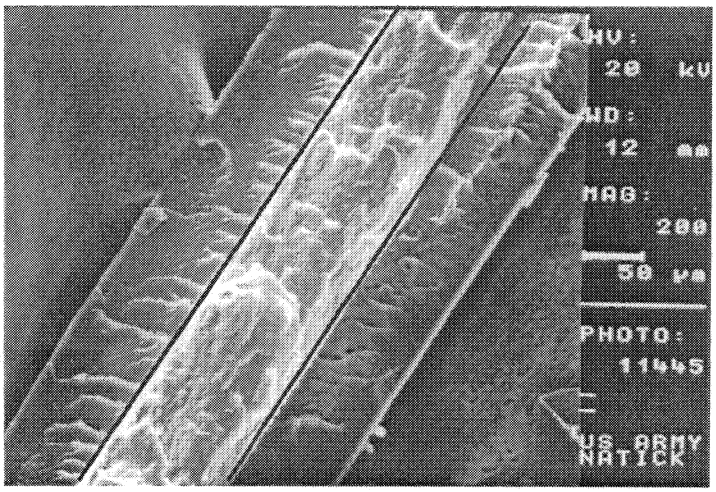

Figure 10. SEM image of the Pure LDPE / Nano LDPE / Pure LDPE multilayer structure

Table 4. Layer thickness measurements based on SEM images

Sample	Pure LDPE Skin Layer	LDPE Nanocomposite Core Layer	Pure LDPE Skin Layer	**TOTAL THICKNESS**
11 mil	3.5	4.7	3.5	11.7
6 mil	2.2	2.2	2.2	6.6

Mechanical results, illustrated in Figure 11, show that the multilayer film has almost a 50% increase in Young's modulus over pure LDPE, and a 130% improvement over the LDPE currently used for the Meal Bag.

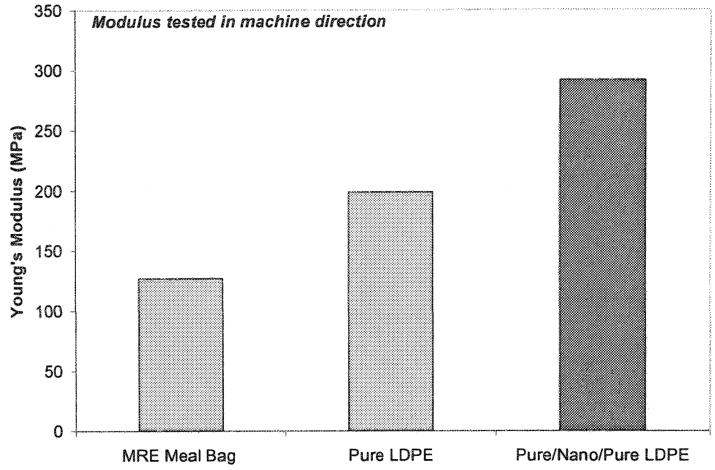

Figure 11. Young's modulus results for LDPE films

Oxygen barrier results, Figure 12, show that the current 11mil MRE Meal Bag, 7mil monolayer LDPE nanocomposite and 7mil multilayer film all have approximately the same oxygen transmission rate. In the case of the monolayer LDPE nanocomposite this equates to a 36% reduction in material, while still maintaining the same barrier properties as the Meal Bag. More importantly, in the case of the multilayer film with the LDPE nanocomposite core there is still a 36% reduction in material, but there is more than a 65% reduction in the amount of nanocomposite LDPE, which is a significant cost reduction due to the price of nanoparticles.

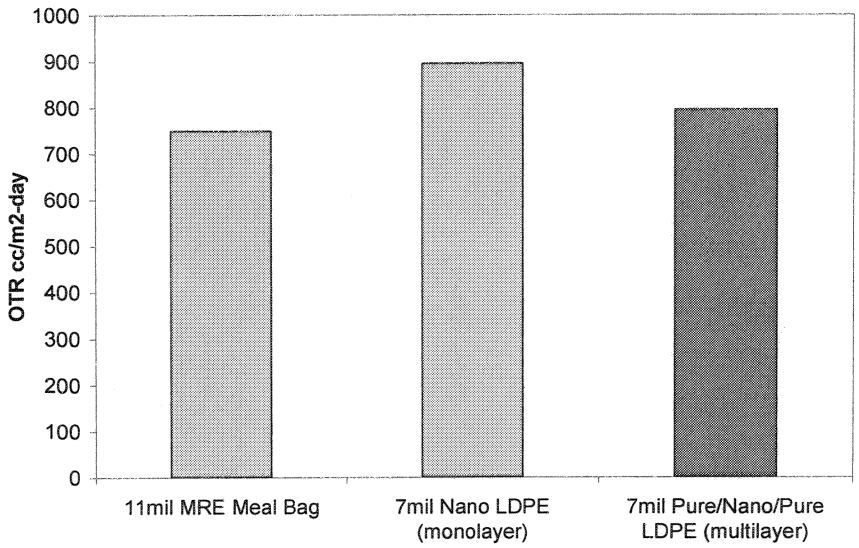

Figure 12. Oxygen barrier results for the Meal Bag and LDPE and Nanocomposite of LDPE/MLS

The multilayer films were tested for insect resistance, since they were developed to overcome the rough, grainy surface of the monolayer LDPE nanocomposite. Due to the size of the lab scale films, pouches could not be made to the dimensions of the current Meal Bag. Instead pouches large enough to hold the accessory packed were constructed. The accessory packet was chosen because this is the only food-containing component that does not have foil-based packaging, so it was assumed that this is the item insects are attracted to. The insect test was modified slightly from the first round of testing, and included three test methods: (1) test

pouches filled with accessory packets, (2) test films with food, and (3) test films without food. The test set-up for these methods is shown in Figure 13. All films and pouches were tested for 12 weeks, and removed every 4 weeks to determine if any of pouches or films had been penetrated, chewed or scratched.

a.) b.)

Figure 13. Test set-up for insect study a.) pouches filled with accessory packets b.) film testing with and without food

It appears that the films tested will provide adequate protection from insect infestation. Only one film failed (test 2- Blown 6 mil nano LDPE) after 12 weeks exposure. As in the earlier study, it appears that the course texture of this film gives the insects a surface that they could grip with their mandibles. With a few exceptions the seals were tight and only a few leaks were noted. It could not be determined if the insects could detect food odors through the films.

5.1.6 Vibration and Drop Testing of LDPE Nanocomposite Meal Bags Results

The inspection of the MRE's from the drop testing found no failures in Nanocomposite box labeled #1. However, there were three failures in Nanocomposite box labeled #2. Two of the bags split along the top seal and one of the bags ripped where the corner of the meal box contacts the film. The MRE boxes had one failure in each case, both rips were where the corner of the meal box was in contact with the film. All the bags that failed were in the corner of the cases and all the bags in the center of the case did not fail. The bags that did fail were in the top row and in the corner of the cases. Overall the Nanocomposite boxes did well when compared to the current MRE meal bags, 12.5% of nano bags failed while 8.3% of the current MRE bags failed. More drop testing will be done with the multilayer LDPE nanocomposite films, and additional testing will be done with boxes at room and frozen temperatures to simulate different environmental conditions seen during shipment and storage of MRE cases.

5.2 Meal Bag - PLA Nanocomposite Study

5.2.1 MLS Selection

Selection of the optimum montmorillonite MLS was done by analysis of the x-ray patterns of the extruded nanocomposite pellets from the DACA mini-extruder. These patterns illustrate the degree of dispersion and exfoliation of MLS within the polymer matrix. The frequency of the MLS platelets as well as the d-spacing of the MLS galleries can be observed in the x-ray diffraction patterns. Figure 14 illustrates the x-ray diffraction patterns of both PLA/Cloisite 20A and PLA/Cloisite 25A nanocomposite pellets processed using the DACA mini-extruder. By comparing the d-spacing of the nanocomposite to the d-spacing of the MLS, it is possible to determine which system has the greatest amount of polymer between the MLS layers. It is this gallery layer spacing that will be used to classify the degree of exfoliation/intercalation in the system.

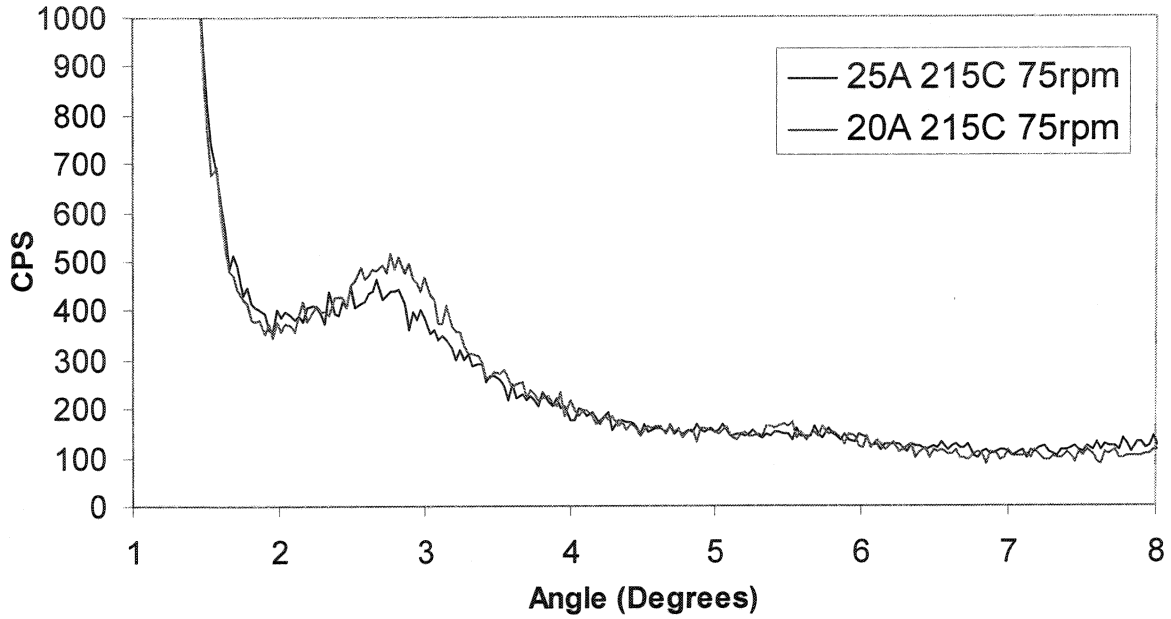

Figure 14. X-Ray diffraction patterns for optimum PLA/20A and PLA/25A systems

Table 5 lists the initial d-spacing of Cloisite 25A as well as Cloisite 20A. This table also lists the measured d-spacing after processing with PLA and the amount of change observed in this gallery spacing. It is clear from this table that the MLS gallery spacing has increased with processing of the PLA polymer. This is a sign that the polymer is achieving penetration between the MLS layers and increasing the distance between the layers. It is also apparent that the layers of Cloisite 25A have been separated the most by the PLA polymer and this was selected for the nanocomposite film study.

Table 5. Amount of D-Spacing Measured in Montmorillonite MLS Galleries

MLS Platelet	Initial D-Spacing (Angstroms)	Final D-Spacing After Processing	Change in D-Spacing
20A	24.00	34.75	+10.75
25A	18.00	35.53	+17.53

5.2.2 Morphology

The next step in nanocomposite analysis was to examine how the gallery d-spacing was affected by the parameters in blown-film processing. To measure this, x-ray diffraction was done on the PLA/MLS 25A nanocomposite blown films processed at various processing conditions. Figure 15 illustrates the diffractions patterns seen for 4 of the nanocomposite films. Processing parameters that were varied for these patterns include the extruder screw speed as well as the pellet feed rate.

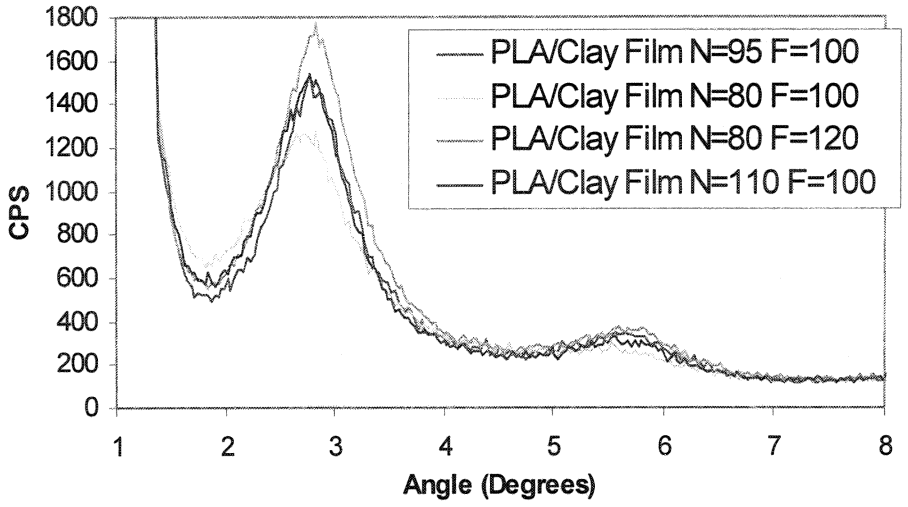

Figure 15. X-Ray diffraction patterns for nanocomposite films at various processing parameters

Table 6 shows the d-spacing values associated with the diffraction patterns seen in Figure 15. Evaluation of the spectra along with the tabulated data seems to suggest that the processing conditions were not as significant in dispersing and exfoliating the nanocomposite. The largest change in the spectra appears when the feed rate of the extruder was increased to 120. At this higher feed rate, the degree of exfoliation had substantially decreased relative to the films processed at the lower feed rate. Optimum results appeared at low screw speeds and low feeding rates. Knowing this, it was possible to test the barrier, thermal, and mechanical properties of the nanocomposite films to determine if exfoliation of the MLS particles improved these properties.

Table 6. d-Spacing Values Measured for Nanocomposite Blown-Films

PLA/MLS Sample	Screw Speed (rpm)	Feed Rate (Arbitrary)	D-Spacing (Angstroms)
PLA/MLS 1	80	100	32.62
PLA/MLS 2	110	100	32.18
PLA/MLS 3	95	100	31.75
PLA/MLS 4	80	120	31.54

Figure 16 shows the TEM of the PLA/MLS nanocomposite with dispersion and alignment in the low magnification photograph and the delamination of MLS platelets in the high magnification photograph.

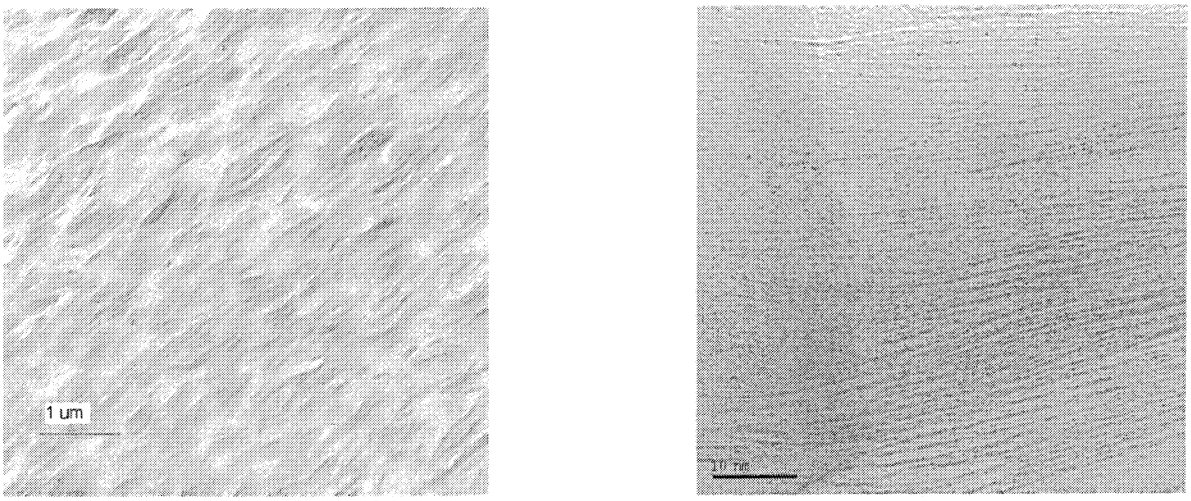

a.) b.)

Figure 16. TEM of PLA/MLS nanocomposites of a.) low magnification and b.) high magnification

5.2.3 Mechanical Properties

All data presented is shown in the machine direction. Generally speaking, the processing conditions did not appear to have a direct influence on the mechanical properties of the films. As observed from the GPC data in Table 7, the PLA nanocomposite films processed at the highest screw speeds exhibited a 17% loss in molecular weight, a result of increased heat and shearing effects. Nanocomposite films processed at the lowest screw speeds exhibited an average molecular weight loss of only 6%, which is reasonable for melt processing.

Table 7. GPC Results for Processed PLA and PLA Pellets

Sample	Heat Histories (#)	Mw (D)	Mn (D)	PDI
Pure PLA Pellet	0	202584	125669	1.61
Pelletized PLA	1	191006	118452	1.61
Pelletized Nano PLA	1	194254	128926	1.51
Pure PLA Film #1	2	189599	124750	1.52
Nano PLA Film #1	2	186602	121903	1.53
Pure PLA Film #2	2	196164	133207	1.47
Nano PLA Film #2	2	167208	104257	1.60
Pure PLA Film #4	2	194975	124582	1.57
Nano PLA Film #4	2	174657	112585	1.55

Organically modified MLS can act as excellent reinforcing agents for polymer materials if dispersed correctly in the polymer matrix. The dispersed MLS platelets allow for stress transfer to the high-surface area MLS reinforcements, strengthening and toughening the polymer. This type of behavior was exhibited in our PLA/MLS nanocomposite films (Figure 17 and Figure 18). On average, the Young's modulus for the nano-PLA samples (Figure 17) was about 30–40% greater than that of the neat polymer. However, incorporation of the MLS into the PLA matrix produced no significant change in the tensile strength of the resulting films. Adding filler to a plastic typically decreases the elongation significantly, but this was not the case with the MLS in this system. Indeed, elongation was about 16–40% greater for the nano-PLA films than for the neat films (Figure 18.) Giannelis has recently reported on dramatic enhancements in elongation to break (140%) and toughness (700%) for a nanocomposite consisting of polyvinylidene fluoride (PVDF) and a surfaced modified MLS. No improvement in toughness was observed for the non-modified MLS/PVDF system.

Although the PLA/MLS system did not see these highly significant enhancements, the toughness is at least maintained in the PLA/MLS nanocomposites unlike other filled polymeric systems. Giannelis attributes this enhancement to a new energy-dissipation mechanism during deformation and that the MLS induces structural and morphological changes that increases chain mobility as compared to micrometer-size fillers.

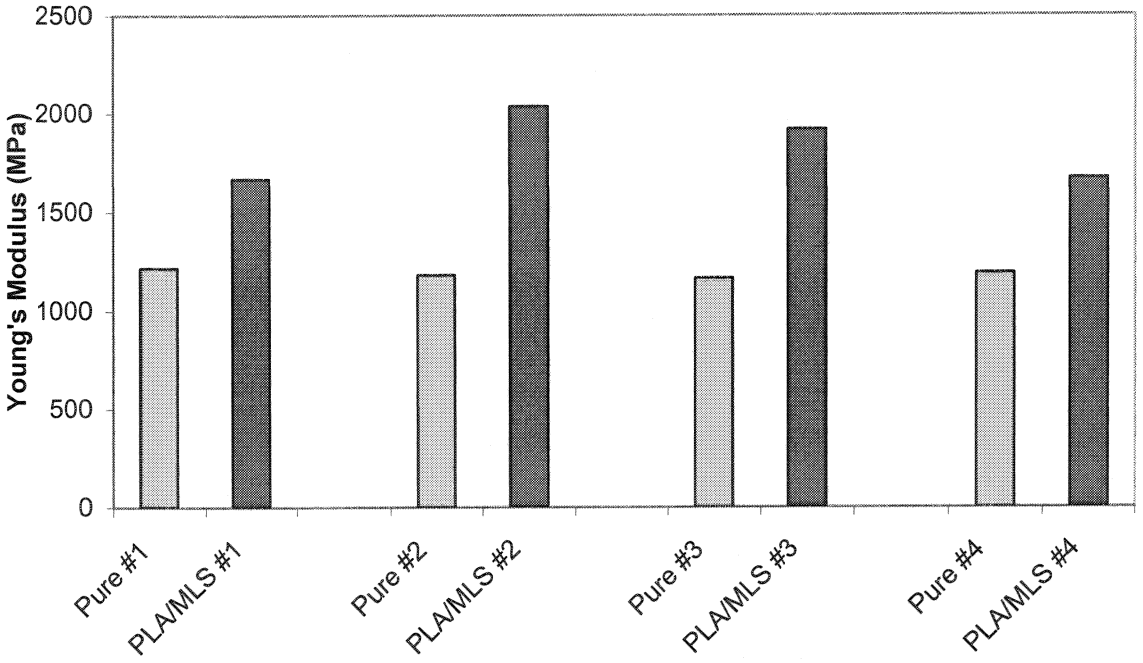

Figure 17. Young's modulus of PLA and PLA nanocomposites

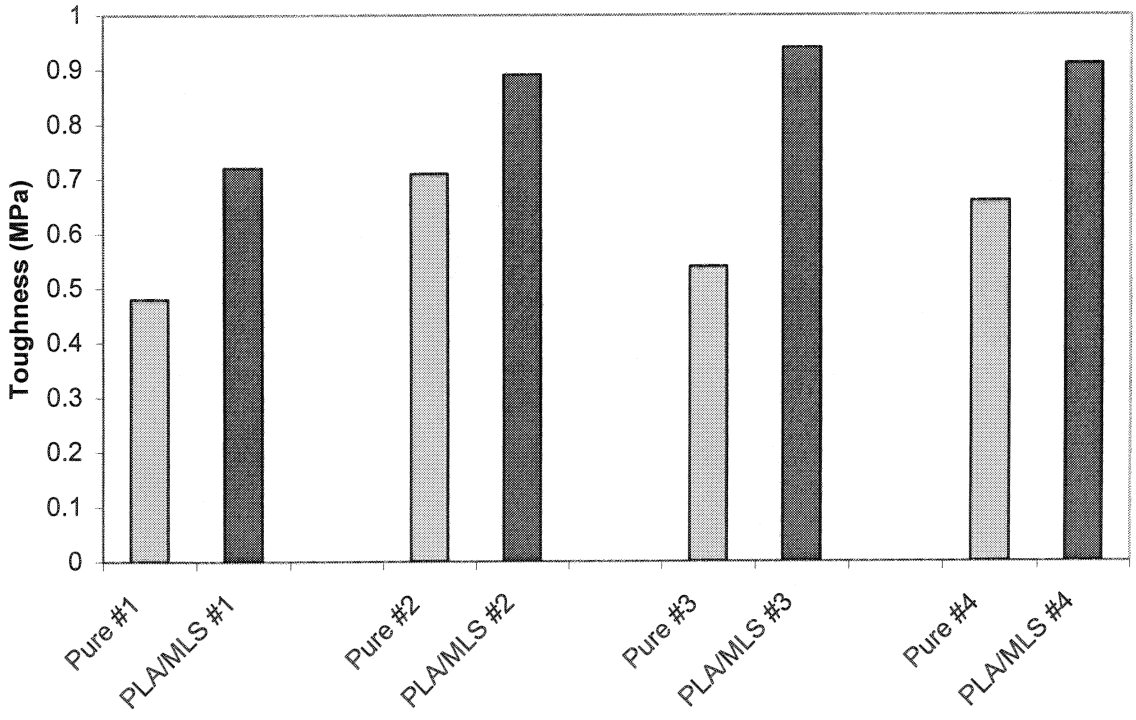

Figure 18. Toughness of PLA and PLA nanocomposites

5.2.4 Barrier Properties

Permeation analysis was carried out on the neat PLA samples as well as the nanocomposite using both the MOCON Ox-tran and Perma-tran units. Neat PLA does not have strong barrier properties to water and oxygen. The incorporation of plasticizer into the process only decreases the already weak barrier performance of PLA. Table 8 lists the oxygen and water vapor permeation results for the neat PLA film as well as the nanocomposite film.

Table 8. MOCON Results From Water Vapor and Oxygen Permeation Testing

Sample	Water Vapor Permeation Coefficient (g*mil/(m²-day))	Oxygen Permeation Coefficient (cc*mil/(m²-day))
Pure PLA 1	367	855
Pure PLA 2	303	554
Pure PLA 3	419	749
Pure PLA 4	328	551
PLA/MLS 1	151	470
PLA/MLS 2	166	477
PLA/MLS 3	158	438
PLA/MLS 4	191	471

5.2.5 Biodegradation Properties

Table 9 displays the biodegradation data for PLA and PLA nanocomposites in soil. Carbon dioxide production in the control soil is a result of mineralization of the native soil organic matter, which proceeded in a linear fashion at a rate of about 0.13 mg CO_2-C d^{-1} throughout the 180-day test exposure. Mineralization of the positive control (cellulose) proceeded slowly at first (with a lag period of about 8 days) but then increased rapidly from about DAY 8 to DAY 21. After DAY 21, net CO_2 production continued to increase in a near-linear fashion for another nine weeks–though at a much slower rate–before approaching a plateau at about DAY 104. The time required to achieve 60% net mineralization was ca.76 days, which was well within the 180-day time-frame set out in the ASTM standards.

In general, the net mineralization curves are characterized by a small, but relatively rapid increase in CO_2 production during the first 7–10 days of the test exposure, followed by a much slower, but relatively constant, increase in net CO_2 production during the remainder of the exposure. During this latter phase, net mineralization of both the neat and nano-layered materials was best described using a linear model, with rate constants ranging from about 0.005 to 0.013 mg CO_2-C d^{-1} (Table 9) The initial (more rapid) mineralization phase was most likely a result of microbial attack along exposed end groups as well as the mineralization of low molecular weight fragments in the polymer matrix and the acetyltriethyl citrate plasticizer.

Table 9. Mineralization of the PLA-clay Nanocomposite Films and Positive Control (cellulose) During a 180-day Test Exposure in Soil at 22 ± 1°C and a Moisture Content of 55 ± 5% WHC

Test Material	Lag [a] (days)	----- Mineralization -----			r_{pdp} [d] (mg C d^{-1})	t_{60} [f] (days)
		Max-CO_2C [b] *(mg)*	$ThCO_2$ (%)	RBI[c]		
Cellulose powder	8	175.5 ± 10.9	70.5 ± 4.4	---	4.13 ± 1.19 (1.51 ± 0.05)[e]	76
neat PLA	IND	2.07 ± 0.36	0.83 ± 0.14	0.01	0.010± 0.001	IND
PLA/CE	IND	2.51 ± 2.18	1.01 ± 0.87	0.01	0.005± 0.003	IND
PLA/MLS	IND	2.63 ± 0.73	1.06 ± 0.29	0.02	0.013± 0.002	IND
PLA/MLS/CE	IND	2.93 ± 0.83	1.28 ± 0.18	0.02	0.012± 0.002	IND

[a] Time required for net mineralization to reach 10% of the MAX-CO_2. Note: In those cases where the net mineralization curve did not reach a plateau, the LAG was defined as the time required for net CO_2-C evolution to reach 5% $ThCO_2$. IND = indeterminate.

[b] The maximum amount of CO_2-C evolved during the 180 day test exposure.

[c] Relative biodegradation index = (% mineralization of the TEST SAMPLE ÷ % mineralization of the POSITIVE CONTROL); positive control = cellulose.

[d] Average rate of mineralization during the primary degradation phase: defined as the slope of the linear least-squares regression line plotted between the end of the lag period and start of the plateau region (i.e., the point where net mineralization = two-thirds MAX-CO_2). Note: for the PLA samples there was no distinct lag period and the linear model gave the best fit to the net mineralization curves; therefore, the rate constant was calculated as the slope of the linear least-squares regression equation.

[e] Values in parentheses are the rate (± the 95% confidence interval) during the slower mineralization phase (i.e.,

5.3 Food Pouch - EVOH Study

5.3.1 Monolayer Nanocomposites

5.3.1.1 Morphology

XRD and TEM are often referred to as complimentary techniques for studying polymer/nanoparticle morphology; each filling in gaps of information the other technique cannot obtain. XRD was performed first to obtain a general understanding of how the MLS and polymer matrix interacted and to determine *d*-spacing of the MLS in the EVOH. Figure 19 shows the XRD curves for the nanocomposite pellets and film as well as the pure 25A. This figure also displays film with 3 and 6% MLS, processed at screw speeds of 50 and 90 rpm. All the curves indicate an intercalated morphology that appears to be independent of processing. The intensity of the peak is dependent on the concentration of the MLS, with 6% MLS nanocomposites having the highest intensity peak. The peak pattern in Figure 20 for the nanocomposite film (3% MLS) shows a significant shift to the left, in comparison to the pure 25A MLS, indicating interaction between the MLS and polymer. The increase in MLS *d*-spacing from 18.7 Å, in the pure 25A MLS, to 31.2 Å after blown film processing, indicates that the extrusion process assisted in dispersion of the MLS. It is also important to point out that there was slight increases in d-spacing from 29.0 Å to 31.2 Å between melt compounding and blown film, signifying additional MLS dispersion during blown film extrusion. As reported by Dennis et al., an average *d*-

spacing between 20–30 Å indicates an intercalated system[5]; therefore suggesting that this EVOH/MLS nanocomposite system, with a *d*-spacing of 31.2 Å, is highly intercalated. Dennis et al. reports that full exfoliation does not occur until *d*-spacing has reached 80-100 Å.[5]

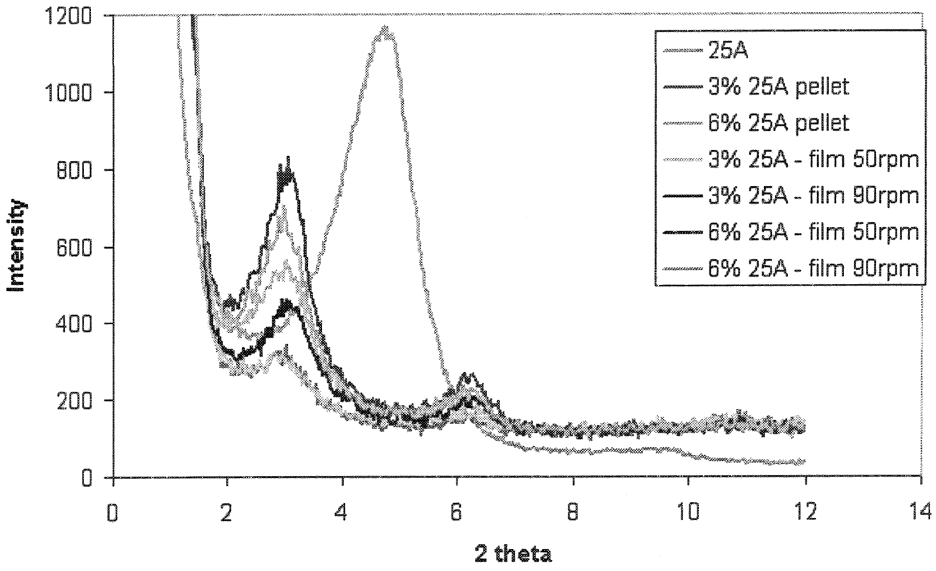

Figure 19. XRD curves for pure 25A MLS and E-105 with 3% and 6% 25A loading at 50 and 90 rpm

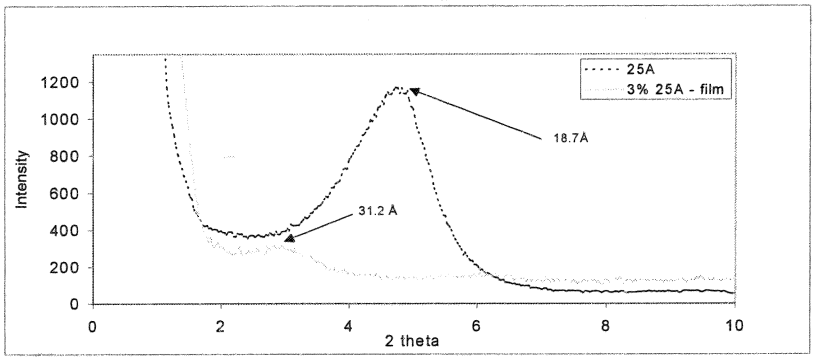

Figure 20. XRD curves for pure 25A MLS and E-105 with 3% 25A loading

The TEM images of both the compounded pellet and blown film compliment the XRD results, and provide a better understanding of how 25A is dispersed within the polymer matrix. Figure 21a and Figure 21b show low magnification TEM images of the compounded pellet and blown film, respectively. These images reveal enhanced MLS alignment in the blown film, in comparison to the pellet. This is most likely due to the biaxial orientation the film is exposed to when exiting the die during blown film extrusion. Figure 21c and Figure 21d show higher magnification images of the pellet and film, respectively. At this magnification it is apparent that the platelets are better dispersed in the blown film. There does appear to be some degree of MLS dispersion in the pellet, however not to the extent shown in the blown film. From this X-ray and TEM data, it was then decided to focus on the 3% MLS nanocomposites for further characterization.

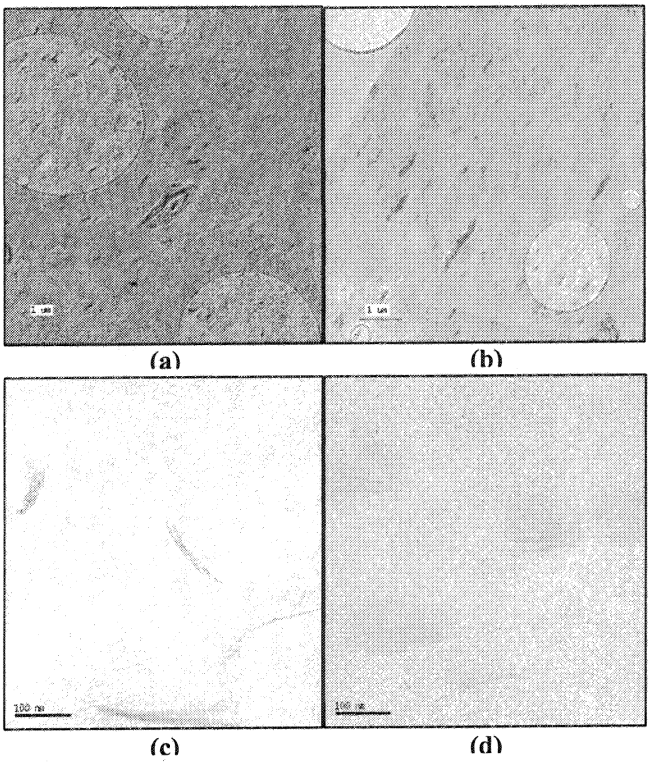

Figure 21. TEM images E-105 with 3% 25A (a) compounded pellet at low magnification, (b) blown film at low magnification, (c) compounded pellet at higher magnification, (d) blown film at higher magnification

5.3.1.2 Mechanical Properties

Examination of mechanical properties in the machine direction for the pure EVOH and nanocomposites blown and cast film as a function of moisture content are shown in Figure 22 and Figure 23 respectively. For both pure and nanocomposite cast and blown films, the same trend occurs. The Young's modulus decreased as the RH increased. For the blown films at relatively high humidity, the nanocomposite had a higher Young's modulus than the pure E-105 film (58% improvement). At dry conditions (0% humidity), there is no improvement in the modulus value for the nanocomposite. This is not expected since there is an intercalated morphology and the stiff MLS platelets normally increase the mechanical properties. The cast film has a 23% increase at 0% RH but only an 11% improvement from the pure EVOH at the 93% RH.

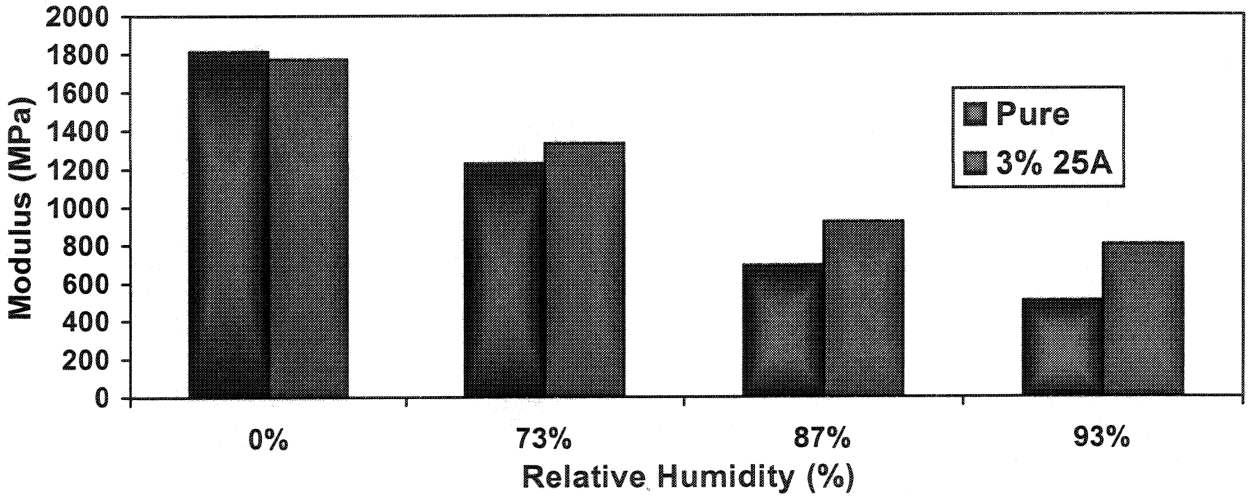

Figure 22. Young's modulus of EVOH blown films

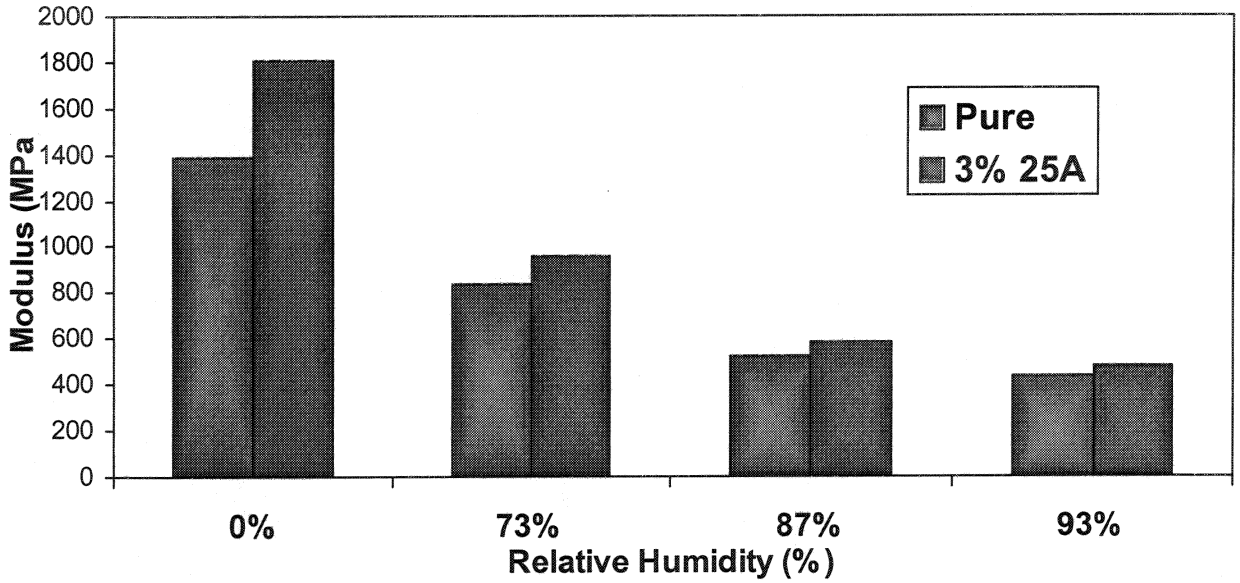

Figure 23. Young's modulus of the cast films. Pure EVOH and EVOH nanocomposite as a function of RH

5.1.1.3 Barrier Properties

Figure 24 illustrates the oxygen barrier data for the cast and blown films at 0% RH. For the pure EVOH, the cast film is a much better oxygen barrier than the pure blown film. For the nanocomposites, there is a 57% improvement in barrier for the cast film, but a decrease of 14 % for the blown film samples compared to the pure EVOH controls.

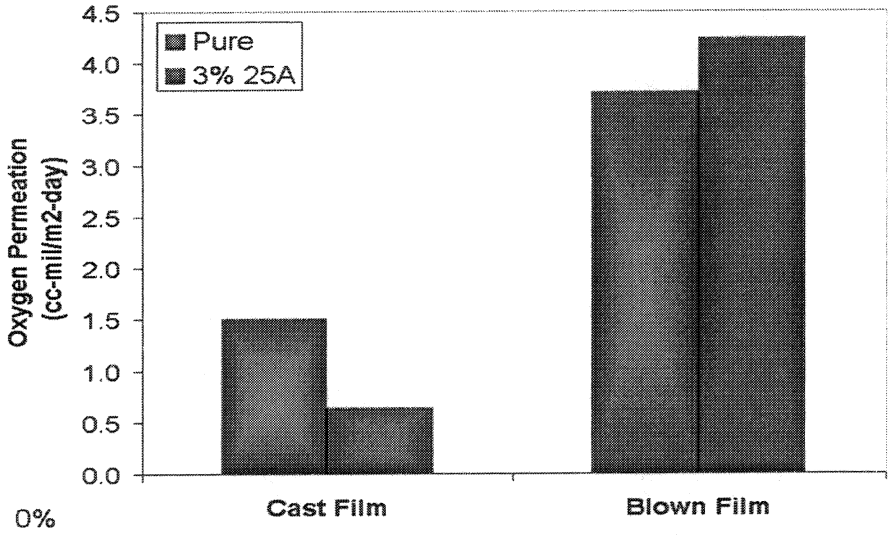

Figure 24. Oxygen permeation data at 0% RH for cast and blown film EVOH and EVOH nanocomposites

In previous studies of EVOH and EVOH nanocomposites, the barrier properties were better for the bi-axially oriented blown films, as opposed to the cast films.[34] More experiments need to be performed for both cast and blown films to investigate why these differences are occurring. Segmental motion of the polymer chains may attribute to the barrier properties as well as the degree of orientation and degree of crystallinity.

Permeability in nanocomposites can be influenced by the MLS orientation in the polymer matrix, the MLS sheet length as well as the state of aggregation and dispersion. An increased diffusion path length (tortuous path) is produced in the polymer/MLS systems by the overlapping of MLS platelets. Platelets must align parallel to the surface of the film to obtain the advantage of the tortuous path. If the platelet orientation is altered, then this can alter the enhancement of barrier properties. Bissot has studied the effect of platelet orientation of oxygen barrier properties with EVOH and platelet-type fillers (mica, talc, and aluminum flake). [35] Cast, blown and co-extruded films were processed and the barrier properties were dependent on this orientation.

Sharastri studied the orientability and effect of orientation on high barrier films including pure EVOH. He was orienting in the solid state and actually was not successful at orienting the EVOH. However, for a vinylidene chloride/vinyl chloride (VDC) copolymer, there was 1.5 times higher permeability in the unoriented film with biaxial orientation than with a cast film.[36] The crystallinity of the bi-axially oriented film was actually less 24% versus the 33% of the extrusion cast film. Sharastri believes that microvoids can develop during the orientation and also the size of the crystallites may change, both factors influencing permeability.

Also, the decreased barrier effect of nanoparticles in the blown film, as compared to the improved barrier of the cast film, could be attributed to the effect of orientation on alignment of nanoparticles therefore reducing the projected area of the particles parallel to the surface.

displays the oxygen barrier data at 90% RH for the cast films. For the pure EVOH, there is an 11 times decrease in the barrier properties from the 0% RH sample, and a 9 times decrease for the nanocomposite. The nanocomposite displays a 24% better OTR barrier than the pure EVOH at 90%RH.

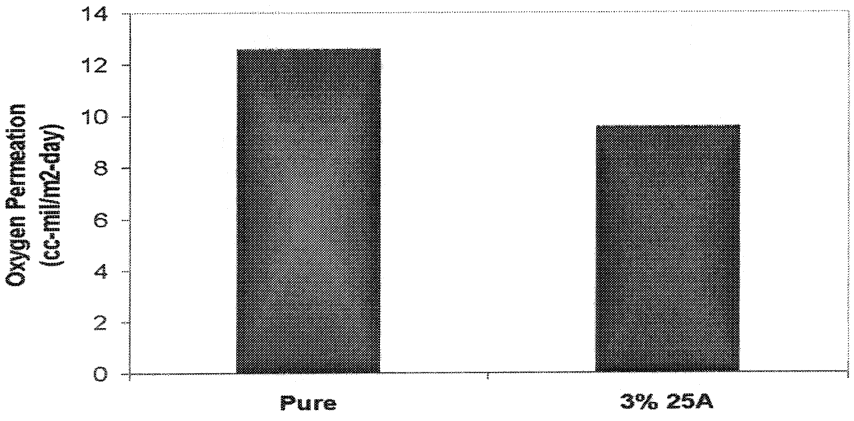

Figure 25. Oxygen barrier data at 90% RH and 23°C for pure EVOH and EVOH/MLS nanocomposite

Figure 26 displays the water vapor permeation for the cast and blown films. There is the same trend for the cast and blown film that was viewed for oxygen. The blown film nanocomposite displays a worse water vapor barrier than the pure EVOH by 34%, while the cast film nanocomposite shows a 29% improvement over the pure EVOH. This again can be attributed to the orientation in the EVOH and the nanoparticle in the matrix.

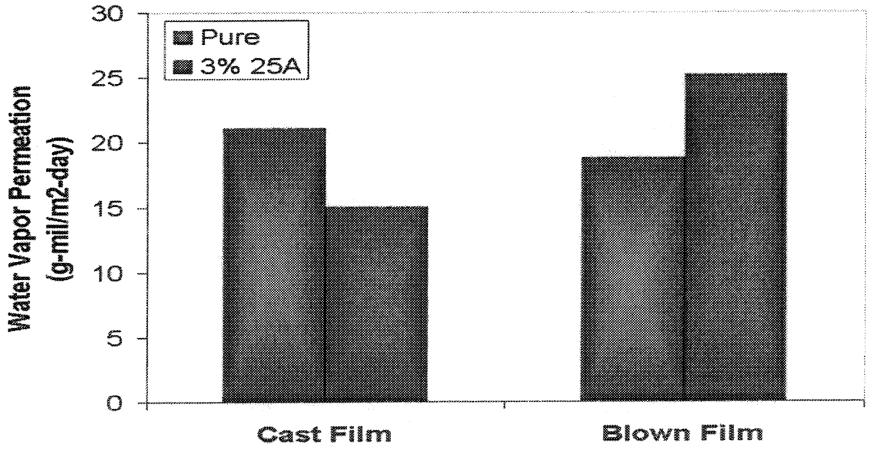

Figure 26. Water vapor transmission rate of cast vs. blown film at 90% humidity and 37.8°C

Figure 27 shows weight loss as a function of temperature for both pure E-105 and E-105/MLS nanocomposite blown film. The addition of MLS slightly increases the onset degradation temperature of E-105 by almost 2°C, as shown in Table 10. More interesting is the slope of the degradation curves. The pure E-105 curve drops off quickly indicating a high rate of degradation. Whereas the nanocomposite curve shows a more gradual slope, indicating a significantly slower degradation rate. This data is also representative for the cast films. This reduction in degradation rate was also apparent in prior EVOH nanocomposite research reported by Lucciarini et al., however an increase in onset degradation temperature of the nanocomposite film was not achieved in this study.[34]

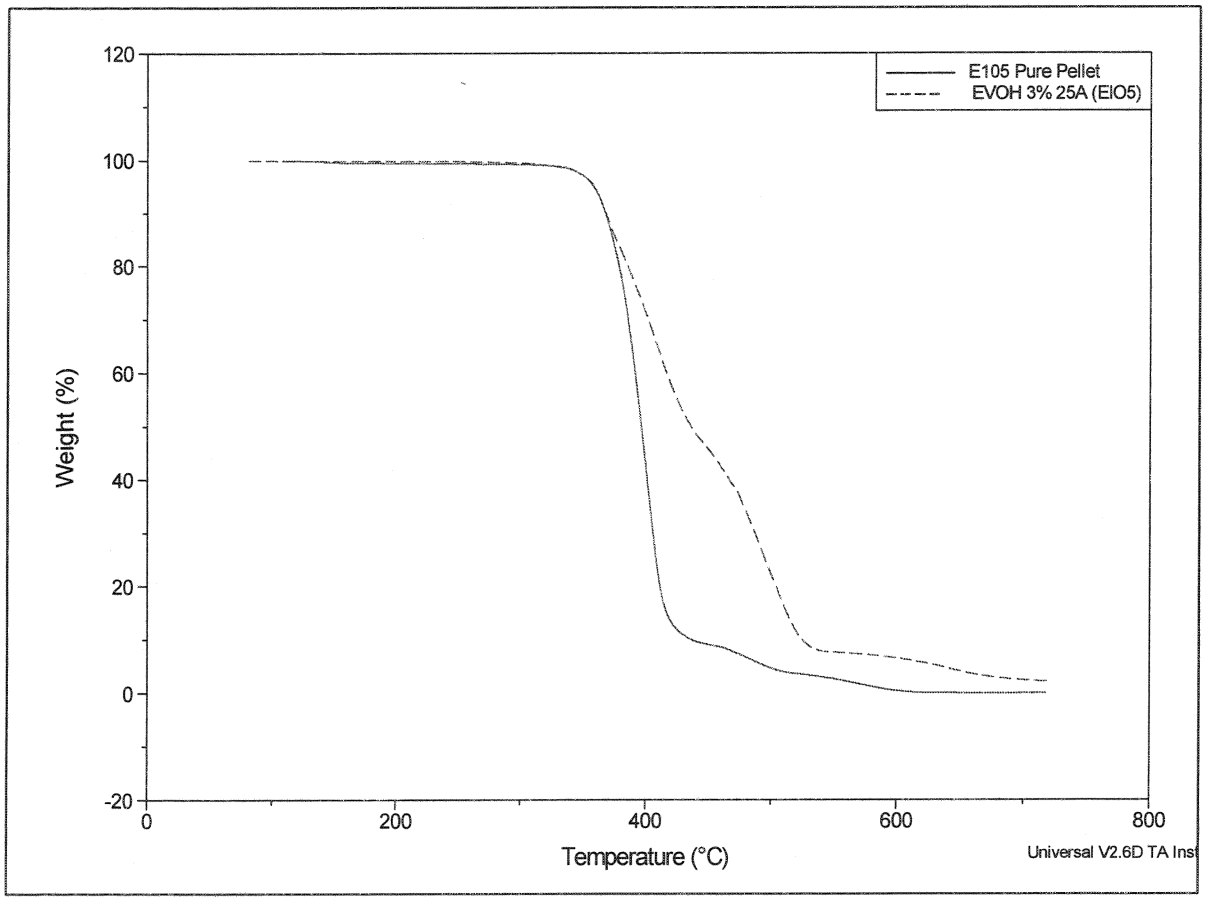

Figure 27. TGA results for pure EVOH and EVOH/MLS nanocomposite blown film

Table 10. TGA data for the Pure EVOH and the EVOH/MLS Nanocomposite.

Sample	Onset Degradation (°C)
Pure E-105	356.6
E-105 + 3% 25A	358.1

Table 11 shows the DSC data for the Tm (peak) and the enthalpy. The melting temperature for the EVOH in the nanocomposites did not vary from pure EVOH. There was also no change for the cast film or blown film. The enthalpy for the blown film nanocomposite was slightly higher than the pure EVOH indicating perhaps some enhanced crystallinity in this sample.

Table 11. DSC Melting Temperature and Enthalpy for EVOH and EVOH/MLS Nanocomposites

Sample	Peak Temperature (°C)	ΔH (J/g)
Cast EVOH Neat	166	77.8
Cast EVOH + 3% 25A	166	75.8
Blown EVOH Neat	166	77.9
Blown EVOH + 3% 25A	166	81.2

5.3.2 Multilayer Films

Figure 28 displays the 5-layer LDPE/Tie layer/EVOH/ Tie layer/ LDPE Scanning Electron Microscopy (SEM) photograph. By using this technique, we can measure the thickness of each layer.

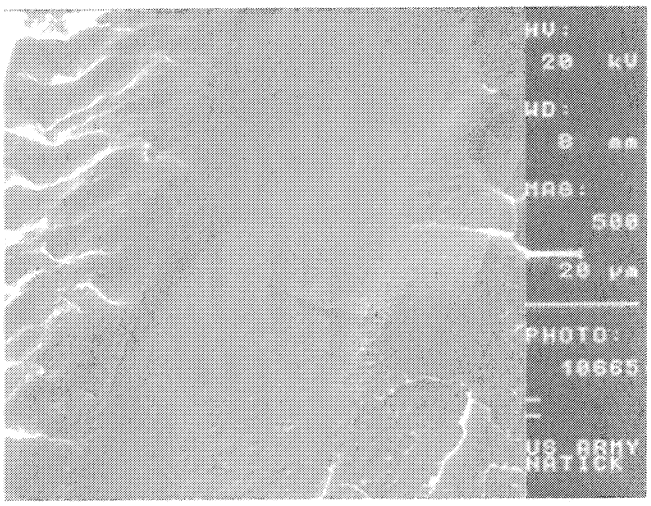

Figure 28. Scanning electron microscopy of the 5-layer EVOH/LDPE/tie layer structure

Table 12. Oxygen transmission data for EVOH/LDPE co-extruded film

Sample	EVOH Thick. (microns)	WVTR (g/m^2-day)	OTR - 0%RH (cc/m^2-day)	OTR - 90%RH (cc/m^2-day)
Sample 1	85	0.59	0.46	1.88
Sample 2	100	0.53	0.25	0.67

Table 12 demonstrates that oxygen barrier is improved with a thicker EVOH layer, while the water vapor barrier values do not change significantly. This data was for only the pure EVOH. Figure 29 contains oxygen barrier data for the co-extruded nanocomposite films containing 3% 25A in the nanocomposite EVOH layer and 7.5% 20A in the LDPE nanocomposite layer. The multilayer film containing the pure LDPE and pure EVOH had better oxygen barrier data than the sample with EVOH/MLS nanocomposite and LDPE nanocomposite.

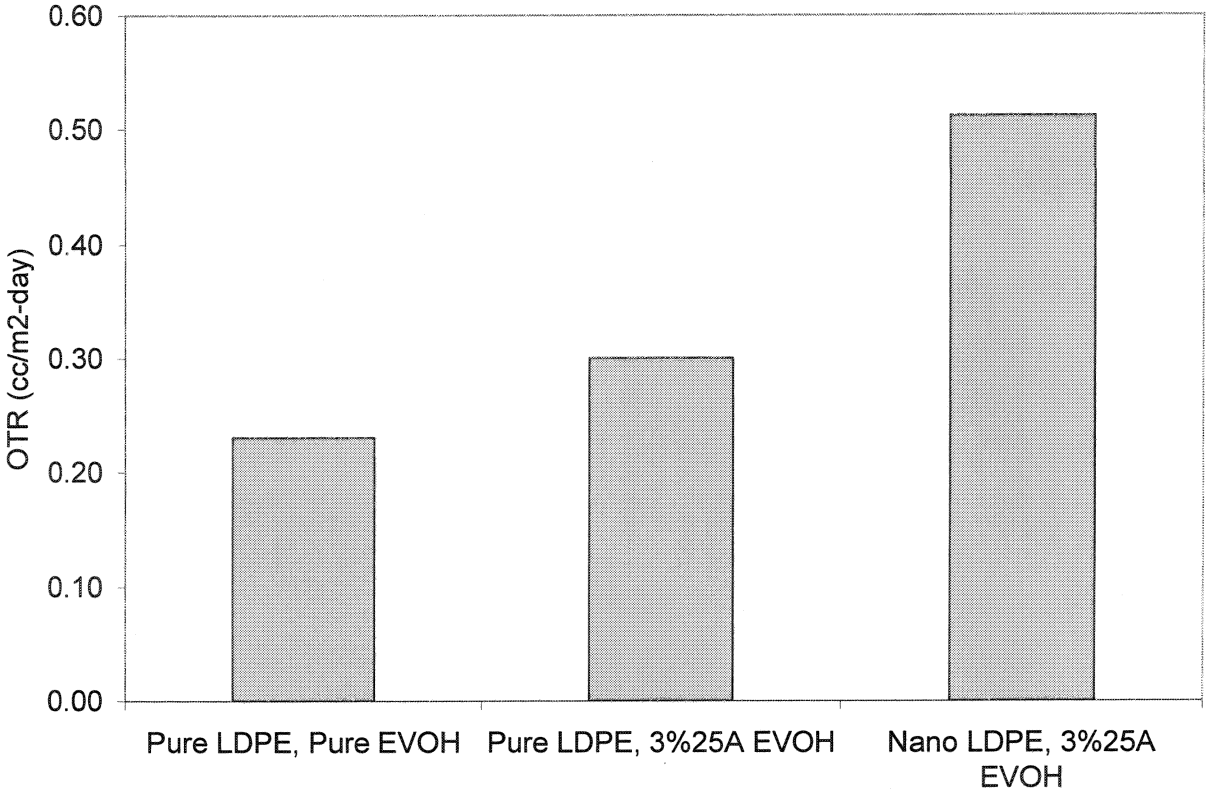

Figure 29. OTR for EVOH/LDPE co-extruded film

5.3.3 Retort Studies of EVOH/LDPE Multilayer Films

The MRE includes items that are sterilized using retort, which subjects the packaging to extreme heat and pressure while submerged in water. Two retort studies were conducted to determine the effect of retort conditions on the integrity of several packaging films. These trials included multilayered film structures supplied by Cryovac and EVALCA, as well as LDPE and PP films processed at NSC. A list of films included in these trials is shown in Table 13. The following properties were tested before and after retort to determine the affect of retort on the package: seal strength (ASTM D 882), tensile properties (ASTM D 638), and oxygen permeability (ASTM D 3985), in addition the pouches were subjected to a visual inspection to determine if any of the seals had ruptured after the retort trial was complete.

Table 13. Nanocomposite Films Included in Retort Study

Films Supplied By	Film ID	Film Description	Retort Trial
Cryovac	74759-1	Sealant/Tie/Barrier*/Tie/Abuse	1
Cryovac	74766-4B	Sealant/Tie/Barrier*/Tie/Abuse	1
Cryovac	74767-6	Sealant/Tie/Barrier*/Tie/Abuse	1
EVALCA	XEF-630	Barrier Coating/PET/Barrier Coating	2
NSC	Blown	LDPE/tie/EVOH/tie/LDPE	1
NSC	Cast	PP	2
NSC	Blown	PP	2

*core barrier layer is a proprietary blend of Nylon and EVOH

To begin the study, the films were converted into pouches using a Vertan Impulse Sealer. Optimal seal settings were defined for each material by testing the seal strength and identifying which settings produced the strongest seal. Once constructed the pouches were filled with a pre-measured amount of distilled water and were refrigerated overnight to create a uniform temperature of 40°F. The films were retorted at 250°F for 30 minutes at a pressure of 24 psig, using a Validator 2000.

Visual inspection of the pouches revealed that all seals passed the retort trial, however not all the pouches maintained their original size and color. The LDPE/EVOH multilayer pouches shrunk to half their original dimensions and changed from translucent to opaque. Due to the severe deterioration of the LDPE /EVOH multilayer film, post retort testing could not be conducted. It was determined that LDPE was not suitable for the extreme conditions of retort, and therefore focus was shifted to a retortable PP, which was tested during the second retort trial. The Cryovac films, which were also transparent at the start of the study, turned slightly cloudy, but retained their original shape. The other samples were visually unaffected by the retort process.

Seal strength results, before and after retort, are shown in Figure 30. All of the pouches, with the exception of Cryovac 74759-1, showed no reduction in seal strength after the retort process. Cryovac 74766-4B actually showed an improvement in seal strength after retort. NSC's blown PP showed consistent seal strength before and after retort, however the values were more than four times lower than the other retorted samples, including the cast PP. This may be due to the film being significantly thinner than the other samples.

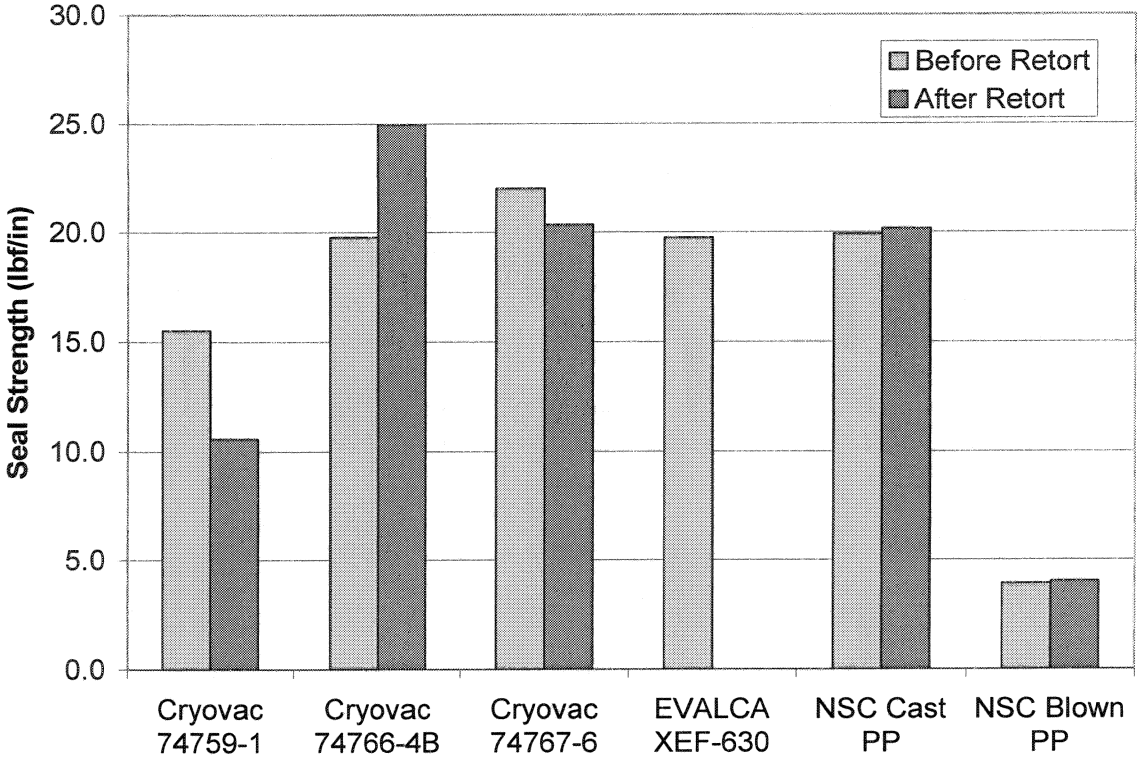

Figure 30. Seal strength before and after retort

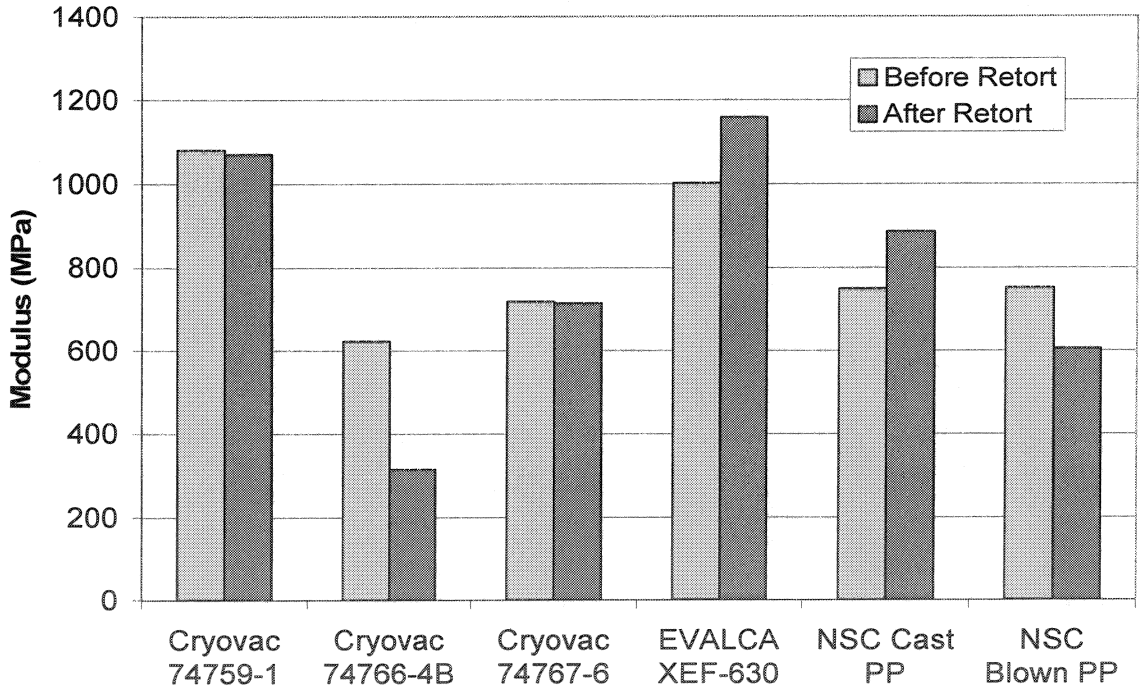

Figure 31. Young's modulus before and after retort for nanocomposite films

Mechanical testing was also performed before and after retort. Results on the film's Young's modulus is shown in Figure 31. The majority of the films showed consistent, if not higher Young's modulus, after the retort process. Cryovac 74766-4B, which showed better seal strength after retort, actually showed a decrease in Young's modulus. NSC's blown film showed a slight decrease in Young's modulus after retort, whereas the cast film showed a slight increase in modulus.

Oxygen transmission rate (OTR) was also measured before and after retort. The OTR for the Cryovac and EVALCA samples, shown in Figure 32, was measured within three hours of retort, and the recorded values are after the films had dried out and maintained equilibrium. All the films showed a significant increase in OTR after being subjected to the retort process. The EVALCA film had the best barrier before retort and recovered better after retort, with an OTR eight times higher than before retort. The Cryovac films did not recover as well after retort, and showed an OTR of 25-33 times higher than before retort. The Cryovac films incorporate both EVOH and nylon in the barrier layer, both of which show increased oxygen permeability in the presence of moisture. EVOH undergoes "retort shock" meaning that it shows a dramatic increase in OTR immediately after retort, and only regains a percentage of its original barrier properties after it dries out. As you can see from Figure 33, Cryovac film 74759-1 shows the least amount of retort shock and dries out quicker than the other two films. The OTR of the PP cast and blown films were also measured before and after retort. As shown in Figure 34, the cast PP shows a 28% increase in OTR after the retort process, whereas the blown film showed almost a 10% decrease in OTR after the retort process, despite the fact that it showed a decrease in Young's modulus and a low seal strength.

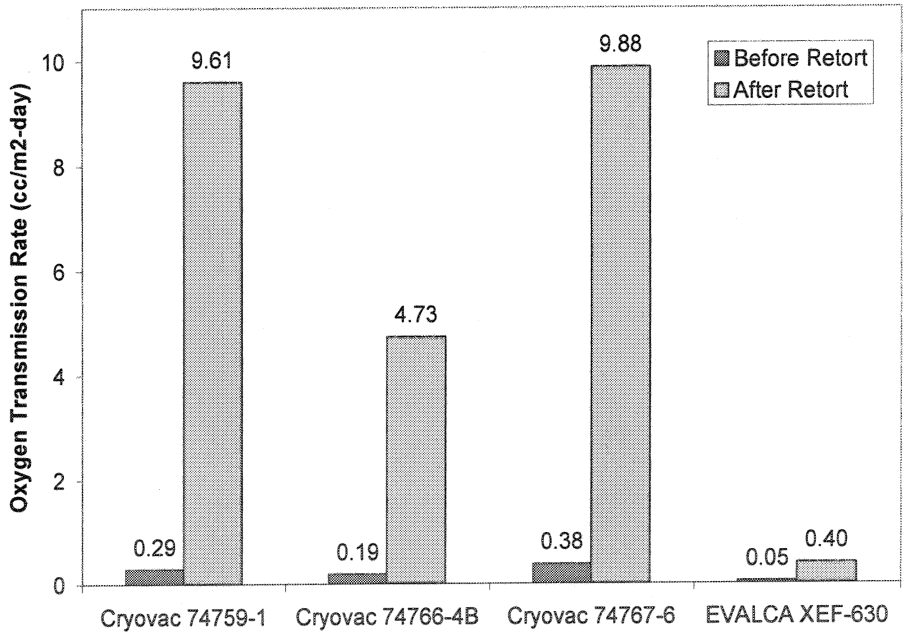

Figure 32. Oxygen transmission rate of Cryovac and EVALCA films before and after retort

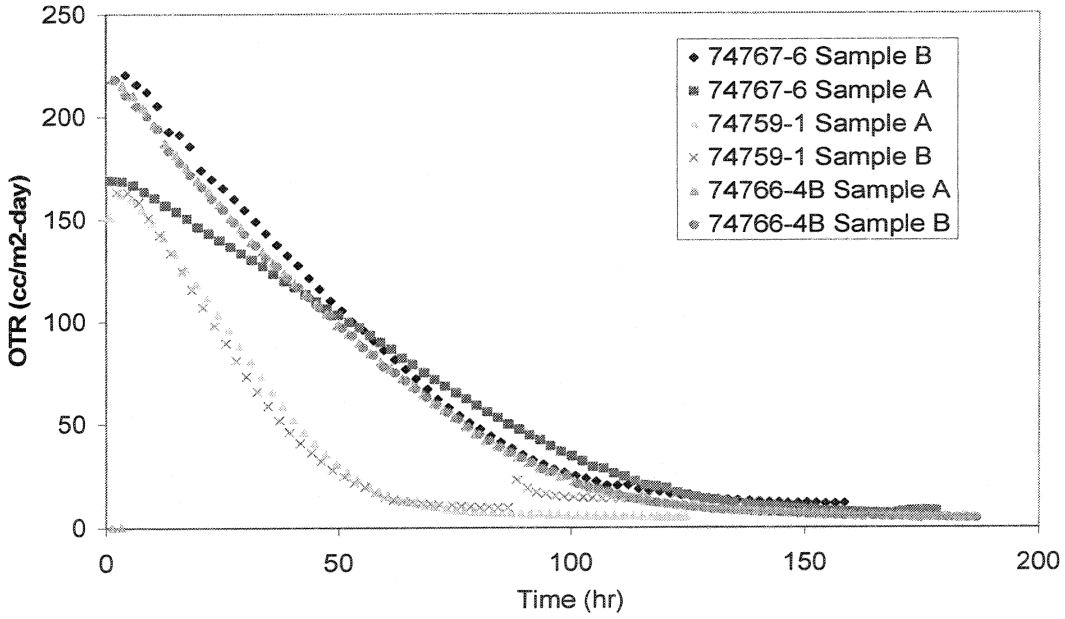

Figure 33. Oxygen transmission rate of Cryovac films during dry-out

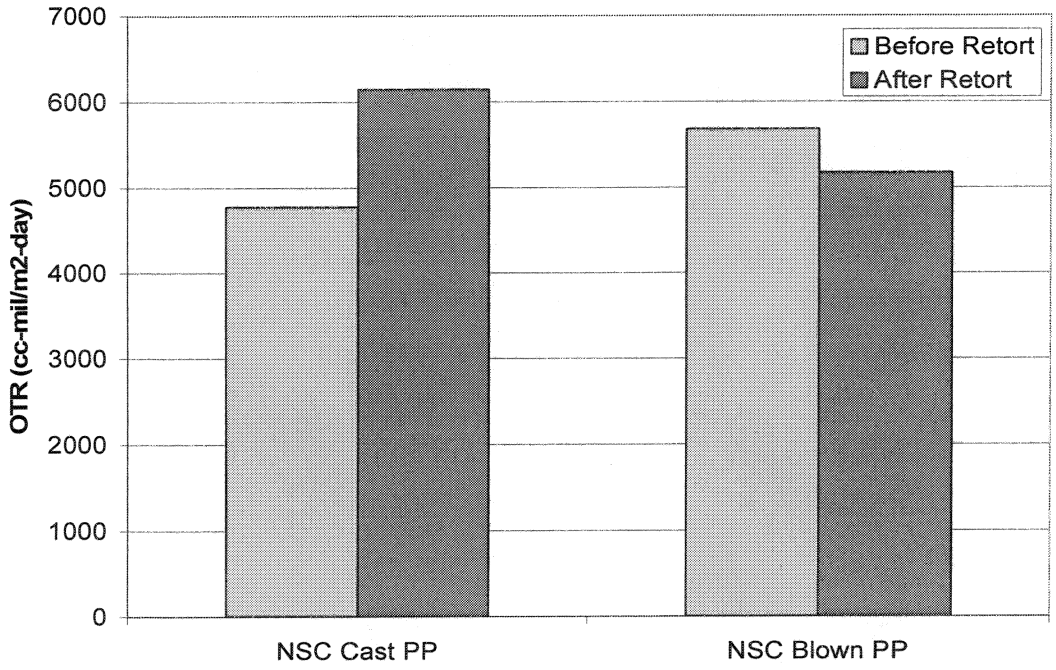

Figure 34. Oxygen transmission rate of PP cast and blown films before and after retort

5.4 Food Pouch - Nylon Nanocomposite Study

5.4.1 Monolayer Nylon Films

5.4.1.1 Neat Nylon Films

5.4.1.1.1 Mechanical Properties

Neat monolayer nylon films were characterized, primarily for barrier properties, to determine which nylon would be used as a base material for the nanocomposite films. Mechanical analysis of the nylons is illustrated in Table 14. The mechanical properties of the films determined through tensile testing are quite similar between the three nylons. The only property showing a significant difference between the samples was Young's modulus. In this case, the Capron films had the highest modulus of the three. Given this data, it was decided that the Capron nylon 6 would be used as the base nylon control for the nanocomposite work.

Table 14. Tensile Properties of Neat Nylon Films

Nylon Film Samples	Young's modulus (MPa)	Yield Stress (MPa)	Yield Strain (mm/mm)
Capron	2014	59	.05
Zytel 42A	1723	57	.05
Novamid	1465	55	.06

5.4.1.1.2 Barrier Properties

Figure 35 indicates that the Capron nylon 6 films exhibited the lowest OTR of the 3 control samples once the data was normalized to thickness. This was not unexpected, as nylon 6 materials tend to provide better barrier to oxygen than nylon 6,6 materials do. [20]

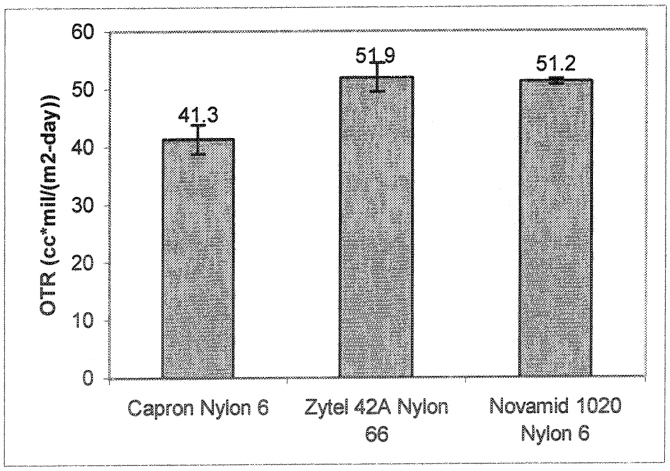

Figure 35. OTR of neat nylon films

5.4.1.2 Nanocomposite Monolayer Films

5.3.1.2.1 Morphology

Nanocomposite films, extruded in the same fashion as the neat nylon films, were examined in comparison to the neat films. The ease of processing allowed these materials to be extruded at similar processing conditions, eliminating changes in film performance related to processing differences. Figure 36 illustrates a low magnification TEM image of the monolayer Aegis NC73ZP nanocomposite film that shows MLS dispersion. Notice that the MLS platelets are oriented in one direction. The film extrusion process is the most likely cause of this orientation in the machine extrusion direction.

Figure 36. TEM Image of Aegis NC73ZP Nanocomposite Extruded Film

5.4.1.2.2 Barrier Properties

Barrier properties of these films to both oxygen and water vapor are presented in Figure 37. These results show that the nanocomposite nylon provided a barrier to oxygen at 0%RH that was roughly 40% better than the neat nylon film. Barrier to water vapor also improved by 30% over the neat film.

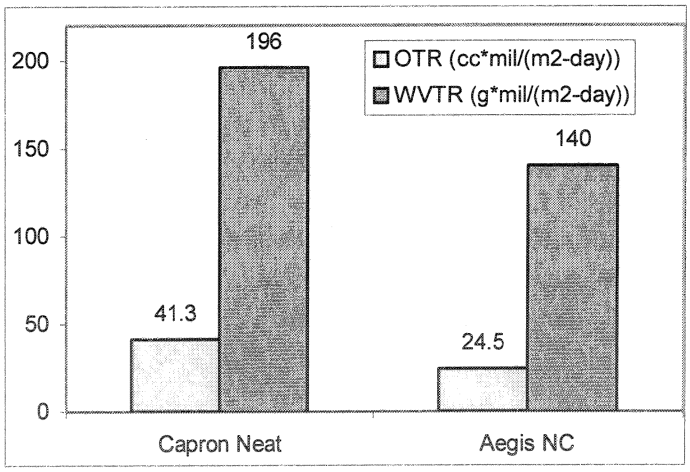

Figure 37. OTR and WVTR of neat nylon 6 and nylon 6 nanocomposite films at 0%RH

5.4.1.2.3 Thermal Properties

Thermal analysis of the films through TGA and DSC is presented in Figure 38 and Figure 39 respectively. It is clear from Figure 38 that the nanocomposite film exhibits a small decrease in thermal stability over the neat material (~4°C). Fornes et.al [18] discusses this phenomenon in detail and relates the degree of polymer degradation and thermal stability to the surfactant structure in the MLS additive. The organic component of many MLSs begins to breakdown at temperatures as low as 180°C, therefore small shifts in polymer stability may occur when processing with nylon materials in the range of 250-270°C.

DSC analysis showed that the Tg of the nylon 6 was not significantly altered by the MLS. The measured Tg (half-height) of the neat and nanocomposite nylon films was 53.0°C and 52.9°C respectively. Figure 36 illustrates the melting transitions of the neat and nanocomposite nylon films measured through DSC. Again, there is very little difference between the two curves. Both curves show similar onset Tms and crystal melting behavior. A small exothermic peak is observed just prior to melting in both curves. This is indicative of crystal perfection, where small less-perfect crystals melt below their thermodynamic melting point and then re-crystallize into larger, more perfect crystals that will melt again at a higher temperature. It is apparent that the MLS additives have not affected these thermal properties.

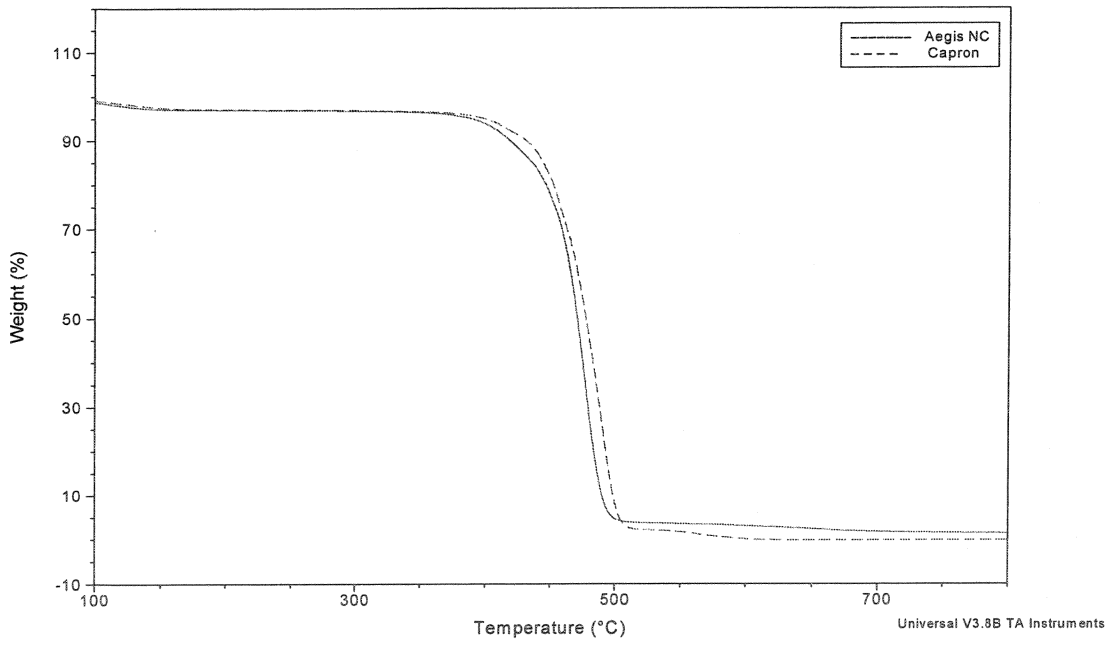

Figure 38. TGA of neat nylon 6 and nylon 6 nanocomposite films

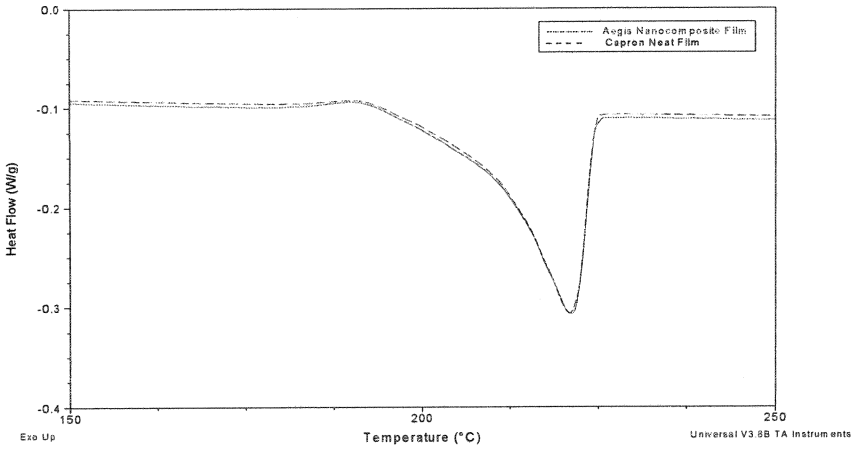

Figure 39. Melting transition of neat nylon 6 and nylon 6 nanocomposite films through DSC

5.4.1.3 Multilayer Nylon Nanocomposite and Neat Films

5.3.1.3.1 Barrier Data

To protect the nylon materials from atmospheric moisture and high humidity environments, multi-layer samples were co-extruded. The material used for the tie layers and outer shell remained the same throughout the experiment, while the nylon barrier layer was varied. The neat Capron, MXD6 nylon, the Aegis nylon nanocomposite, and a high-barrier nylon MXD6 nanocomposite material called "Imperm 105" were used as the nylon barrier layer. Figure 40 illustrates the barrier properties of these multilayer films in comparison to one another. It is important to note that due to the fact that the multi-layer samples are non-homogeneous, the transmission rate values were not normalized to thickness. Therefore, thickness values of each film are reported in Figure 40, below each sample name.

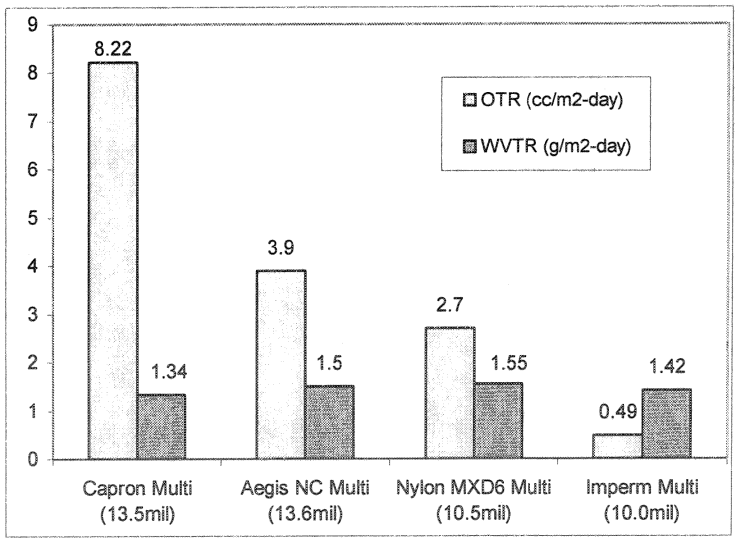

Figure 40. Barrier data for multilayer nylon nanocomposite films

It is clear from Figure 40 that the multilayer Aegis nanocomposite film provided a 53% better barrier to oxygen, at the same thickness, than the un-filled Capron multilayer film sample. The same effect is not observed with respects to barrier against water vapor. The nanocomposite had very little effect on the barrier to water vapor. Finally, a high-barrier nylon material based on nylon MXD6 (Imperm 105) chemistry was substituted as the nylon barrier layer. This polymer is reported to offer high barrier at various RH values. The results of the barrier test show that a 10-mil thick film sample containing this Imperm nylon provided the highest degree of barrier to oxygen at 0%RH.

5.5 Food Pouch - PETG Nanocomposite Study

5.5.1 Morphology

Table 15 shows the platelet spacing observed in XRD and TEM of the nanocomposite films. No concentration effect of MLS was observed on the peak position but intensity increased with concentration. The basal spacings observed in XRD matched the one observed in TEM.

Table 15. TEM platelet spacing for PET Nanocomposites

	PETG Nanocomposites		PETG + MA nanocomposites	
	X-ray	TEM	X-ray	TEM
Clay	19 A°	-	19 A°	-
1%	35 A°	30 A°	37 A°	40 A°
2%	37 A°	35 A°	37 A°	35 A°
3%	39 A°	36 A°	37 A°	38 A°
5%	35 A°	35 A°	39 A°	35 A°

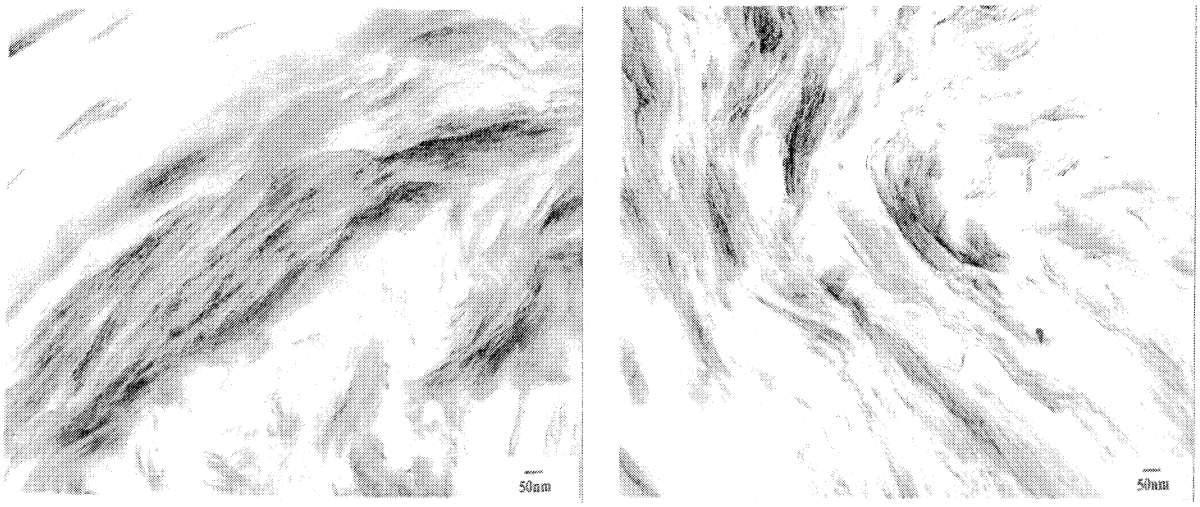

Figure 41. TEM of 1% PETG Nanocomposites

Table 16 and Table 17 show the full width half maxima (FWHM) of 001 and 002 peaks. The peaks became narrower with increase in MLS concentration. This is an indication of a strong intercalation behavior. Vaia has also reported similar results in nylon nanocomposites. The decreased FWHM behind this strong effect attributes to strong platelet-to-platelet interaction.[36]

MA present nanocomposites showed larger FWHM values compared to nanocomposites without MA. This indicates more structural disorder due to presence of MA as a compatibilizer. Low molecular weight MA acted as a coupling agent and a better dispersion was observed (**Figure 41**).

Table 16. FWHM, PETG Nanocomposites

Name	Peak (001) FWHM	Peak (002) FWHM
Cloisite 20A	1.1	1.02
1% MLS	.43	.75
2% MLS	.30	.69
3% MLS	.30	.69
5% MLS	.35	.54

Table 17. FWHM PETG-MA Nanocomposites.

Name	Peak (001) FWHM	Peak (002) FWHM
Cloisite 20A	1.1	1.02
MA+1% MLS	.46	.83
MA+2% MLS	.41	.69
MA+ 3% MLS	.34	.68
MA+ 5% MLS	.30	.58

5.5.2 Mechanical Properties

Table 18 and Table 19 show the mechanical properties of PETG nanocomposites. Nanocomposites without MA showed a maximum of 10% increase in UTS and 16% increase in modulus. Low molecular weight MA played a dominant role and a 5% decrease in UTS was observed in MA MLS nanocomposites compared to neat PETG.

Table 18. Mechanical Properties of PET Nanocomposites

Type	UTS, Mpa	Strain to Failure	Modulus, GPa
PETG	53	.049	1.2
PETG + 1%MLS	55	.048	1.2
PETG + 2%MLS	56	.044	1.2
PETG + 3%MLS	56	.041	1.3
PETG + 5%MLS	58	.041	1.4

Table 19. Tensile PETG-MA Nanocomposites.

Type	UTS, Mpa	Strain to Failure	Modulus, GPa
PETG+MA	46	.052	1.0
PETG+MA+1% MLS	47	.041	1.3
PETG+MA+2% MLS	50	.040	1.3
PETG+MA+3% MLS	48	.034	1.3
PETG+MA+5% MLS	49	.035	1.2

5.5.3 Barrier Properties

PETG nanocomposites showed improved resistance towards helium gas. No concentration dependent effect was observed and 1% nanocomposite showed best results. These measurements were made at the University of North Texas due to the quality of films, data could not be obtained with NSC's MOCON apparatus.

5.5.4 Thermal Properties

Figure 42 shows the effect of MLS on the Tg of PETG. A decreasing trend of Tg was observed in PETG nanocomposites. The T_g of PETG and PETG with MAwas observed to be the same, indicating no effect of plasticizing on PETG chains due to low molecular weight MA. All nanocomposite samples showed plasticization of the polymer due to MLS. It is likely that the chains do not pack tightly on the silicate surface and are therefore more mobile. Further since there is an intercalated dispersion, which is concentration independent, it is likely that a fixed fraction of chains is trapped between the platelets and therefore there are significant unconstrained polymer chains in each nanocomposite, which increases with MLS concentration.

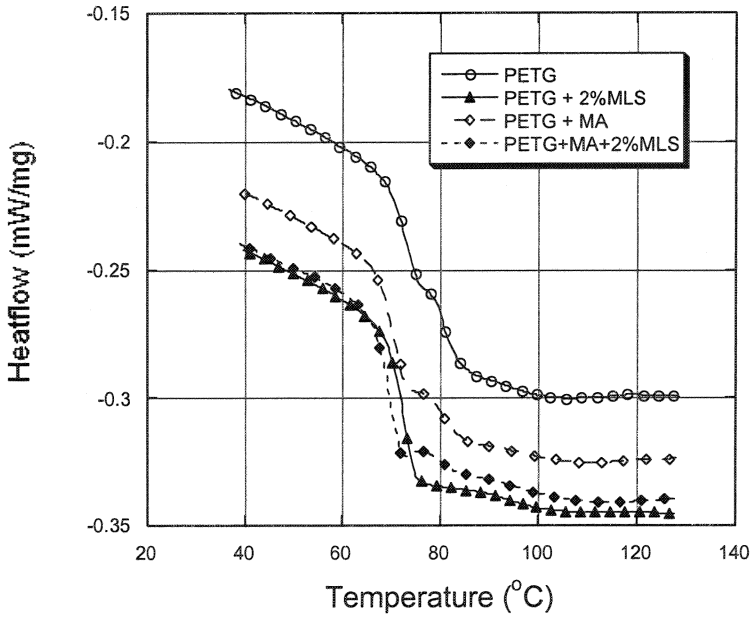

Figure 42. DSC Thermograms of Nanocomposites

TGA was performed on Closite-20A to study the decomposition behavior of the MLS. Closite-20A has a decomposition temperature of 305°C. PETG processing was done below 300°C. Previous studies show that a better compatibility between polymer and MLS can be achieved between MLS and polymer by using a modifier, which is stable at the polymer processing temperature.

Figure 43 shows the degradation behavior of PETG nanocomposites. All PETG nanocomposites showed roughly a 3-5% drop in the onset degradation temperature. MLS is

treated with organic modifier. The initial weight loss in the TGA studies corresponds to degradation of this organic treatment. The onset temperature drop was from 426°C to 400°C, which is well above the working temperature of PETG. While the surfactant degradation was not accompanied by any significant weight loss, it is apparent that the degraded surfactant reacted and accelerated the degradation of the PETG.

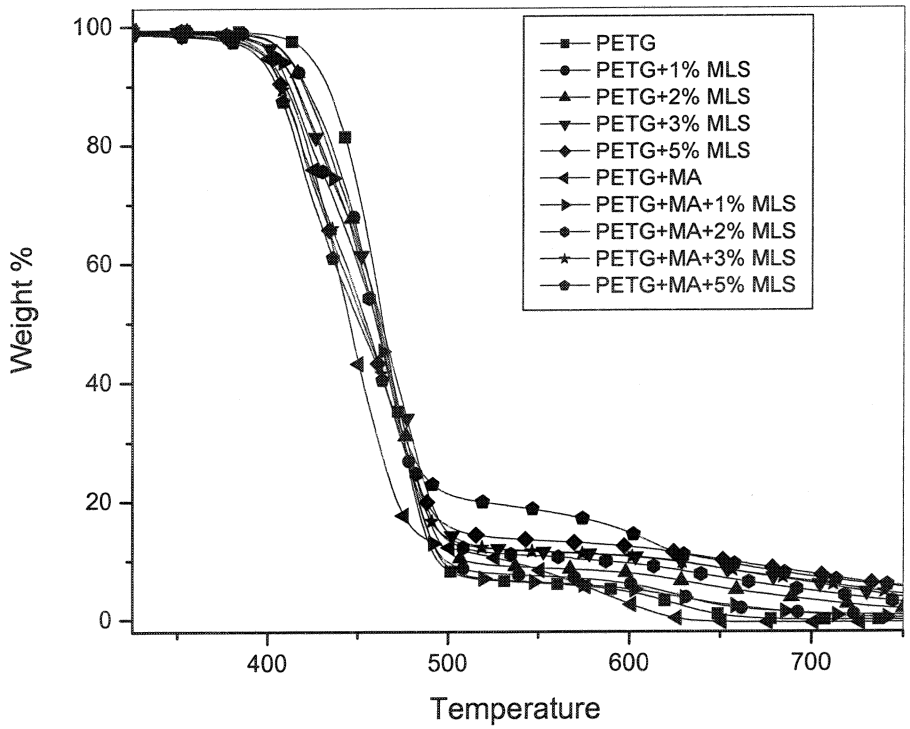

Figure 43. Thermal degradation behavior of PETG

5.5.5 Thermal Analysis

DSC analysis of the films provided an interesting glimpse into the thermal properties of the PET/MLS nanocomposites. Figure 46 shows an overlay of a DSC scan in which the films are being cooled at a controlled rate of 10°C/min from the melt state. The peaks shown represent the crystallization onset temperature and the degree of crystallization in the films. The scans indicate that the degree of crystallization is higher in the nanocomposites and that the MA did not substantially affect this. The onset of crystallization was also observed at higher temperatures indicating that the MLS were acting as nucleating agents for crystal formation within the films. The Tgs of the films dropped by 1-4°C with the addition of the MLS.

Another important property of the films that was examined was thermal stability. Through TGA experiments, it was possible to determine how the MLS and MA agent affected the polymer's degradation temperature. Figure 47 shows an overlay of numerous TGA experiments. It is important to note the temperature at which the sample begins to significantly lose weight and degrade. The neat PET film appears to demonstrate the highest thermal stability of all samples tested. The addition of MLS alone causes a depression in degradation temperature

and thermal stability. A chemical reaction between the PET and MLS treatment may be the cause of this depressed stability. A similar effect is observed in the maleated PET samples without MLS. Again, the thermal stability of the samples is depressed by as much as 10°C when 0.5% MA is incorporated into the system. In this set of experiments, the maleated PET without the MLS additive displays the least thermal stability. The degradation mechanism of PET and MA is currently under investigation.

5.6 Food Pouch - PET Nanocomposite

5.6.1 Morphology

Presented in Figure 44are the XRD patterns for the MLS samples before compounding, along with the patterns for the nanocomposite pellets formed from PET and 2% by weight of the MLS. As indicated by the shifts in the pattern peaks, the d-spacing of the MLS 20A has increased from 24.4Å to 34.1Å after processing with PET in the twin-screw extruder. This indicates that polymer is penetrating between MLS platelets, but it is an intercalated system. However, examination of the XRD pattern for the PET/MLS 30B sample shows that the MLS peak is primarily absent from the scan. This indicates a shift toward a more intercalated/exfoliated nanocomposite sample. TEM images listed in Figure 45 show the aligned structure of the PET/MLS 20A sample while the PET/MLS 30B image shows a slightly better dispersion confirming the intercalated structure. Therefore, it was decided that Cloisite 30B would be the best choice for our PET nanocomposite. Figure 46 shows a TEM image of a PET/MLS 30B nanocomposite sample after the pelletization process. Notice the intercalated structure as well as a small degree of exfoliated platelets.

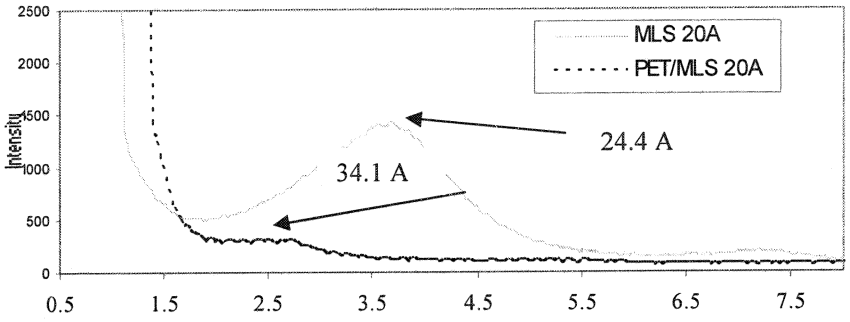

(a)

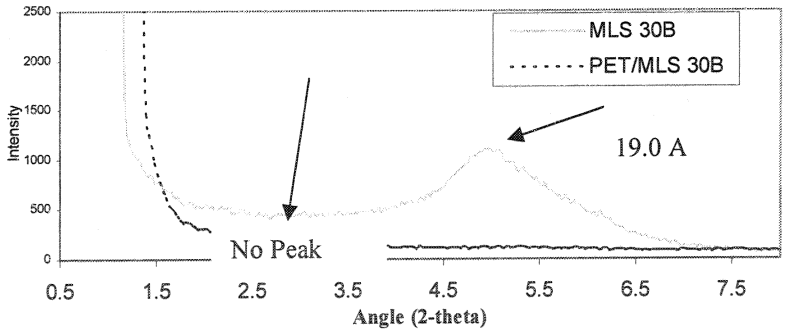

(b)

Figure 44. XRD patterns for MLS 20A (a) and 30B (b) before and after compounding with KOSA PET

(b)

(b)

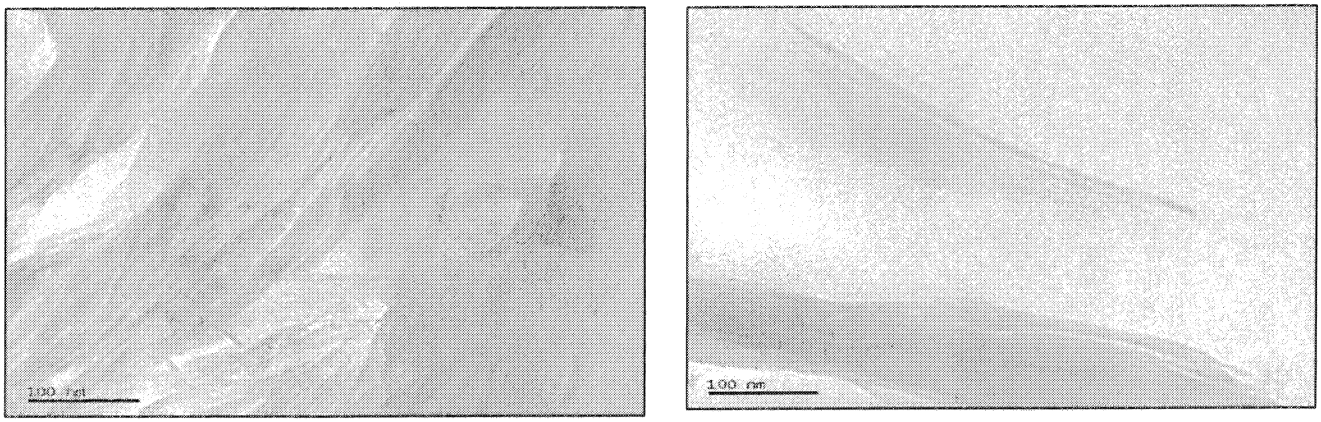

(a) (b)

Figure 45. TEM Images of PET/MLS 20A (a) and PET/MLS 30B (b) pellets

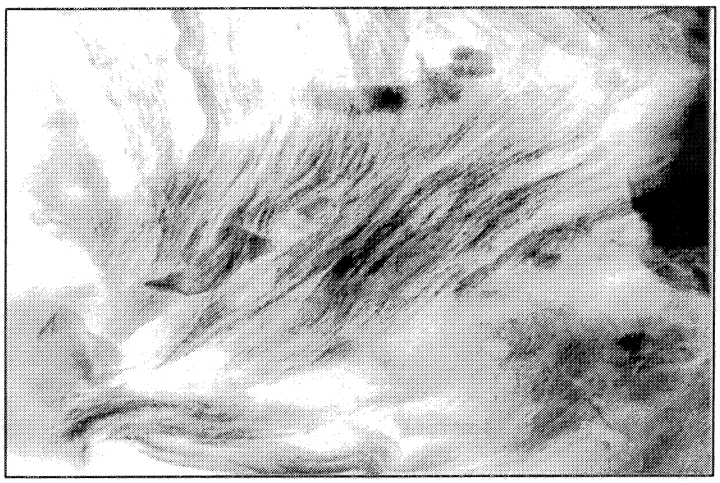

Figure 46. TEM image of an intercalated PET/MLS 30B nanocomposite

5.6.2 Mechanical Properties

Mechanical analysis of the nanocomposite films shows that the mechanical properties of the PET were substantially altered by the incorporation of MLS and MAto the polymer. Young's modulus of the nanocomposite was enhanced by 11% at a 5% MLS loading. The maleated samples showed slightly lower modulus values when compared to their non-maleated counterparts. The greatest effect of the MLS and MA on the PET appears upon examination of the toughness and ultimate strain properties of the film. While neat PET and maleated PET samples show similar toughness and strain values, nanocomposite samples with and without the MA show a tremendous loss in these properties. Figure 47 illustrates the dramatic effect that the MLS had on the ultimate strain of the PET films. Possible causes for this behavior include

inadequate MLS modification or polymer degradation. Analysis of the film molecular weight through gel-permeation chromatography (GPC) will support this hypothesis.

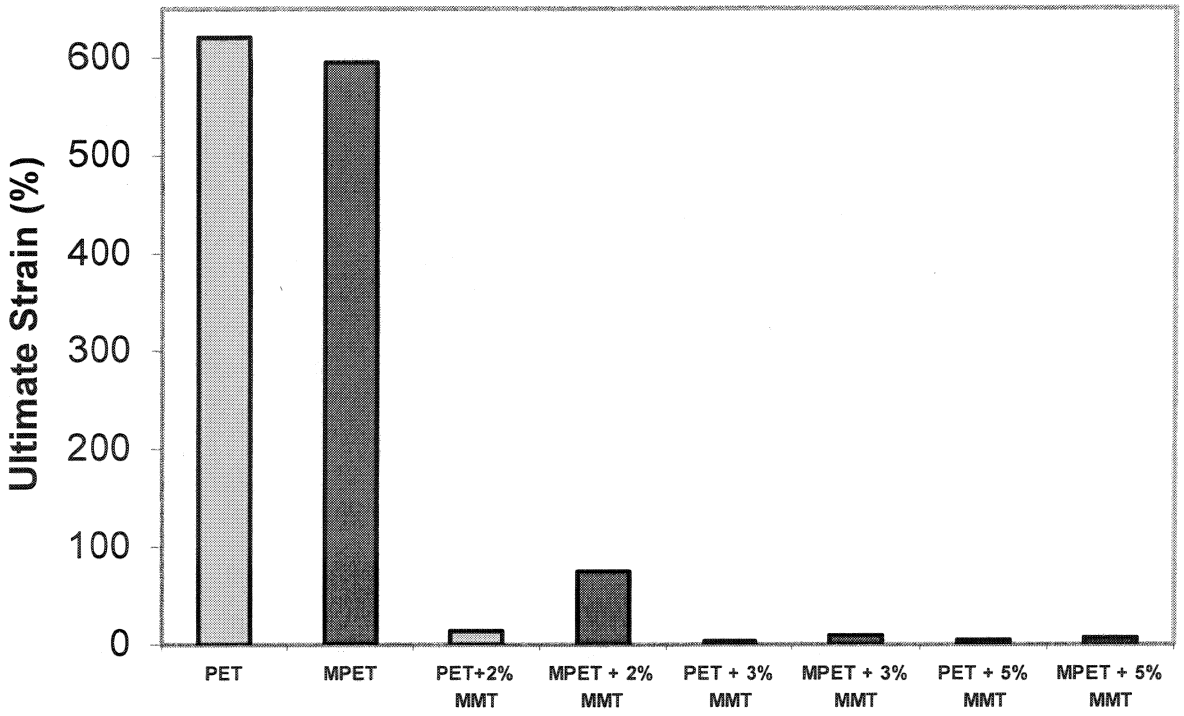

Figure 47. The effect of MLS and MA on the ultimate strain of PET films

5.6.3 Thermal Properties

Presented in Figure 48 is the TGA of the PET nanocomposite films that describes the material's thermal stability. From Figure 48 it is clear that the MLS platelets caused a small shift in the onset of thermal degradation of the PET to slightly lower temperatures. As the loading level of the MLS increased, the onset of degradation shifted to lower temperatures indicating a reaction between the MLS and PET at elevated temperatures that causes early thermal degradation and weight loss. When the MA is introduced into the system, a completely different result is obtained. When MLS is added to the maleated PET system, a slight increase in thermal stability is observed at all clay loading levels. The shifts observed in this figure are relatively small and result in thermal stability changes of only a few degrees in either direction.

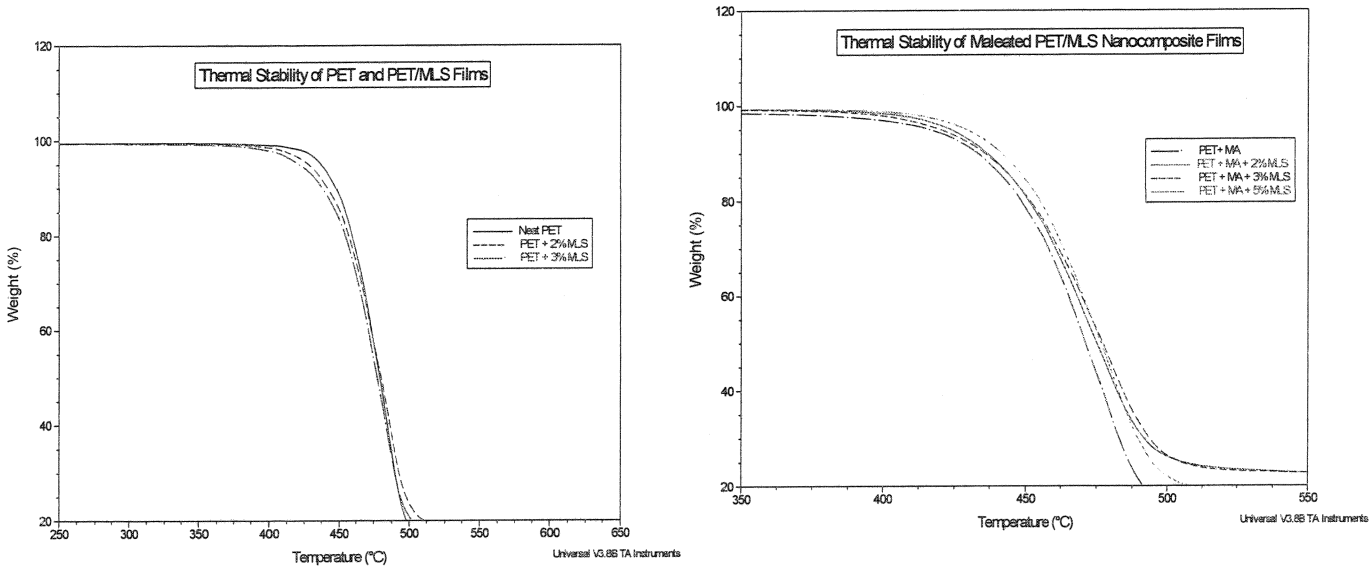

Figure 48. Thermal stability of PET, PET/MLS, and PET/MLS/MA nanocomposite films

Analysis of the DSC thermograms of the films indicates that both the MA and the MLS act as nucleating agents for crystal growth in the PET film. Figure 49 illustrates this nucleating effect. It is evident that upon cooling from the melt state, crystallization begins to occur at higher temperatures for both the maleated PET as well as the maleated PET nanocomposites. These scans also show that the degree of crystallization was higher in the nanocomposites, indicating that the MLS itself acts as a nucleating agent for crystal formation and growth.

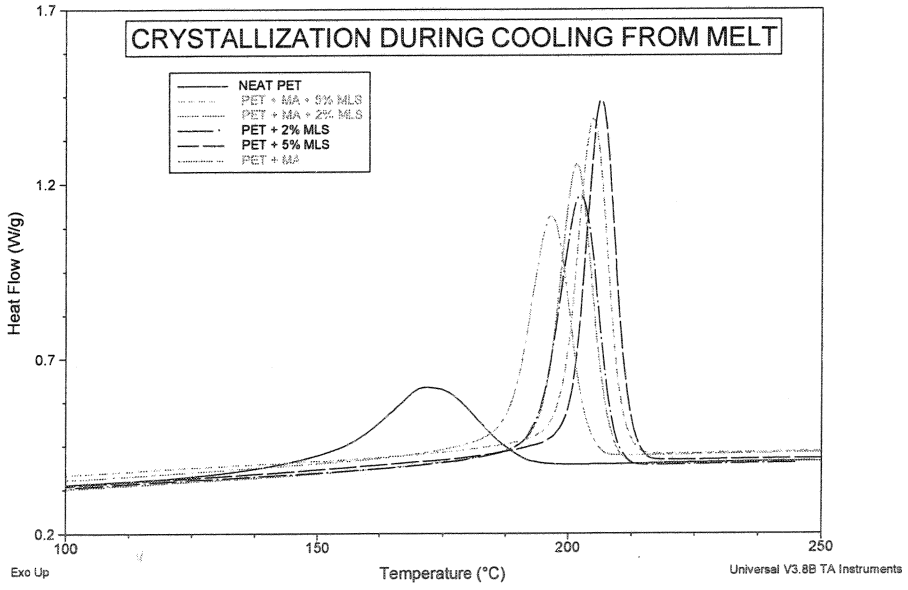

Figure 49. Nucleating effect of MA and MLS on PET films

5.6.4 Barrier Properties

Analysis of the oxygen barrier properties of these films is presented in Figure 50. Oxygen permeation values are taken once the measured permeation has leveled out and has reached equilibrium. Clearly, the nanocomposites provided higher barrier properties than the neat PET films. What is unclear is whether or not the incorporation of MA affected the barrier properties. There is no clear pattern observed in Figure 50 that directly relates the percent of MLS or the use of MA to a change in barrier properties. At this time, the only statement that can be made regarding these results is that the incorporation of MLS into PET has improved the barrier properties to oxygen by as much as 33% when using MLS loadings levels in the 3-5% range.

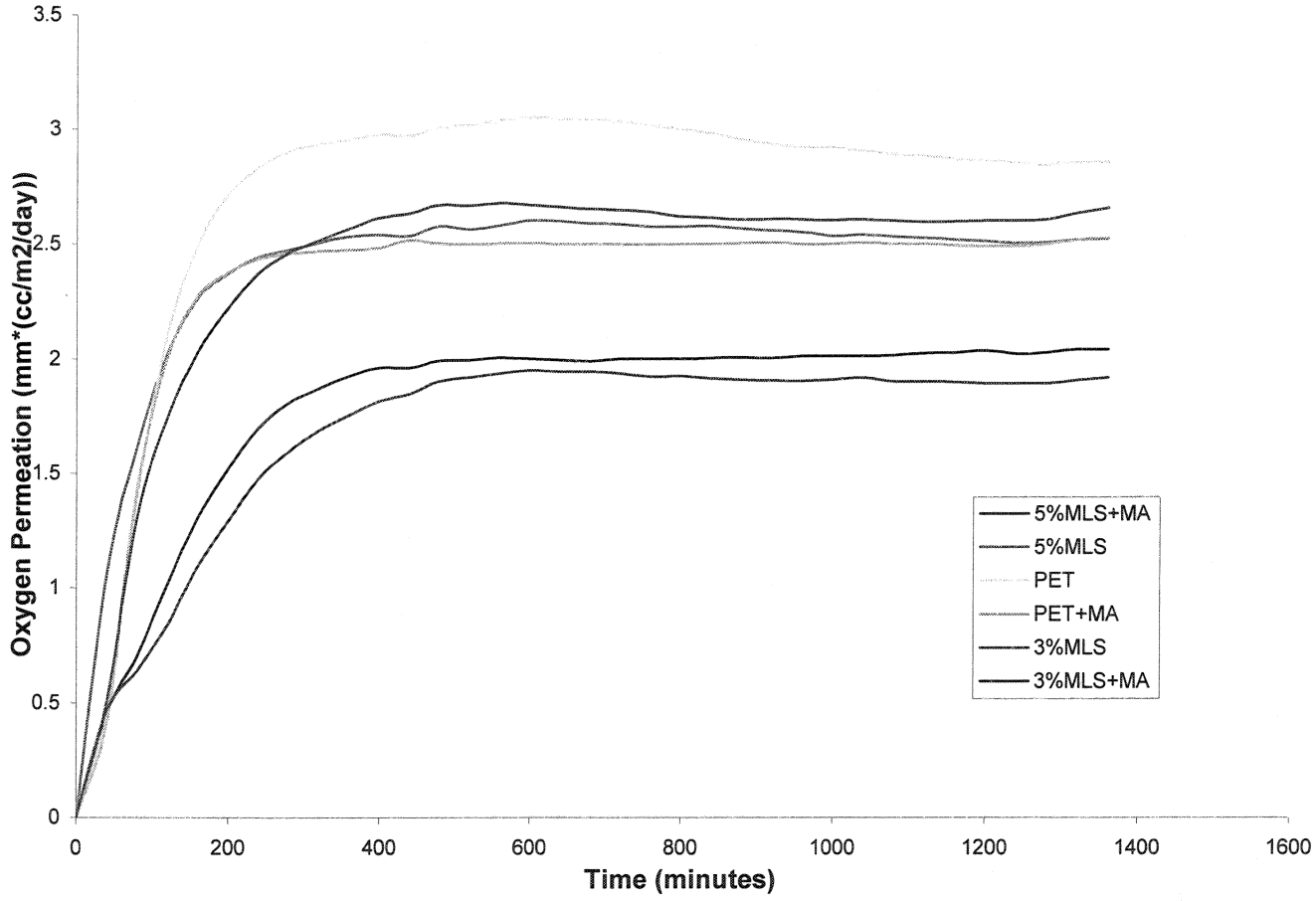

Figure 50. Barrier Properties of PET Nanocomposite films

6. Conclusions

The barrier, mechanical and thermal properties of the nanocomposite films produced in this research were improved significantly over the base-films for certain polymer/MLS formulations. In particular, there was success to replace the existing MRE Meal Bag with nanocomposite packaging that is approximately half the thickness of the current polyethylene material, and a potential to reduce production of plastic waste by over 800 tons a year from this ration item alone. This engineering accomplishment will lighten the load for the soldier and decrease the amount of solid waste generated by the Army; the latter is the highly prioritized environmental requirement that is addressed in this SERDP program. The properties of each nanocomposite system are addressed below.

Recyclable nanocomposite film consisting of low-density polyethylene (LDPE) and montmorillonite was the replacement for the MRE Meal Bag. The organically modified montmorillonite was combined at low loadings (7.5%) with a compatibilized LDPE and processed as a blown film to give improved thermal, mechanical and barrier properties. Transmission electron microscopy (TEM) of the films at various processing parameters showed that the 7.5% loading had a high degree of intercalation and dispersion. The Young's modulus of the film increased by 80% for the 7.5% montmorillonite nanocomposite in comparison to the pure LDPE. The oxygen barrier improved also with the 7.5% nanocomposite having almost twice the barrier of the pure LDPE. This LDPE/MLS formulation passed the insect resistance tests and the vibration and drop tests required for the MRE meal bag.

The ability of the LDPE/MLS nanocomposite to significantly improve the properties of the pure LDPE was consistent between both laboratory (3-5lbs) and pilot scale trials (300lbs). Successful scale-up is an essential milestone in proving the validity of the research, verifying the producibility of polymer nanocomposites, and transitioning the technology to advanced development. This nanocomposite MRE Meal Bag meets all the military requirements, yet further tests will be done upon further scale up of this material. Further scale-up to a 1000 lb processing run is currently being planned and executed.

Plasticized PLA/ MLS nanocomposites showed improvement from the pure PLA, but not enough improvement to be considered for the MRE Meal Bag packaging. XRD and TEM determined that the compounded pellets and the blown film PLA/MLS nanocomposites were intercalated. Mechanical properties of the nanocomposites showed that the Young's modulus increased by 20% and the ultimate elongation of the nanocomposites were not sacrificed in comparison to the neat samples. Nanocomposite films show a 48% improvement in oxygen barrier and a 50% improvement in water vapor barrier in comparison to the neat PLA. The thermogravimetric analysis (TGA) showed an overall 9°C increase in the decomposition temperature for all of the nanocomposites. Differential scanning calorimetry (DSC) has determined that the glass transition, cold crystallization and melting point temperatures were not significantly influenced by the presence of MLS. Biodegradation rates in soil were slightly greater for the PLA/MLS nanocomposite than the pure PLA; however, none of the PLA pure and nanocomposites achieved significant biodegradation levels after 180 days.

EVOH/MLS nanocomposites of blown and cast films were processed and characterized to obtain an optimal formulation for multilayer extrusion films. EVOH barrier resins need to be utilized in co-extruded structures as a packaging film, but an understanding of the EVOH nanocomposites' mechanical and barrier properties as a function of moisture are crucial. The morphology of all the nanocomposites showed intercalated systems with some degree of MLS dispersion. The mechanical properties of the films changed significantly with respect to RH. The barrier properties are also influenced by the amount of moisture in the sample. However, the orientation of the MLS platelets from the cast and blown film extrusion methods may be the underlining factor that is affecting the permeation properties. Thermal properties were somewhat affected by the addition of MLS. The onset of degradation temperature was slightly increased, and the rate of thermal degradation was significantly reduced.

Five-layer EVOH/tie/LDPE co-extruded films were prepared and barrier properties were measured. Systematic scale-up processing and characterization studies have been performed to obtain a non-retortable and/or retortable EVOH nanocomposite multilayer film for the MRE. Collaborations with EVALCA, suppliers of the EVOH resin, have been initiated and established The nylon nanocomposites will be used in the multilayer structure along with EVOH. The barrier properties of monolayer nylon 6 films to oxygen and water vapor were improved by 40% and 30% respectively through the addition of MLS. Multilayer nylon films formed through co-extrusion processing provided similar results and are examined for packaging applications. Multilayer films based on nanocomposite nylon MXD6 technology demonstrated the highest barrier against oxygen. Oxygen permeation through this 10-mil thick film at 0%RH was 0.49cc/m^2-day. Initial testing of these films at higher RH values shows greater barrier performance than at dry conditions. Thermal stability of the neat nylon film is roughly 4°C higher than that of the nanocomposite. Monolayer nylon and nylon nanocomposite films were processed and characterized. MLS additives did not significantly affect the Tg and Tm of the nylon 6.

The PET/MLS nanocomposites unfortunately did not have promising results for use in the MRE packaging. Intercalated dispersion was observed in x-ray diffraction and TEM confirmed the platelet spacing observed in x-ray diffraction. Non-maleated nanocomposites showed 10% increase in ultimate tensile strength and 16% increase in Young's modulus. Barrier properties towards helium gas were found improved in the nanocomposites compared to the pure PET film. MA served as an effective compatibilizer for PETG/MLS films, but the un-reacted MA contributed to decreased thermal stability due to reactivity with the hydrogenated tallow. Stiff platelets with intercalated dispersions resulted in decreased chain packing and increased free volume with a decreased T_g.

An intercalated PET/MLS film has been produced through film extrusion processing. XRD analysis and TEM microscopy has shown that the d-spacing of the MLS platelets had increased as a result of melt processing, but layered-structures were still present in the samples. The PET/MLS systems with and without the MA-coupling agent demonstrated an increased Young's modulus along with a substantial loss in film toughness and elongation. Maleated PET/MLS systems did not show any improvement in mechanical properties over the non-maleated PET/MLS films. Incorporation of MLS into PET has improved the barrier properties to oxygen by as much as 33% when using MLS loadings levels in the 3-5% range. This

improvement cannot be attributed to only the MLS, as the MA may be influencing the barrier properties by acting as a nucleating agent. The MLS also appears to plasticize the PET, as the Tg of the PET/MLS systems is lower than the neat PET film. This effect is not observed in the maleated PET sample; therefore it was directly related to the MLS.

This SERDP effort studied and characterized many nanocomposite systems. The effort was transitioned in FY06 to a 6.3 Army Solid Waste Reduction Program. This 6.3 research program, Nanocomposites for Optimized Packaging System (NANOPS), will focus on the MRE Meal Bag and Non-Retortable and Retortable Food Pouches. In this program, the LDPE/MLS nanocomposites will go thru another scale up on commercial size extruders and the characterization and military performance tests will be performed. Also, the EVOH nanocomposites are being scaled up at the 25, 100, 300 lb level as cast films and then characterized for barrier properties. Multilayer films of EVOH/MLS and Nylon/MLS nanocomposites are being targeted for both food pouches.

This document reports research undertaken at the U.S. Army Research, Development and Engineering Command, Natick Soldier Center, Natick, MA, and has been assigned No. NATICK/TR-06/023 in a series of reports approved for publication.

7. References

1. Giannelis, E.P. (1996), Advanced Materials, Vol. 8, pp. 29-35.

2. LeBaron, Peter C., Wang, Zhen et al. (1999), Applied Clay Science, Vol. 15, pp. 11-29.

3. Dagani, Ron, (1999), Chemical & Engineering News, June 7, 1999, pp. 25-37.

4. Miller, B. (1997), Plastics Formulating and Compounding, Vol. 3, pp. 30-32.

5. Dennis, H.R.; Hunter, D.L.; Chang, D.; Kim, S.; White, J.L.; Cho, J.W.; Paul, D.R. (2001), Polymer, Vol. 42, pp. 9513-9522.

6. Hu, G.H.; Feng, L.F. (2003) Macromol.Symp.Vol.195, pp. 303-308.

7. Hambir, S.; Bulakh, N.; Jog, J.P. (2002), Polymer Engineering and Science, Vol. 42, No. 9 pp. 1800-1807.

8. Alexandre, M.; Dubois, P.; Sun, T.; Garces, J.; Jerome, R. (2002), Polymer, Vol. 4, pp. 2123-2132.

9. Jeon, H.; Jung, H.; Lee, S.; Husdon, S. (1998), Polymer Bulletin, Vol. 4, pp. 107-113.

10. Hotta, S.; Paul, D.R.; (2004), Polymer, Vol. 45, Issue (22), pp.7639-7654.

11. Pandey, J.; Singh, Ray P. (2004), e-Polymers http://www.epolymers.org/papers/singh_140804.

12. Bae, J. H.; Ryu, S. H.; Chong, Yong, W. (2004), ANTEC, 62nd, Vol. 2, pp. 2196-2200.

13. Zhang, J.; Wilke, C. (2003), Polymer. Vol. 80, Issue (1), pp. 163-169.

14. Wang, K. H.; Cheng, M.; Chung, I. J. (2003), Journal of Applied Polymer Science, Vol. 89, Issue (8), pp. 2131-2136.

15. Lunt, J. (1998), Polymer Degradation and Stability, Vol. 59 pp.146.

16. Ke, T.; Sun. X.S. (2003), Journal of Applied Polymer Science, Vol. 88, pp. 2948.

17. Martin, O.; Averous L. (2001), Polymer, Vol. 42, pp. 6209.

18. Pluta, M.; Galeski, A.; Alexandre, M.; Paul, M.A.; Dubois, P. (2002), Journal of Applied Polymer Science, Vol. 86, pp.1497.

19. Ray, S.S.; Yamada, K.; Okamoto, M.; Ogami, A.; Ueda, K. (2003), Chem. Mater. Vol. 15, pp. 1456.

20. Koene, B.E.; Singh, A.K.; Triton Systems, Inc. SBIR Phase II, Contract #DAAD16-99-C-1039, Robert Trottier Technical Monitor

21. EVAL® Key Properties and Applications
EVALCA Technical Bulletin.

22. Usuki, A.; Koiwai, A.; Kojima, Y.; Kawasumi, M.; Okada, A.; Kurauchi, T.; Kamigaito, O. (1995), Journal of Applied Polymer Science, Vol. 55, pp. 119.

23. Fornes, T.D.; Yoon, P.J.; Paul, D.R. (2003), Polymer, Vol. 44, pp. 7545-7556.

24. Ranade, A.; D'Souza, N.; Gnade, B.; Dharia, A. (2003), Society of Plastics Engineers Annual Technical Conference Proceedings.

25. Massey, L. (2003), Plastics Design Library/William Andrew Publishing, Norwich, NY.

26. Ranade, A.; D'Souza, N.; Gnade, B.; Ratto, J. (2004), Society of Plastics Engineers Annual Technical Conference Proceedings, pp. 2405-2409.

27. Mai, Y.W.; Wong, J.S.S.; Li, R.K.Y.; Lu, C. (2004), Society of Plastics Engineers Annual Technical Conference Proceedings, pp.1785-1789.

28. Mueller, C.; Kaas, R.; Fillon, B.; Tournier, S.; Jean-Jacques, L. "Thermoplastic films containing polymeric nanocomposites with improved barrier and mechanical properties" US. Patent No. 6403231 (2001).

29. Brydson J. (1999), Plastics materials, Butterworth Heinemann.

30. Saunders K.J. (1988), Organic Polymer Chemistry, Chapman and Hall.

31. Ke, Y.; Long, C.; Qi, Z. (1999), Journal of Applied Polymer Science, Vol. 71, pp. 1139-1146.

32. Ou, C. F.; Ho, M. T.; Lin, J. R. (2003), Journal of Polymer Research, October, pp. 127-132.

33. Sanchez-Solis, A.; Garcia-Rejon, A.; Manero, O. (2003), Macromol. Symp., Vol. 192, pp. 281-292.

34. Lucciarini, J. M., Ratto, J., Koene, B.E., Powell, B., , SPE ANTEC Proceedings, Dallas, TX (2001).

35. Bissot T.C. In Koros WJ (ed), ACS Symposium Series Barrier Polymers and Structures, American Chemical Society Washington, DC (1989); 225.

36. Shrastri R. S. In Koros WJ (ed), ACS Symposium Series Barrier Polymers and Structures, American Chemical Society Washington, DC (1989); 178.

8. Appendix

List of Technical Publications

Articles in Peer-Reviewed Journals

Thellen, C.; Orroth, C.; Froio, D.; Ziegler, D.; Lucciarini, J.; Farrell, R.; D'Souza, N.A.; and. Ratto, J. "Influence of montmorillonite layered silicate on plasticized poly(l-lactide) blown films" Polymer, 46, 11716 (2005).

Ranade, A.; D'Souza, N. A.; Ratto, J.; and Thellen, C. "Surfactant concentration effects on amorphous PETG-montmorillonite layered silicate blown films: creep, dispersion and crystallinity", Polymer, 46, 7323 (2005)

Conference/Symposium Proceedings

Culhane, E.; Froio, D.; Thellen, C.; Orroth, C.; Lucciarini, J.; Ratto, J. "A Study of Laboratory and Pilot Scale Extruded LDPE Nanocomposite Films" *Society of Plastics Engineers Annual Technical Conference Proceedings*, (2005), 63rd, 1916-1919.

Pendse, S.; Ratto, J.; D'Souza, N.A. "Essential Work of Fracture in PET Nanocomposites" *Society of Plastics Engineers Annual Technical Conference Proceedings*, (2005), 63rd.

Pendse, S.; Ratto, J.; D'Souza, N.A. "Deformation in Polymer Nanocomposites" *Society of Plastics Engineers Annual Technical Conference Proceedings*, (2005), 63rd.

Froio, D.; Lucciarini, J.; Ratto, J.; Thellen, C.; Culhane, E. "Developments in High Barrier Non-Foil Packaging Structures for Military Rations" *Flex Pack Conference*, Orlando, FL. March 15, (2005). (Invited Presentation)

Lucciarini, J.; Ratto, J., "Polymer Nanocomposites for Combat Ration Applications", Research & Development Associates, November (2005).

Froio, D.; Ziegler, D.; Orroth, C.; Thellen, C.; Lucciarini, J.; Ratto, J. "The Effect of Montmorillonite Layered Silicates on the Properties of Ethylene Co-Vinyl Alcohol Blown Film Nanocomposites" *Society of Plastics Engineers Annual Technical Conference Proceedings*, (2004) 62nd, (Vol. 2), 2415-2419.

Ranade, A.; D'Souza, N.A.; Gnade, B.; Ratto, J. "Permeability Measurement of Polymers and Layered Silicate Nanocomposites" *Society of Plastics Engineers Annual Technical Conference Proceedings*, (2004) 62nd, (Vol. 2), 2406-2408.

Pendse, S.; Ranade, A.; D'Souza, N.A.; Ratto, J. "Effect of Montmorillonite Layered Silicates (MLS) on Crystallization Growth Rate in Semi-Crystalline PET Nanocomposites." *Society of Plastics Engineers Annual Technical Conference Proceedings*, (2004) 62nd, (Vol 2), 2342-2348.

Orroth, C.; Thellen, C.; Ziegler, D.; Froio, D.; Stenhouse, P.; Shaffer, C.; Ratto, J. "A Processing and Characterization Study of a Biodegradable Nanocomposite" *Materials Research Society Annual Fall Meeting,* Boston, MA, (2003).

Thellen, C.; Orroth, C.; Froio, D.; Lucciarini, J.; Ratto, J. "The effect of maleic anhydride coupling agent on melt processed semi-crystalline PET nanocomposite films". Annual Technical Conference - Society of Plastics Engineers (2004), 62nd (Vol. 2), 2130-2134.

Froio, D.; Thellen, C.; Lucciarini, J.; Ratto, J. The Effect of Montmorillonite Layered Silicates on the Properties of Ethylene Co-vinyl Alcohol Nanocomposites, Proceedings of the Society of Plastics Engineers' Annual Technical Meeting (ANTEC), Chicago, IL. May 2004.

Thellen, C.; Orroth, C.; Ratto, J. Thermal Analysis of Nanocomposites: An Overview of Selected Polymer/Montmorillonite Layered Silicate Systems", Proceedings of the Society of Plastics Engineers' Annual Technical Meeting (ANTEC), Chicago, IL May 2004.

Ratto, J.; Lucciarini, J.; Froio, D.; Thellen, C. Nanocomposite Research for Combat Ration Packaging, Army Science Conference, Orlando, FL 2004.

Technical Abstracts and Presentations

Thellen, C.; Orroth, C.; Ratto, J. "An Investigation of Biodegradable Polylactic Acid/Montmorillonite Blown Film Nanocomposites". ***Seventh Annual Green Chemistry and Engineering Conference [CD-ROM]; The National Academies, Washington, DC.*** (2003); Paper # 2.

Ratto, J. "Army Environmental Research Efforts for Military Packaging" USDA Biobased Roundtable Symposium, December 8, (2005) (Invited Presentation)

Ratto J.; Lucciarini, J.; Froio, D.; Thellen, C. Strategic Environmental Research and Development Program Annual Symposium, November, 2004 and 2005 (Posters)

Pendse, S.; Ratto, J.; D'Souza, N.A. "Essential Work of Fracture Approach in Determination of Toughening Mechanism in PET Nanocomposites in Relation to Matrix Modification" Flex Pack, March (2005). (Poster)

Ratto, J. "Developing Improved Polyethylene Nanocomposite Film Products for Army Food Packaging", Third Annual Polymer Symposium at Lyondell Chemical Company, April 21, (2005). (Invited Presentation)

Ratto, J. " Nanotechnology for Military Packaging", Batelle, Columbus Ohio, April 2005. (Invited Presentation)

Lucciarini, J. Ratto, J. "Polymer Nanocomposites for Ration Packaging Applications" Nanotechnology for Defense Conference July, 26 2005. (Invited Presentation)

Thellen, C.; Ratto, J. "Nanotechnology in Military Food Packaging" The Future of Nanomaterials Conference, Pira International, Miami, FL. February 22, (2005). (Invited Presentation)

Ratto, J., Lucciarini, J. "Nanoparticles Enhanced Polymer Films for Food Packaging" International Food Technology Annual Meeting, Las Vegas Nevada, July 12-16, (2004). (Invited Presentation)

Ranade, A.; D'Souza, N.; Gnade, B.; Ratto, J.; Thellen, C. "Permeability "PET Nanocomposites with Expandable Layered Smectites." Strategic Partnerships for Research in Nanotechnology Conference, Austin, Texas, August 25, (2004).

Ranade, A.; D'Souza, N.; Gnade, B.; Ratto, J., "Permeability modeling of nanocomposite films" Strategic Partnerships for Research in Nanotechnology Conference, Dallas, Texas, April, 20, (2004).

D'Souza, N.A.; Ranade, A.; Gnade, B.; Ratto, J.; Fairbrother, D. "Amorphous and Semicrystalline PET Nanocomposites: Barrier Properties" FlexPack 2004, March 15, (2004). (Invited Presentation)

Ratto J.; Thellen, C., "Montmorillonite Layered Silicate Nanocomposites for Military Packaging Applications. Presented at Nanocomposites 2004 Conference, Brussels, Belgium, March 18, (2004). (Invited Presentation)

Ranade, A.; D'Souza, N.; Gnade, B.; Ratto, J., "Semicrystalline PET Nanocomposites" Strategic Partnerships for Research in Nanotechnology Conference, Austin, Texas, April, 21 (2003).

Ranade, A.; D'Souza N.A.; Gnade, B.; Thellen, C.; Orroth, C.; Froio, D.; Ratto, J., "Effect of coupling agent on the dispersion of PETG montmorillonite nanocomposite films" Materials Research Society, November, (2003). (Poster)

Ranade, A.; D'Souza, N.; Gnade, B.; Ratto, J.; Thellen, C. "PETG Nanocomposites with Expandable Layered Smectites" Polymers for Advanced Technology Conference, September 9, (2003).

Book Chapter

Ratto, J.; Lucciarini, J.; Froio, D.; Thellen, C. "Melt Processed Polymer/Montmorillonite layered silicate nanocomposites for high barrier food applications" for "Packaging Nanotechnology" to be published by American Scientific Publishers (www.aspbs.com)
(Invited book chapter; in preparation due August, 2006)

Dissertations

Thellen, Christopher, "Investigation of the processing and characterization of blown film nanocomposites consisting of polylactic acid and organically modified montmorillonite clay." Master's Thesis in Plastics Engineering at the University of Massachusetts Lowell, May, (2003).

Ranade, Ajit, " Barrier and long term creep properties of polymer nanocomposites" Doctor of Philosophy (Materials Science and Engineering) University of North Texas, December (2004).

9. List of Acronyms

DSC	Differential Scanning Calorimetry/Calorimeter
EVOH	Poly (ethylene co-vinyl alcohol)
FWHM	Full width half maxima
LDPE	Low Density Polyethylene
MA	Maleic Anhydride
MLS	Montmorillonite Layered Silicates
MRE	Meal Ready-To-Eat
NSC	Natick Soldier Center
OTR	Oxygen Transmission Rate
PB	Polybond
PET	Polyethylene Terephthalate
PETG	Polyethylene Terephthalate Glycol
PLA	Polylactic Acid
PP	Polypropylene
PVDF	Polyvinylidene Fluotide
PVOH	Polyvinyl alcohol
RH	Relative Humidity
SERDP	Strategic Environmental Research and Development Program
SEM	Scanning Electron Microscopy
TEM	Transmission Electron Microscopy
TGA	Thermogravimetric Analysis
WHC	Water Holding Capacity
WVTR	Water Vapor Transmission Rate
XRD	X-ray Diffraction